Heat-induced gene positioning in *Caenorhabdidtis elegans*: *hsp-16* promoter drives transcription-dependent nuclear pore association

Inauguraldissertation

zur
Erlangung der Würde eines Doktors der Philosophie
vorgelegt der
Philosophisch-Naturwissenschaftlichen Fakultät
der Universität Basel

von
Sabine Rohner
aus Rebstein SG

Basel, 2013

Genehmigt von der Philosophisch-Naturwissenschaftlichen Fakultät

auf Antrag von

Prof. Dr. Susan M. Gasser
Dr. Julie Ahringer

Basel, den 13. November 2012

Prof. Dr. Jörg Schibler
Dekan

creative commons

Namensnennung-Keine kommerzielle Nutzung-Keine Bearbeitung 2.5 Schweiz

---

Sie dürfen:

das Werk vervielfältigen, verbreiten und öffentlich zugänglich machen

Zu den folgenden Bedingungen:

Namensnennung. Sie müssen den Namen des Autors/Rechteinhabers in der von ihm festgelegten Weise nennen (wodurch aber nicht der Eindruck entstehen darf, Sie oder die Nutzung des Werkes durch Sie würden entlohnt).

Keine kommerzielle Nutzung. Dieses Werk darf nicht für kommerzielle Zwecke verwendet werden.

Keine Bearbeitung. Dieses Werk darf nicht bearbeitet oder in anderer Weise verändert werden.

- Im Falle einer Verbreitung müssen Sie anderen die Lizenzbedingungen, unter welche dieses Werk fällt, mitteilen. Am Einfachsten ist es, einen Link auf diese Seite einzubinden.
- Jede der vorgenannten Bedingungen kann aufgehoben werden, sofern Sie die Einwilligung des Rechteinhabers dazu erhalten.
- Diese Lizenz lässt die Urheberpersönlichkeitsrechte unberührt.

Quelle: http://creativecommons.org/licenses/by-nc-nd/2.5/ch/ Datum: 3.4.2009

Table of Contents

Abstract

The DNA of eukaryotic cells is packaged into transcriptionally active euchromatin and repressed heterochromatin. These two chromatin types are non-randomly distributed within the nucleus. Indeed, at the nuclear periphery, heterochromatin is enriched near the nuclear lamina whereas euchromatin is found in the vicinity of nuclear pores. Interestingly, in budding yeast, several stress inducible genes interact with nuclear pores upon activation, although the relevance of this in higher eukaryotes has been unclear. In this thesis I characterise the spatial distribution of a heat shock gene (*hsp16.2*) in embryos of the nematode worm *Caenorhabditis elegans*. I find that *hsp-16.2* is preferencially found at the nuclear periphery, where it interacts with the nuclear pore complex. Using two different types of ectopically integrated *hsp-16.2* promoters, I investigated the molecular mechanism of the pore-gene interaction. I find that both types of transgenes show the same distribution, even though to a lesser extent. The results presented here shed light on the promoter elements and proteins essential for the perinuclear gene localisation and suggest conservation of gene-pore interactions in yeast, worm and fly.

Chapter 1: Introduction

In the process of evolution, organisms with traits that contribute to improved survival are selected for, becoming the dominant population of a given species. This allows for the transmission of favourable heritable information to the next generation. The heritable information that is subject to this selection process, is encoded within polymers of deoxyribonucleic acid (DNA), which contain protein coding sequences called genes. Genes can be transcribed into a ribonucleic acid (RNA) polymer, which in turn can be translated into chains of amino acids and folded into proteins. Other RNAs, also transcribed from DNA, serve as structural elements in ribosomes and other macromolecular machines. RNA and proteins provide the functional machinery that ensures the synthesis and maintenance of most of the structural and metabolic components of an organism.

Heritable information in eukaryotes is sequestered in the nucleus

One of the major changes that occurred during evolution from prokaryotes to eukaryotes is the compartmentalisation of the cell, and most notably sequestration of the genome away from other elements of the cell. For most of the eukaryotic cell cycle, chromosomes are clustered into the nucleus, which is separated from the cellular cytoplasm by a double membrane with a lumen, called the nuclear envelope. A number of proteins line the inner face of the nuclear envelope, attached to the membrane by membrane spanning domains. In eukaryotes with an open mitosis, the nuclear envelope breaks down during mitosis, and the nucleus reforms in early G1 phase. In eukaryotes with a closed mitosis, the nuclear envelope remains intact through mitotic division.

Nuclear pores form the gateway between the nucleus and the cytoplasm

To maintain transport of macromolecules, high-energy intermediates of metabolism and other signalling molecules between the nucleus and the cytoplasm, the nuclear envelope is interspersed by large proteinaceous pores which function as gateways (Grunwald and Singer, 2012). A single pore is built from about 30 different proteins that form together the nuclear pore complex (NPC) with a molecular weight of 90 – 120 MDa. The pore assumes the shape of a cylinder with octagonal symmetry (Grunwald and Singer, 2012; Lim and Fahrenkrog, 2006; van Steensel, 2011).

Electron-microscopy has revealed three structural parts of the vertebrate NPC (Fahrenkrog et al., 2004). A central framework is positioned within the nuclear envelope, piercing the nuclear envelope, while on the cytoplasmic side filaments protrude and on the nuclear side a basket like structure is attached. This architecture – as well as the protein components – is conserved from yeast to vertebrates (Fahrenkrog et al., 2004). The overall diameter of an NPC is about 120 nm and the channel has a

diameter of about 50 nm with a length of about 90 nm (Beck et al., 2004; Huve et al., 2008; Stoffler et al., 2003).

Ions and small molecules up to a size of 40 to 60 kDa can diffuse passively through the NPC. Larger cargo is transported with the help of transport factors termed importins, exportins and karyopherins and depend on the presence of a nuclear localisation sequence (NLS) or a nuclear export sequence (NES). The translocation per se is not energy dependent, but gradients of specific metabolic energy are maintained across the nuclear membrane (Grunwald and Singer, 2012). For import complexes the dwell time was between 1 and 100 ms whereas for β-actin mRNA it was between 180 ms and more than 2s, which still is considerably short (Dange et al., 2008; Grunwald and Singer, 2010; Kubitscheck et al., 2005; Sun et al., 2008). The export of mRNAs, well studied for β-actin mRNA in mammalian cells, can be split into three steps: docking (80 ms), transport (5 to 20 ms) and release (80 ms) (Grunwald and Singer, 2010). Transport rates through individual nuclear pores are amazingly high with about 1000 transport complexes with cargo traversing the pore every second (Grunwald and Singer, 2012).

Interesting also is lifetime of nucloporins before they get renewed. While scaffold proteins are quite stably associated and are exchanged about every 10 hours to 3 days, peripheral nucleoporins are renewed within seconds up to about 10 minutes (Rabut et al., 2004).

In addition to their essential role in transport and communication, nuclear pores play also a role in the organisation of the nuclear architecture and in fine tuning gene expression (Capelson et al., 2010). However, many of the nucleoporins playing a role in gene expression were shown to be found as well in the nucleoplasm in a soluble state and being not only part of the nuclear pore complex. For example only about 50% of Nup153 are found in the nuclear pore basket and the rest is found in the nuclear lumen (Capelson et al., 2010; Kalverda and Fornerod, 2010)).

Nuclear lamina serves as a scaffold and as a binding platform for chromatin

Together with the inner nuclear membrane, the nuclear lamina, a filamentous meshwork of intermediate filament proteins, is involved in the organisation of nuclear structure and function. It is generally found in all somatic cells of metazoans as a thin filamentous layer between the nuclear membrane and the peripheral chromatin (Prokocimer et al., 2009). There it has a scaffold function to keep the nuclear shape and to correctly space nuclear pores, but it serves also as a binding platform for chromatin and numerous proteins involved in chromatin organisation and other various nuclear functions (for review see (Dechat et al., 2010)). In single-celled eukaryotes with closed mitosis, the nuclear pores function in the absence of the nuclear lamina, leading researchers to propose that the essential role of the lamina is to mediate the reformation of the nucleus after mitosis and to enable terminal differentiation, during which large amounts of the genome generally become associated in a repressed state with the nuclear lamina (for review see (Dechat et al., 2010)).

The major proteins of the nuclear lamina are called lamins and are one of the most ancient members of the intermediate filament family. They have the typical tripartite structure of intermediate filament proteins with an α-helical rich central rod domain flanked by a short globular amino-terminal head and a longer carboxy-terminal tail domain. Head-to-tail associations between lamin monomers form 10 – 200 nm thick lamin filaments, a structural organisation that is evolutionarily conserved. All metazoan cells encode lamins; while vertebrates encode mainly four types of lamin, invertebrates usually encode only one, except *Drosophila*, which encodes two (Prokocimer et al., 2009). Since the experimental part of this thesis focuses on the role of active genes interacting with nuclear pores at the nuclear periphery, I do not go into further details about the nuclear lamina.

DNA is compacted into chromatin

Within the nucleus we find a large amount of DNA; in human cells with a diameter of about 6 µm for example 2 meters. In order to fit into the nucleus, genomic DNA is associated with multiple proteins to form chromatin. The basic repeating unit of chromatin is the nucleosome, where 147 bp of DNA is wrapped around a histone octamer (two copies each of H2A, H2B, H3 and H4) (Luger et al., 1997). To allow for the necessary compaction to fit the linear DNA molecule within the nucleus, arrays of nucleosomes are further compacted and stabilised by additional DNA binding proteins, such as the linker histone H1. Compaction of the nucleosomal fiber into higher-order structures generally inhibits the binding of other DNA binding factors such as transcription factors, providing a further layer of transcriptional control.

Accessibility of DNA is guaranteed by at least three different means

Indeed, regulated DNA accessibility affects all DNA based cellular activities such as transcription, replication and repair. In order to make use of the additional layer of regulation, accessibility needs to be regulated. To do this cells contain at least three different means to modulate DNA accessibility according to the immediate need. A first possibility is to remodel chromatin in an ATP-dependent manner by chromatin remodelers. Another possibility is to alter the biochemical composition of histones within nucleosomes, while the third is to covalently modify histones to generate, directly or indirectly improved access to the DNA (Zlatanova and Thakar, 2008). In the following paragraphs I would like to describe these possibilities more in detail.

Chromatin remodelers can increase the accessibility of DNA by disrupting chromatin, but they are also very important to organise the genome by assembling and spacing nucleosomes. There are many chromatin remodelling enzymes in eukaryotes, all use ATP hydrolysis to change DNA – nucleosome interactions, but yet they have specific cellular roles (Clapier and Cairns, 2009). The SWI/SNF (switching defective/sucrose non-fermenting) complex is not involved in chromatin assembly but rather slides and ejects nucleosomes for various processes (Mohrmann and Verrijzer, 2005), whereas the ISWI (imitation switch) enzymes regulate nucleosome spacing either for chromatin

assembly or for transcriptional repression (Florescu et al., 2012). The INO80 (inositol requiring 80) complex, in contrast, is especially important for promoting DNA repair and replication fork restart (Chambers and Downs, 2012).

By changing the composition of nucleosomes, accessibility of DNA can be changed in a direct or indirect manner. Interestingly, although histones are some of the most conserved proteins known, variant forms exist of histones H2A and H3. These histone variants can impart new properties onto the nucleosome and have critically important functions within the cell. For example, the conserved H3 variant CENP-A in humans (Cse4 in *S. cerevisiae* and CID in *Drosophila*), plays an important role in centromere function and chromosome segregation (for review see (Talbert and Henikoff, 2010) and (Rando and Winston, 2012)). Another example is the exchange of histone H2A for the histone variant H2A.Z. This histone variant is also conserved in evolution and is essential for viability in many organisms (Zlatanova and Thakar, 2008). Interestingly, H2A.Z is incorporated into chromatin by the ATP-dependent chromatin remodelling complex called SWR1 in yeast, or SRCAP in mammals (Kobor et al., 2004; Krogan et al., 2003; Mizuguchi et al., 2004). In yeast, H2A.Z is often incorporated in the -1 and +1 nucleosome next to a nucleosome-free region, which corresponds to the promoter region of many genes. Nucleosome-free regions are approximately 150 bp in length, are located about 200 bp upstream of transcription start sites and include transcription factor binding sites as well as poly(A) and poly(T) rich sequences (Yuan et al., 2005). In housekeeping genes the two flanking nucleosomes are well positioned, whereas in stress genes, generally containing a TATA box, they are less well positioned (Rando and Winston, 2012). In yeast it has been shown that in some promoters H2A.Z plays an important role in the proper recruitment of RNA polymerase II as well as TBP (TATA Binding Protein), two factors that are crucial for transcription (Adam et al., 2001).

Last but not least, histones can be modified by a large number of different post-translational modifications of amino acid residues, which often occur within the histone tail domains. They thus can either bind proteins or regulate the compaction of the nucleosomal fiber, and through both mechanisms they influence the accessibility of the underlying DNA sequence. Of these modifications, lysine acetylation and lysine methylation are perhaps the two best understood, and both have been shown to affect chromatin structure and accessibility. The acetylation of lysines reduces the positive charge of the lysine residue, and results in chromatin with a less compact structure. This generally facilitates access to different macromolecular machineries (Bannister and Kouzarides, 2011). As a result, multiple types of histone acetylation are enriched at gene promoters, where they facilitate the access of transcription factors and recruit chromatin remodelers (Wang et al., 2008). Acetyl marks are set by histone acetyl transferases (HAT) and removed by histone deacetylases (HDAC) (Bannister and Kouzarides, 2011). Methylation of histones is not thought to directly impact the folding of the nucleosomal array, but rather provides a binding platform for various factors that recognize mono-, di- or tri-methylated states of specific lysines. There are a large number of methyl binding motifs, the most famous of which are the chromodomains,

Tudor domains, or PhD fingers, which are found in proteins known as “readers” of the methylation marks. As an example, tri-methylation of lysine 9 in H3 (H3K9me3) recruits HP1, a chromodomain protein, the binding of which results in chromatin compaction and facilitation of heterochromatin formation (Bannister et al., 2001; Lachner et al., 2001).

Different types of chromatin are non-homogeneously distributed in the nucleus

The different histone modifications, the ligands they attract, as well as the presence of histone variants create chromatin that is compacted to different degrees. Very early it was observed by microscopic techniques that chromosomal domains having different degrees of compaction were non-homogenously distributed within the nucleus. Uranyl acetate staining coupled with electron microscopy, revealed the presence of high and low density chromatin regions. Interestingly, these high and low density regions were found in some cases to identify distinct regions of the nucleus, such as the nuclear envelope or perinucleolar sites (Belmont and Bruce, 1994; Dehghani et al., 2005; Monneron and Bernhard, 1969; Olins and Olins, 1974). The dense staining regions were classically called hetereochromatin, whereas lighter staining parts contained less compacted chromatin and was called euchromatin. These descriptions have long been thought to be functionally relevant as heterochromatin is typically transcriptionally silent and euchromatin transcriptionally active (Rouquette et al., 2009; Visser et al., 2000).

Recent studies argue that this model of two different types of chromatin may be too simplistic. Studies in *Drosophila* and human cells that analysed combinations of chromatin binding proteins as well as histone modifications defined at least 2-3 subclasses of euchromatin and of heterochromatin (Filion et al., 2010; Kharchenko et al., 2008; Ram et al., 2011). They are differentiated by distinct sets of protein ligands, such as polycomb group proteins, histone acetylases or histone H1 in combination with different histone modifications such as H3K4me2 or H3K9me2 (Filion et al., 2010). This suggests a more subtle role of chromatin compaction in the definition of chromatin types, and even the contribution of chromatin compaction to repression remains a topic of debate (Bell et al., 2011; van Steensel, 2011).

In summary we can say that even though DNA is highly compacted within the nucleus, it is well organised and accessibility is guaranteed by molecular machines like chromatin remodelers. In *Drosophila* the combination of post-translational modifications and specific sets of DNA-binding proteins, led to a robust identification of five different types of chromatin.

Heterochromatic domains tend to cluster at the nuclear lamina

From the above mentioned electron microscopy studies, a functional, non-homogenous, subnuclear organisation of chromatin within the nucleus was proposed with active and

inactive genome segments clustered into functional domains, where heterochromatic domains often cluster along the nuclear envelope, except immediately under nuclear pores (Akhtar and Gasser, 2007). Evidence for this phenomenon was shown in different organisms such as *Drosophila*, *C. elegans* and human, but significant differences were observed among different cell types within one species. Croft and colleagues revealed that the gene-poor, rather heterochromatic, chromosome 18 was mainly found at the periphery and at the edge of the nucleolus in human lymphocytes, whereas the gene-rich, euchromatic chromosome 19 was localized in the nucleoplasm (Croft et al., 1999). Also in rodents, cattle and birds, gene-poor chromosomes are often found close to the nuclear periphery whereas gene-rich ones tend to locate in the nuclear interior (for review see (Cremer and Cremer, 2010)).

Using a fusion of lamin with the *E. coli* DNA adenine methyltransferase (Dam) to identify transient and stable DNA-lamin interactions via DNA methylation (DamID) *in vivo*, the group of Bas van Steensel identified about 500 genes in the *Drosophila melanogaster* Kc cell line that interact with the nuclear lamina (Pickersgill et al., 2006). Applying the same technique in cultured human lung fibroblasts, the same group published two years later another study, where they identified lamina-associated domains (LADs). The mean gene density within these LADs is about half the density outside the LADs and genes within LADs are generally 5- to 10-fold less active compared to genes outside LADs (Guelen et al., 2008). More recently using Chromatin Immuno-Precipitation (ChIP) followed by analysis on microarrays, it could be shown in *C. elegans,* that chromosome regions interacting with LEM-2 (LAP2, Emerin, Man-1), a transmembrane protein, have a relatively poor content of genes (Ikegami et al., 2010). Taken together these studies support the hypothesis that gene content and transcriptional activity are quite low close to the nuclear lamina and that the nuclear lamina could be important for the nuclear organisation by tethering parts of the chromatin to the nuclear envelope.

Tethering genes to the nuclear lamina often results in repression

In agreement with the observation that inactive, silent loci are found in the vicinity of the nuclear envelope, several studies targeted a locus to the nuclear lamina and investigated the effect. In yeast, the mating type locus *HMR*, deprived of an effective silencer, was targeted to the periphery, which resulted in silencing (Andrulis et al., 1998). This was later shown to be due to the tethered locus being close to clusters of telomeres, which are bound to the nuclear envelope and sequester the silencing factors (Taddei et al., 2009). In mouse fibroblasts the recruitment of some genes to the inner nuclear membrane can result in their transcriptional down-regulation (Reddy et al., 2008). Similarly, artificial tethering of human chromosomes to the nuclear lamina of cultured cells resulted in the repression of some but not all genes (Finlan et al., 2008). A study performed in mammalian cells showed a similar transcription activity of a locus independent of whether or not it was targeted to the nuclear periphery (Kumaran and Spector, 2008). In summary, this indicates that association with the nuclear periphery causes repression of some but not all genetic loci, with the variability most likely depending on the nature of the promoter.

Developmenally regulated genes relocate to the nuclear lumen or get sequestered at the nuclear lamina depending on their expression status

In contrast to the nuclear periphery, where primarily inactive genes are localized, we often find active genes in the lumen of the nucleus, particularly in differentiated cells. In a study performed in human, mouse and rabbit lymphocytes the inactive β-globin gene was localised at the nuclear periphery, whereas the ubiquitously expressed and thus active α-globin localised in the nuclear lumen (Brown et al., 2001). In several organisms developmentally regulated genes move from the nuclear periphery, where they are located in their inactive state, towards the nuclear interior when they get activated. This was observed in human lymphocytes using Fluorescence In Situ Hybridisation (FISH) where immunoglobulin loci are preferentially localised at the nuclear periphery in hematopoietic progenitors and pro-T cells in which the genes are silent, whereas they are often located in the nuclear centre in pro-B nuclei where the genes are active (Kosak et al., 2002). In mice several loci shift towards the nuclear interior upon activation: the GFAP (glial fibrillary acidic protein) gene during astrocyte differentiation, the β-globin locus during erythroid development, the C-maf (MusculoAponeurotic Fibrosarcoma oncogene homolog) locus during T-cell development, the MyoD (Myogenic Differentiation) locus during myoblast development and the Mash1 locus during neural development. In humans, the CFTR (Cystic Fibrosis Transmembrane Conductance Regulator) locus moves inwards in cells where it is expressed (for review see (Egecioglu and Brickner, 2011)).

Two studies in *C. elegans* showed that for developmentally regulated genes are randomly distributed in embryonic cells that are undifferentiated and uncommitted. In differentiated cells, localisation of muscle- and gut-specific transgenes within the nucleus is dependent on their activity: in their inactive state the loci are sequestered to the nuclear lamina, whereas they are enriched in the nuclear lumen in their active state (Meister et al., 2010; Towbin et al., 2010).

Interestingly it was shown that the inner nuclear envelope needs to be intact for efficient gene silencing. In somatic cells of Drosophila, ablation of $LamDm_0$ resulted not only in detachment of testes-specific clusters from the nuclear envelope but also to their selective transcriptional up-regulation (Shevelyov et al., 2009). Also in animals depleted for the *C. elegans* lamin homologue LMN-1 or associated proteins, transcription of promoters on transgenic, heterochromatic arrays is strongly up-regulated (Towbin et al., 2010). Similarly in mammalian cells lacking lamins or other nuclear lamina components genes expression was miss-regulated. (Frock et al., 2006; Vergnes et al., 2004).

In a genome wide study performed in three consecutive development stages of mouse cells – pluripotent embryonic stem cells (ESC), multipotent neuronal precursor cells (NPC) and terminally differentiated astrocytes (AC) – Peric-Hupkes and colleagues analysed the interaction of loci with the nuclear lamina by applying DAM-ID. In agreement with the studies mentioned above, genes that were activated from one cell

type to the other moved away from the nuclear lamina. The group made two other observations: if a gene is inactivated from one cell type to the next, the locus is sequestered to the nuclear lamina, similar to what was found in *C. elegans* upon cell differentiation. The other interesting finding was, that genes expressed in AC cells, will already move away from the nuclear periphery in NPC cells without increased transcription, most probably in order to be already prepared for activation (Peric-Hupkes et al., 2010).

This shows in summary that genetic loci are spatially differently organised in their inactive compared to their active state and that a movement from the nuclear lamina to the nuclear lumen and vice versa occurs in several species.

Chromatin within the nucleus is highly mobile

A direct prediction from this observation is that some genes must, upon activation, get relocated from one position to another. Chromatin is indeed highly dynamic inside the nucleus, although usually within a restricted volume, that ranges from 30% to less than 1% of the nuclear volume, depending on the species analysed. Centromeric chromatin in yeast is constantly moving in a near-random walk with a specific chromosome being confined to a very small nuclear subregion (Marshall et al., 1997). It was suggested that microtubules play an important role in the confinement of centromeres to sites near the spindle pole body in yeast, since depolymerisation of microtubules by the chemical compound nocodazole increased movement and displaced tagged centromere towards the nuclear center (Marshall et al., 1997) (Bystricky et al., 2004; Heun et al., 2001). The tethering by microtubules is true for yeast centromeres, but not for tagged loci found along the chromosomal arms. Non-centromeric chromatin in yeast also moves in a subdiffusive manner that is highly mobile, within a radius of constraint ranging from 0.4 to 0.6 m. The movement is microtubule independent and moves on average about 0.2 µm in a 10 second interval with occasional larger displacements bigger than 0.5 µm (Heun et al., 2001). Both telomeric and centromeric chromatin is much more restrained than internal chromosomal regions due to their attachment to the nuclear envelope (Heun et al., 2001).

Splicing speckles are a binding platform for active genes in mammalian cells

Mammalian cells have additional subnuclear domains, called nuclear speckles. Some active genes cluster to these dynamic sub-compartments of the nucleus that are enriched in pre-mRNA splicing factors. Using immunofluorescence microscopy, 20-50 irregularly shaped structures that vary in size are visible (Spector and Lamond, 2011). Based on the fact that gene-rich stretches of chromatin are more often found at nuclear speckles than gene-poor ones, Shopland and collegues suggested that the periphery of the speckles might create a euchromatic environment (Shopland et al., 2003). Recently it has been shown that in mammalian cells a transgene containing the *Hsp70* promoter

was preferentially associated with nuclear speckles upon heat induction (Hu et al., 2010).

Nuclear pores serve as a platform for active genes

In flies and both fission and budding yeasts, several stress-inducible genes were observed to interact with the nuclear periphery, where they interact with the nuclear pore complex. This phenomenon is understood best in budding yeast, where systematic studies showed hundreds of active genes interacting with the nuclear pore complex (Casolari et al., 2005; Casolari et al., 2004). In studies investigating specific genes that are active at the nuclear pore complex, different genes in yeast were found that are activated by growth in low sugar media or upon heat shock (Brickner and Walter, 2004; Cabal et al., 2006; Casolari et al., 2005; Dieppois et al., 2006; Schmid et al., 2006; Taddei et al., 2006).

Some of the studies mentioned above tested the necessity of different parts of a gene for peripheral localisation and active transcription. For the yeast subtelomeric gene *HXK1*, the 3'UTR is necessary, whereas for the internal gene *GAL2*, the 3'UTR is dispensable (Dieppois et al., 2006; Taddei et al., 2006). Also the coding sequence of *GAL2* is not required for pore association, but the promoter is. This was also shown for *GAL4* where the promoter with an intact TATA box is required for interaction with the nuclear pore complex (Schmid et al., 2006). For *INO1*, the group of Jason Brickner identified two gene recruitment sequences (GRS I and GRS II) that are required for targeting to the nuclear periphery and suggest that they function as a "DNA zip code". Acting redundantly, only the loss of both GRS I and GRS II blocks the targeting of *INO1* to the nuclear periphery, but not one alone.

The multi-protein complex SAGA is crucial for stress-induced gene activation

As mentioned above, many stress-inducible genes have been shown to interact with the nuclear pore complex. About 10% of yeast genes belong to this category and their activation is largely dependent on the transcriptional coactivator SAGA (Spt-Ada-Gcn-Acetyltransferase). This multi-protein complex is composed of 21 different proteins and has a size of about 1.8 MDa (Samara and Wolberger, 2011). It has two catalytic activities, the histone acetyltransferase activity (HAT) and the histone deubiquitination activity (Daniel and Grant, 2007; Daniel et al., 2004; Garcia-Oliver et al., 2011; Grant et al., 1997; Sterner et al., 1999). Both provoke a shift from compact and inactive chromatin to open and active chromatin. SAGA has four different modules: the deubiquination module (DUBm), the histone acetyl transferase (HAT/core) module, the TAF (TATA-binding protein associated factors) module and the SPT (suppressor of Ty) module (Garcia-Oliver et al., 2011). While the HAT recognises methylated H3K4, where SAGA will bind, the TAF module helps to recruit the basal transcription machinery and the SPT module helps in the assembly of the pre-initiation complex (Garcia-Oliver et al., 2011). By deubiquiting monoubiquinated histone H2B the Ctk1 kinase is recruited, which

phosphorylates the C-terminal domain of RNA Pol II resulting in transcriptional elongation (Wyce et al., 2007). All these activities originally described for the yeast SAGA complex are largely conserved in the *Drosophila* and human SAGA (Garcia-Oliver et al., 2011).

The TREX / AMEX complex links transcription and mRNA export

Located at the inner face of the nuclear pore complex is another multi-protein complex called TREX-2 in yeast and plants (which stands for TRanscription and Export) or AMEX in *Drosophila* and mammals, which functionally links transcription and mRNA export. In yeast it is thought that the interaction between SAGA and TREX-2 mediates gene recruitment to the nuclear pore complex. In *Drosophila* it was described to promote the association of the TREX/THO complex with nascent RNA and in human AMEX facilitates the mRNA movement from transcriptional foci to the nuclear periphery (Garcia-Oliver et al., 2011).

Sus1, a protein present in the SAGA and TREX complex, serves as linker between active genes and the nuclear pore complex

On a molecular level, Sus1, a protein present both in SAGA and the TREX-2 complex was described to be implicated in pore association and / or transcriptional activity. Different groups described the dependency of yeast *GAL* gene induction on Sus1, namely *GAL1, GAL7* and *GAL10* (Cabal et al., 2006; Dieppois et al., 2006; Rodriguez-Navarro et al., 2004). Also in yeast, Brickner and Walter found that the transcriptional activity of *INO1*, another gene shown to shift to nuclear pores upon induction, is dependent on Sus1. In a similar manner, the peripheral anchoring of *Hsp70* in *Drosophila* S2 cells requires E(y)2/ENY-2, the homologue of Sus1, which colocalises weakly with nucleoporins and Xmas2, the homologue of the TREX-2 subunit Sac3 (Kurshakova et al., 2007). Sus1 binds directly the nuclear pore protein Nup1 and anchors TREX-2 to the NPC. This mediates gene recruitment upon transcriptional activation and appears to facilitate mRNA processing (Garcia-Oliver et al., 2011). This suggests, but does not prove that pore association is linked to mRNA processing and/or export. It is unclear which of the many steps in mRNA maturation might be regulated by the NPC during gene induction.

Interaction with pores is essential for full transcriptional activity of some genes

The recruitment to the periphery of stress-inducible genes raises the question about the functional significance of this behaviour. This has been investigated in yeast but remains controversial. By tethering *INO1* to the nuclear periphery, transcription is promoted in the absence of its antagonizer (Brickner and Walter, 2004). Also for *HXK1* interaction with the nuclear pore is essential for maximal transcriptional activity (Taddei et al., 2006). In contrast, in two other studies it was observed that for *GAL* genes as well as for *HSP104*, transcription occurs away from the nuclear pore complex as efficiently as when the genes interact with pores (Cabal et al., 2006; Dieppois et al., 2006). In most cases,

total mRNA levels are quanitified, thus it is not elongation efficiency but total accumulation of mRNA that was scored. The discrepancies among these studies may reflect true differences in transcriptional control, but may also reflect the different experimental tools used to release the genes from the pore. It is likely that specific aspects of transcriptional regulation, including processing, packaging and export rates of the mRNA, might influence the different impact of pore association or pore release, of the above mentioned genes. In a study of the yeast Arp6 protein, a component of the SWR1 remodeler, it was shown that SWR1 controlled genes associate with the nuclear pore in an Arp6-dependent manner. In the case of ribosomal protein genes, most genes actually showed higher rates of transcription when they were not held near the nuclear pore (Yoshida et al., 2010). In metazoans functional significance of pore association is poorly understood, even though the well-studied *Hsp70* locus in flies also shows a reduction in mRNA level upon release from pores using RNAi (Kurshakova et al., 2007).

Three hypotheses try to explain the functional relevance of pore proximal activation of stress-inducible genes

Even though there are many different explanations for why genes might interact with the nuclear pore complex upon activation, there are three hypotheses that I would like to address.

Already in 1985, Günther Blobel hypothesized that the proximity to nuclear pores would spatially facilitate mRNA export in general, but also its delivery to distinct cytoplasmic domains in asymmetric cells (Blobel, 1985). Another explanation that arose more recently is the idea that the proximity of genes to nuclear pores establishes an epigenetic state, which confers to transcriptional memory, facilitating reactivation of stress-inducible genes. In yeast it was shown that after a first recruitment to the periphery upon change of medium, *INO1* and *GAL1* remain there for several generations and can be reactivated much more rapidly than long term repressed forms of these genes localised in the nuclear centre (Brickner et al., 2007). Similarly Tan-Wong and colleagues found that *HXK1* forms a so called “memory gene loop” between the promoter and its 3’ end. In this paper it was predicted that within this loop transcription factors are retained and help a faster recruitment of Pol II to restart transcription (Tan-Wong et al., 2009).

A third hypothesis for peripheral localisation of heat-inducible genes is the fact that some components of the RNAi machinery are also preferentially localised at pores. In *S. pombe* and human, Dicer interacts with nuclear pores (Ando et al., 2011; Emmerth et al., 2010) and in addition the loss of Dicer caused an increase in expression levels of different heat shock genes in a non-heat shock condition in *S. pombe* (Woolcock et al., 2012). This indicates that Dicer is important to keep the transcription rate of heat-inducible genes at an appropriate level. Similarly, in *Drosophila* Cernilogar and colleagues found that a depletion of *DCR2* and *AGO2*, both components of the RNAi machinery as well, resulted in an increased expression prior to but not during heat stress at the *Hsp70* and *Hsp68* (Cernilogar et al., 2011). Taken together this implies that stress-inducible genes might localise to nuclear pores because components of the RNAi

machinery, such as Dicer, can regulate the expression level of heat-inducible genes and fine tune their expression levels.

Heat activation and its molecular details

Environmental insults have a strong impact on all kinds of creatures. Selective pressure drives the retention of genes that ensure survival under extreme conditions, and these are transmitted from one generation to the next. The class of genes responsible for an adequate reaction of cells to environmental changes was termed stress-inducible genes. An example for these genes is the group of evolutionary ancient and well conserved heat shock genes (Robert, 2003). Not only exposure to elevated temperatures but also to different kinds of stress such as hypoxia, heavy metals, radiation, calcium increase or glucose deprivation cause the activation of heat shock genes (Anckar and Sistonen, 2011). In higher eukaryotes even microbial infections and cancer can cause their activation (Robert, 2003). In general, heat shock proteins (HSP) protect cells and organisms from severe damage by preventing protein aggregates and thus lead to a higher thermotolerance (Robert, 2003; Schoffl et al., 1998).

Based on structural homologies, the well conserved Hsps are grouped in 3 classes: *Hsp83*, *Hsp70* / *Hsp68* and several small Hsps (Robert, 2003). Heat shock proteins were discovered as early as in 1962, when Ferruccio Ritossa worked with salivary glands of *Drosophila bushii* (Ritossa, 1996). Salivary glands of many dipteran flies contain polytene chromosomes, built by several rounds of DNA replication without cell division. Polytene chromosomes show a light and dark banding pattern specific to different chromosomes. By the formation of so called puffs, regions that are swollen and appear to have a looser structure, it is possible to see current transcription. When Ritossa looked at salivary glands that had been exposed to an elevated temperature for about 30 minutes, he observed a changed pattern in the polytene chromosomes that correlated with a high level of RNA synthesis as shown by RNase treatment. After about an hour at normal temperature (25°C) the puffs recede (Ritossa, 1996).

Paused RNA polymerase II is a common feature of fast inducing genes

Changes in the environment or different kinds of insults force an organism to react and activate genes that help to survive. A short reaction time is often crucial for survival, thus genes responding to an environmental insult need to be ready for transcription in a short time.

A prerequisite for fast gene activation is the presence of the transcription machinery. On many stress-inducible genes, RNA Pol II is bound to the promoter region in a poised state. As early as in 1985, the presence of a so called paused RNA Pol II was detected in the promoter region of the uninduced *Drosophila Hsp70* heat shock locus (Gilmour and Lis, 1985). In addition to fast induction, the presence of paused Pol II helps to keep the gene in a more accessible state, so that further Pol II complexes can bind easier (Gilchrist

et al., 2010). Another advantage for efficient transcription might be that the Pol II complexes reassociate with the same promoter instead of being released, as was shown by observing tagged Pol II complexes (Yao et al., 2007).

More recently studies in *Drosophila* embryos, mammalian embryonic stem cells and in lung fibroblasts revealed that paused Pol II is not only present at stress-inducible genes, but is also present at promoters of developmentally regulated genes. It has been suggested that paused Pol II allows a rapid and efficient activation at a very precise development stage (for review see (Levine, 2011)).

The transcription factor HSF1 is essential for activation of heat inducible genes

Another highly conserved key player in the heat shock response is the well characterized heat shock factor 1 (HSF1). This transcription factor is constitutively expressed in most tissues and cell types (Anckar and Sistonen, 2011).

The protein is composed of four different types of domains (Anckar and Sistonen, 2011). At the N-terminus we find the DNA-binding domain that consists of a looped helix-turn-helix motive. Unlike other, similar domains, it does not interact directly with DNA, but stabilizes the connection between DNA and HSF-1 by protein-protein interactions (Littlefield and Nelson, 1999; Vuister et al., 1994). Next to the DNA-binding domain there is an oligomerization domain that is protected by another domain closer to the C-terminus of the protein (Peteranderl and Nelson, 1992; Peteranderl et al., 1999). The trans-activating domain is localised in the centre of the protein and is important for transcriptional activation (Pattaramanon et al., 2007). At the C-terminus is a regulatory domain that interacts with the trans-activating domain in the monomeric form to prevent activation (Anckar and Sistonen, 2011; Green et al., 1995).

In non-heat shock conditions the protein is present in a monomeric, inert form. Upon heat induction it trimerizes and binds in a cooperative manner to Heat Shock Element (HSE) sites on the promoter (Xiao et al., 1991). The sequence of the HSE sites is well conserved from yeast to human and is often found in promoter regions of heat-inducible genes (Fernandes et al., 1994; Guertin and Lis, 2010; Trinklein et al., 2004). In *C. elegans* an additional binding site, termed the Heat Shock Associated Site (HSAS) was found in a bioinformatical screen. Looking at GFP expression from a promoter-GFP fusion indicated that not only HSE but also HSAS plays an important role in heat induction (GuhaThakurta et al., 2002).

Molecular mechanisms occurring on the *Hsp70* promoter upon induction

The promoter-associated changes that correlate with *Hsp70* activation are very well characterized, particularly in *Drosophila*. As mentioned above, Pol II is already present in the uninduced state (Nechaev and Adelman, 2011). In this paused state Pol II is stabilized by DRB (Dichloro-1-β-D-ribofuranosylbenzimidazole) sensitivity inducing factor (DSIF) and the negative elongation factor (NELF)(Levine, 2011). Both bind to the

short RNA of about 25 nucleotides produced by the paused polymerase (Levine, 2011; Rougvie and Lis, 1988). In its paused state Pol II is phosphorylated at serine 5 of the C-terminal domain (Nechaev and Adelman, 2011). Upon activation, the transcription factor HSF1 trimerizes and binds in a cooperative manner to HSE sites. This leads to the recruitment of the P-TEFb (Positive Elongating Factor b), a serine/threonine kinase, which phosphorylates serine 2 in the C-terminal domain of the largest subunit of Pol II as well as DSIF and NELF. This causes the release of DSIF and NELF and allows Pol II to productively transcribe the gene (Fuda et al., 2009). Activation leads to a rapid eviction of nucleosomes after about 30s in a transcription-dependent manner (Petesch and Lis, 2008). It is thought that the activation of PARP (poly (ADP-)ribose polymerase) and its production of PAR molecules result in a decondensation of DNA, which might facilitate the moving of Pol II through nucleosomes (Guertin et al., 2010).

Since survival of environmental insults, in this case elevated temperatures, is crucial for an organism, the response to it is well organised, well orchestrated and also quite well conserved. Many research groups have investigated different aspects of heat shock response and we tried to address these aspects in *C. elegans*, an organism in which it was not yet well explored, and also tried to shed light on new aspects.

Thesis overview

This thesis comprises two parts with experimental data. In Chapter 2, I characterise the small heat shock gene *hsp-16.2* of the nematode *C. elegans*. Looking at embryos, I find that the locus has a preference for peripheral localisation in its uniduced as well as in its induced state. This is not only true for the endogenous locus, but also for two different kinds of promoter-transcripts integrated ectopically in the genome. Using high resolution microscopy and Chromatin Immuno-Precipitation (ChIP) we find that at the periphery, the *hsp-16.2* promoter is preferentially interacting with the nuclear pore complex.

On a molecular level, we find that two specific sequences in the promoter, the HSE sites and the HSAS site are relevant for peripheral localisation. Also Pol II plays an important role in the tethering at the periphery since we find that in Pol II temperature sensitive mutants the interaction with the nuclear periphery is abandoned and *hsp-16.2* is randomly distributed within the nucleus.

Testing ENY-2, the homologue of yeast Sus1, revealed that it is important for peripheral localisation also in *C. elegans* embryos. This protein is present in the SAGA histone acetylation complex as well as in TREX, a complex linking transcription and mRNA export and is known to interact with the nuclear pore complex.

In Chapter 3, I show preliminary data that indicate a possible dependency of the peripheral localisation of *hsp-16.2* on components of the RNAi machinery as well as on RSY-1, a factor that might be involved in splicing. These results indicate that disruption of different components of the RNAi machinery results in the loss of peripheral

enrichment of *hsp-16.2* in the inactive as well as in the active state. Disruption of the *rsy-1* gene only abolishes peripheral localisation after heat induction, which might be due to the fact that only a transcript that needs to be processed makes the link via RSY-1 to the nuclear pore.

Taken together, this thesis sheds light on the mechanisms of gene activation at the nuclear periphery and reveals that not only in yeast and flies, but also in the worm *C. elegans* nuclear pores build a platform for active transcription.

References

Adam, M., F. Robert, M. Larochelle, and L. Gaudreau. 2001. H2A.Z is required for global chromatin integrity and for recruitment of RNA polymerase II under specific conditions. *Mol Cell Biol*. 21:6270-6279.

Akhtar, A., and S.M. Gasser. 2007. The nuclear envelope and transcriptional control. *Nat Rev Genet*. 8:507-517.

Anckar, J., and L. Sistonen. 2011. Regulation of HSF1 function in the heat stress response: implications in aging and disease. *Annu Rev Biochem*. 80:1089-1115.

Ando, Y., Y. Tomaru, A. Morinaga, A.M. Burroughs, H. Kawaji, A. Kubosaki, R. Kimura, M. Tagata, Y. Ino, H. Hirano, J. Chiba, H. Suzuki, P. Carninci, and Y. Hayashizaki. 2011. Nuclear pore complex protein mediated nuclear localization of dicer protein in human cells. *PLoS One*. 6:e23385.

Andrulis, E.D., A.M. Neiman, D.C. Zappulla, and R. Sternglanz. 1998. Perinuclear localization of chromatin facilitates transcriptional silencing. *Nature*. 394:592-595.

Bannister, A.J., and T. Kouzarides. 2011. Regulation of chromatin by histone modifications. *Cell Res*. 21:381-395.

Bannister, A.J., P. Zegerman, J.F. Partridge, E.A. Miska, J.O. Thomas, R.C. Allshire, and T. Kouzarides. 2001. Selective recognition of methylated lysine 9 on histone H3 by the HP1 chromo domain. *Nature*. 410:120-124.

Beck, M., F. Forster, M. Ecke, J.M. Plitzko, F. Melchior, G. Gerisch, W. Baumeister, and O. Medalia. 2004. Nuclear pore complex structure and dynamics revealed by cryoelectron tomography. *Science*. 306:1387-1390.

Bell, O., V.K. Tiwari, N.H. Thoma, and D. Schubeler. 2011. Determinants and dynamics of genome accessibility. *Nat Rev Genet*. 12:554-564.

Belmont, A.S., and K. Bruce. 1994. Visualization of G1 chromosomes: a folded, twisted, supercoiled chromonema model of interphase chromatid structure. *J Cell Biol*. 127:287-302.

Blobel, G. 1985. Gene gating: a hypothesis. *Proc Natl Acad Sci U S A*. 82:8527-8529.

Brickner, D.G., I. Cajigas, Y. Fondufe-Mittendorf, S. Ahmed, P.C. Lee, J. Widom, and J.H. Brickner. 2007. H2A.Z-mediated localization of genes at the nuclear periphery confers epigenetic memory of previous transcriptional state. *PLoS Biol*. 5:e81.

Brickner, J.H., and P. Walter. 2004. Gene recruitment of the activated INO1 locus to the nuclear membrane. *PLoS Biol*. 2:e342.

Brown, K.E., S. Amoils, J.M. Horn, V.J. Buckle, D.R. Higgs, M. Merkenschlager, and A.G. Fisher. 2001. Expression of alpha- and beta-globin genes occurs within different nuclear domains in haemopoietic cells. *Nat Cell Biol*. 3:602-606.

Bystricky, K., P. Heun, L. Gehlen, J. Langowski, and S.M. Gasser. 2004. Long-range compaction and flexibility of interphase chromatin in budding yeast analyzed by high-resolution imaging techniques. *Proc Natl Acad Sci U S A*. 101:16495-16500.

Cabal, G.G., A. Genovesio, S. Rodriguez-Navarro, C. Zimmer, O. Gadal, A. Lesne, H. Buc, F. Feuerbach-Fournier, J.C. Olivo-Marin, E.C. Hurt, and U. Nehrbass. 2006. SAGA interacting factors confine sub-diffusion of transcribed genes to the nuclear envelope. *Nature*. 441:770-773.

Capelson, M., Y. Liang, R. Schulte, W. Mair, U. Wagner, and M.W. Hetzer. 2010. Chromatin-bound nuclear pore components regulate gene expression in higher eukaryotes. *Cell*. 140:372-383.

Casolari, J.M., C.R. Brown, D.A. Drubin, O.J. Rando, and P.A. Silver. 2005. Developmentally induced changes in transcriptional program alter spatial organization across chromosomes. *Genes Dev*. 19:1188-1198.

Casolari, J.M., C.R. Brown, S. Komili, J. West, H. Hieronymus, and P.A. Silver. 2004. Genome-wide localization of the nuclear transport machinery couples transcriptional status and nuclear organization. *Cell*. 117:427-439.

Cernilogar, F.M., M.C. Onorati, G.O. Kothe, A.M. Burroughs, K.M. Parsi, A. Breiling, F. Lo Sardo, A. Saxena, K. Miyoshi, H. Siomi, M.C. Siomi, P. Carninci, D.S. Gilmour, D.F. Corona, and V. Orlando. 2011. Chromatin-associated RNA interference components contribute to transcriptional regulation in Drosophila. *Nature*. 480:391-395.

Chambers, A.L., and J.A. Downs. 2012. The RSC and INO80 chromatin-remodeling complexes in DNA double-strand break repair. *Prog Mol Biol Transl Sci*. 110:229-261.

Clapier, C.R., and B.R. Cairns. 2009. The biology of chromatin remodeling complexes. *Annu Rev Biochem*. 78:273-304.

Cremer, T., and M. Cremer. 2010. Chromosome territories. *Cold Spring Harb Perspect Biol*. 2:a003889.

Croft, J.A., J.M. Bridger, S. Boyle, P. Perry, P. Teague, and W.A. Bickmore. 1999. Differences in the localization and morphology of chromosomes in the human nucleus. *J Cell Biol*. 145:1119-1131.

Dange, T., D. Grunwald, A. Grunwald, R. Peters, and U. Kubitscheck. 2008. Autonomy and robustness of translocation through the nuclear pore complex: a single-molecule study. *J Cell Biol*. 183:77-86.

Daniel, J.A., and P.A. Grant. 2007. Multi-tasking on chromatin with the SAGA coactivator complexes. *Mutat Res*. 618:135-148.

Daniel, J.A., M.S. Torok, Z.W. Sun, D. Schieltz, C.D. Allis, J.R. Yates, 3rd, and P.A. Grant. 2004. Deubiquitination of histone H2B by a yeast acetyltransferase complex regulates transcription. *J Biol Chem*. 279:1867-1871.

Dechat, T., S.A. Adam, P. Taimen, T. Shimi, and R.D. Goldman. 2010. Nuclear lamins. *Cold Spring Harb Perspect Biol*. 2:a000547.

Dehghani, H., G. Dellaire, and D.P. Bazett-Jones. 2005. Organization of chromatin in the interphase mammalian cell. *Micron*. 36:95-108.

Dieppois, G., N. Iglesias, and F. Stutz. 2006. Cotranscriptional recruitment to the mRNA export receptor Mex67p contributes to nuclear pore anchoring of activated genes. *Mol Cell Biol*. 26:7858-7870.

Egecioglu, D., and J.H. Brickner. 2011. Gene positioning and expression. *Curr Opin Cell Biol*. 23:338-345.

Emmerth, S., H. Schober, D. Gaidatzis, T. Roloff, K. Jacobeit, and M. Buhler. 2010. Nuclear retention of fission yeast dicer is a prerequisite for RNAi-mediated heterochromatin assembly. *Dev Cell*. 18:102-113.

Fahrenkrog, B., J. Koser, and U. Aebi. 2004. The nuclear pore complex: a jack of all trades? *Trends Biochem Sci*. 29:175-182.

Fernandes, M., H. Xiao, and J.T. Lis. 1994. Fine structure analyses of the Drosophila and Saccharomyces heat shock factor--heat shock element interactions. *Nucleic acids research*. 22:167-173.

Filion, G.J., J.G. van Bemmel, U. Braunschweig, W. Talhout, J. Kind, L.D. Ward, W. Brugman, I.J. de Castro, R.M. Kerkhoven, H.J. Bussemaker, and B. van Steensel. 2010. Systematic Protein Location Mapping Reveals Five Principal Chromatin Types in Drosophila Cells. *Cell*.

Finlan, L.E., D. Sproul, I. Thomson, S. Boyle, E. Kerr, P. Perry, B. Ylstra, J.R. Chubb, and W.A. Bickmore. 2008. Recruitment to the nuclear periphery can alter expression of genes in human cells. *PLoS Genet*. 4:e1000039.

Florescu, A.M., H. Schiessel, and R. Blossey. 2012. Kinetic Control of Nucleosome Displacement by ISWI/ACF Chromatin Remodelers. *Phys Rev Lett*. 109:118103.

Frock, R.L., B.A. Kudlow, A.M. Evans, S.A. Jameson, S.D. Hauschka, and B.K. Kennedy. 2006. Lamin A/C and emerin are critical for skeletal muscle satellite cell differentiation. *Genes Dev*. 20:486-500.

Fuda, N.J., M.B. Ardehali, and J.T. Lis. 2009. Defining mechanisms that regulate RNA polymerase II transcription in vivo. *Nature*. 461:186-192.

Garcia-Oliver, E., V. Garcia-Molinero, and S. Rodriguez-Navarro. 2011. mRNA export and gene expression: The SAGA-TREX-2 connection. *Biochim Biophys Acta*.

Gilchrist, D.A., G. Dos Santos, D.C. Fargo, B. Xie, Y. Gao, L. Li, and K. Adelman. 2010. Pausing of RNA polymerase II disrupts DNA-specified nucleosome organization to enable precise gene regulation. *Cell*. 143:540-551.

Gilmour, D.S., and J.T. Lis. 1985. In vivo interactions of RNA polymerase II with genes of Drosophila melanogaster. *Mol Cell Biol*. 5:2009-2018.

Grant, P.A., L. Duggan, J. Cote, S.M. Roberts, J.E. Brownell, R. Candau, R. Ohba, T. Owen-Hughes, C.D. Allis, F. Winston, S.L. Berger, and J.L. Workman. 1997. Yeast Gcn5 functions in two multisubunit complexes to acetylate nucleosomal histones: characterization of an Ada complex and the SAGA (Spt/Ada) complex. *Genes Dev*. 11:1640-1650.

Green, M., T.J. Schuetz, E.K. Sullivan, and R.E. Kingston. 1995. A heat shock-responsive domain of human HSF1 that regulates transcription activation domain function. *Mol Cell Biol*. 15:3354-3362.

Grunwald, D., and R.H. Singer. 2010. In vivo imaging of labelled endogenous beta-actin mRNA during nucleocytoplasmic transport. *Nature*. 467:604-607.

Grunwald, D., and R.H. Singer. 2012. Multiscale dynamics in nucleocytoplasmic transport. *Curr Opin Cell Biol*. 24:100-106.

Guelen, L., L. Pagie, E. Brasset, W. Meuleman, M.B. Faza, W. Talhout, B.H. Eussen, A. de Klein, L. Wessels, W. de Laat, and B. van Steensel. 2008. Domain organization of human chromosomes revealed by mapping of nuclear lamina interactions. *Nature*. 453:948-951.

Guertin, M.J., and J.T. Lis. 2010. Chromatin landscape dictates HSF binding to target DNA elements. *PLoS Genet*. 6.

Guertin, M.J., S.J. Petesch, K.L. Zobeck, I.M. Min, and J.T. Lis. 2010. Drosophila heat shock system as a general model to investigate transcriptional regulation. *Cold Spring Harbor symposia on quantitative biology*. 75:1-9.

GuhaThakurta, D., L. Palomar, G.D. Stormo, P. Tedesco, T.E. Johnson, D.W. Walker, G. Lithgow, S. Kim, and C.D. Link. 2002. Identification of a novel cis-regulatory element involved in the heat shock response in Caenorhabditis elegans using microarray gene expression and computational methods. *Genome Res*. 12:701-712.

Heun, P., T. Laroche, K. Shimada, P. Furrer, and S.M. Gasser. 2001. Chromosome dynamics in the yeast interphase nucleus. *Science*. 294:2181-2186.

Hu, Y., M. Plutz, and A.S. Belmont. 2010. Hsp70 gene association with nuclear speckles is Hsp70 promoter specific. *J Cell Biol*. 191:711-719.

Huve, J., R. Wesselmann, M. Kahms, and R. Peters. 2008. 4Pi microscopy of the nuclear pore complex. *Biophys J*. 95:877-885.

Ikegami, K., T. Egelhofer, S. Strome, and J.D. Lieb. 2010. Caenorhabditis elegans chromosome arms are anchored to the nuclear membrane via discontinuous association with LEM-2. *Genome Biol*. 11:R120.

Kalverda, B., and M. Fornerod. 2010. Characterization of genome-nucleoporin interactions in Drosophila links chromatin insulators to the nuclear pore complex. *Cell cycle*. 9:4812-4817.

Kharchenko, P.V., M.Y. Tolstorukov, and P.J. Park. 2008. Design and analysis of ChIP-seq experiments for DNA-binding proteins. *Nat Biotechnol*. 26:1351-1359.

Kobor, M.S., S. Venkatasubrahmanyam, M.D. Meneghini, J.W. Gin, J.L. Jennings, A.J. Link, H.D. Madhani, and J. Rine. 2004. A protein complex containing the conserved Swi2/Snf2-related ATPase Swr1p deposits histone variant H2A.Z into euchromatin. *PLoS Biol*. 2:E131.

Kosak, S.T., J.A. Skok, K.L. Medina, R. Riblet, M.M. Le Beau, A.G. Fisher, and H. Singh. 2002. Subnuclear compartmentalization of immunoglobulin loci during lymphocyte development. *Science*. 296:158-162.

Krogan, N.J., M.C. Keogh, N. Datta, C. Sawa, O.W. Ryan, H. Ding, R.A. Haw, J. Pootoolal, A. Tong, V. Canadien, D.P. Richards, X. Wu, A. Emili, T.R. Hughes, S. Buratowski, and J.F. Greenblatt. 2003. A Snf2 family ATPase complex required for recruitment of the histone H2A variant Htz1. *Mol Cell*. 12:1565-1576.

Kubitscheck, U., D. Grunwald, A. Hoekstra, D. Rohleder, T. Kues, J.P. Siebrasse, and R. Peters. 2005. Nuclear transport of single molecules: dwell times at the nuclear pore complex. *J Cell Biol*. 168:233-243.

Kumaran, R.I., and D.L. Spector. 2008. A genetic locus targeted to the nuclear periphery in living cells maintains its transcriptional competence. *J Cell Biol*. 180:51-65.

Kurshakova, M.M., A.N. Krasnov, D.V. Kopytova, Y.V. Shidlovskii, J.V. Nikolenko, E.N. Nabirochkina, D. Spehner, P. Schultz, L. Tora, and S.G. Georgieva. 2007. SAGA and a novel Drosophila export complex anchor efficient transcription and mRNA export to NPC. *Embo J*. 26:4956-4965.

Lachner, M., D. O'Carroll, S. Rea, K. Mechtler, and T. Jenuwein. 2001. Methylation of histone H3 lysine 9 creates a binding site for HP1 proteins. *Nature*. 410:116-120.

Levine, M. 2011. Paused RNA polymerase II as a developmental checkpoint. *Cell*. 145:502-511.

Lim, R.Y., and B. Fahrenkrog. 2006. The nuclear pore complex up close. *Curr Opin Cell Biol*. 18:342-347.

Littlefield, O., and H.C. Nelson. 1999. A new use for the 'wing' of the 'winged' helix-turn-helix motif in the HSF-DNA cocrystal. *Nat Struct Biol*. 6:464-470.

Luger, K., A.W. Mader, R.K. Richmond, D.F. Sargent, and T.J. Richmond. 1997. Crystal structure of the nucleosome core particle at 2.8 A resolution. *Nature*. 389:251-260.

Marshall, W.F., A. Straight, J.F. Marko, J. Swedlow, A. Dernburg, A. Belmont, A.W. Murray, D.A. Agard, and J.W. Sedat. 1997. Interphase chromosomes undergo constrained diffusional motion in living cells. *Curr Biol*. 7:930-939.

Meister, P., B.D. Towbin, B.L. Pike, A. Ponti, and S.M. Gasser. 2010. The spatial dynamics of tissue-specific promoters during C. elegans development. *Genes Dev*. 24:766-782.

Mizuguchi, G., X. Shen, J. Landry, W.H. Wu, S. Sen, and C. Wu. 2004. ATP-driven exchange of histone H2AZ variant catalyzed by SWR1 chromatin remodeling complex. *Science*. 303:343-348.

Mohrmann, L., and C.P. Verrijzer. 2005. Composition and functional specificity of SWI2/SNF2 class chromatin remodeling complexes. *Biochim Biophys Acta*. 1681:59-73.

Monneron, A., and W. Bernhard. 1969. Fine structural organization of the interphase nucleus in some mammalian cells. *J Ultrastruct Res*. 27:266-288.

Nechaev, S., and K. Adelman. 2011. Pol II waiting in the starting gates: Regulating the transition from transcription initiation into productive elongation. *Biochim Biophys Acta*. 1809:34-45.

Olins, A.L., and D.E. Olins. 1974. Spheroid chromatin units (v bodies). *Science*. 183:330-332.

Pattaramanon, N., N. Sangha, and A. Gafni. 2007. The carboxy-terminal domain of heat-shock factor 1 is largely unfolded but can be induced to collapse into a compact, partially structured state. *Biochemistry*. 46:3405-3415.

Peric-Hupkes, D., W. Meuleman, L. Pagie, S.W. Bruggeman, I. Solovei, W. Brugman, S. Graf, P. Flicek, R.M. Kerkhoven, M. van Lohuizen, M. Reinders, L. Wessels, and B. van Steensel. 2010. Molecular maps of the reorganization of genome-nuclear lamina interactions during differentiation. *Mol Cell*. 38:603-613.

Peteranderl, R., and H.C. Nelson. 1992. Trimerization of the heat shock transcription factor by a triple-stranded alpha-helical coiled-coil. *Biochemistry*. 31:12272-12276.

Peteranderl, R., M. Rabenstein, Y.K. Shin, C.W. Liu, D.E. Wemmer, D.S. King, and H.C. Nelson. 1999. Biochemical and biophysical characterization of the trimerization domain from the heat shock transcription factor. *Biochemistry*. 38:3559-3569.

Petesch, S.J., and J.T. Lis. 2008. Rapid, transcription-independent loss of nucleosomes over a large chromatin domain at Hsp70 loci. *Cell*. 134:74-84.

Pickersgill, H., B. Kalverda, E. de Wit, W. Talhout, M. Fornerod, and B. van Steensel. 2006. Characterization of the Drosophila melanogaster genome at the nuclear lamina. *Nat Genet*. 38:1005-1014.

Prokocimer, M., M. Davidovich, M. Nissim-Rafinia, N. Wiesel-Motiuk, D. Bar, R. Barkan, E. Meshorer, and Y. Gruenbaum. 2009. Nuclear lamins: key regulators of nuclear structure and activities. *J. Cell. Mol. Med.* 13:1059-1085.

Rabut, G., V. Doye, and J. Ellenberg. 2004. Mapping the dynamic organization of the nuclear pore complex inside single living cells. *Nat Cell Biol*. 6:1114-1121.

Ram, O., A. Goren, I. Amit, N. Shoresh, N. Yosef, J. Ernst, M. Kellis, M. Gymrek, R. Issner, M. Coyne, T. Durham, X. Zhang, J. Donaghey, C.B. Epstein, A. Regev, and B.E. Bernstein. 2011. Combinatorial patterning of chromatin regulators uncovered by genome-wide location analysis in human cells. *Cell*. 147:1628-1639.

Rando, O.J., and F. Winston. 2012. Chromatin and transcription in yeast. *Genetics*. 190:351-387.

Reddy, K.L., J.M. Zullo, E. Bertolino, and H. Singh. 2008. Transcriptional repression mediated by repositioning of genes to the nuclear lamina. *Nature*. 452:243-247.

Ritossa, F. 1996. Discovery of the heat shock response. *Cell Stress Chaperones*. 1:97-98.
Robert, J. 2003. Evolution of heat shock protein and immunity. *Dev Comp Immunol*. 27:449-464.
Rodriguez-Navarro, S., T. Fischer, M.J. Luo, O. Antunez, S. Brettschneider, J. Lechner, J.E. Perez-Ortin, R. Reed, and E. Hurt. 2004. Sus1, a functional component of the SAGA histone acetylase complex and the nuclear pore-associated mRNA export machinery. *Cell*. 116:75-86.
Rougvie, A.E., and J.T. Lis. 1988. The RNA polymerase II molecule at the 5' end of the uninduced hsp70 gene of D. melanogaster is transcriptionally engaged. *Cell*. 54:795-804.
Rouquette, J., C. Genoud, G.H. Vazquez-Nin, B. Kraus, T. Cremer, and S. Fakan. 2009. Revealing the high-resolution three-dimensional network of chromatin and interchromatin space: a novel electron-microscopic approach to reconstructing nuclear architecture. *Chromosome research : an international journal on the molecular, supramolecular and evolutionary aspects of chromosome biology*. 17:801-810.
Samara, N.L., and C. Wolberger. 2011. A new chapter in the transcription SAGA. *Curr Opin Struct Biol*. 21:767-774.
Schmid, M., G. Arib, C. Laemmli, J. Nishikawa, T. Durussel, and U.K. Laemmli. 2006. Nup-PI: the nucleopore-promoter interaction of genes in yeast. *Mol Cell*. 21:379-391.
Schoffl, F., R. Prandl, and A. Reindl. 1998. Regulation of the heat-shock response. *Plant Physiol*. 117:1135-1141.
Shevelyov, Y.Y., S.A. Lavrov, L.M. Mikhaylova, I.D. Nurminsky, R.J. Kulathinal, K.S. Egorova, Y.M. Rozovsky, and D.I. Nurminsky. 2009. The B-type lamin is required for somatic repression of testis-specific gene clusters. *Proc Natl Acad Sci U S A*. 106:3282-3287.
Shopland, L.S., C.V. Johnson, M. Byron, J. McNeil, and J.B. Lawrence. 2003. Clustering of multiple specific genes and gene-rich R-bands around SC-35 domains: evidence for local euchromatic neighborhoods. *J Cell Biol*. 162:981-990.
Spector, D.L., and A.I. Lamond. 2011. Nuclear speckles. *Cold Spring Harb Perspect Biol*. 3.
Sterner, D.E., P.A. Grant, S.M. Roberts, L.J. Duggan, R. Belotserkovskaya, L.A. Pacella, F. Winston, J.L. Workman, and S.L. Berger. 1999. Functional organization of the yeast SAGA complex: distinct components involved in structural integrity, nucleosome acetylation, and TATA-binding protein interaction. *Mol Cell Biol*. 19:86-98.
Stoffler, D., B. Feja, B. Fahrenkrog, J. Walz, D. Typke, and U. Aebi. 2003. Cryo-electron tomography provides novel insights into nuclear pore architecture: implications for nucleocytoplasmic transport. *J Mol Biol*. 328:119-130.
Sun, C., W. Yang, L.C. Tu, and S.M. Musser. 2008. Single-molecule measurements of importin alpha/cargo complex dissociation at the nuclear pore. *Proc Natl Acad Sci U S A*. 105:8613-8618.
Taddei, A., G. Van Houwe, F. Hediger, V. Kalck, F. Cubizolles, H. Schober, and S.M. Gasser. 2006. Nuclear pore association confers optimal expression levels for an inducible yeast gene. *Nature*. 441:774-778.
Taddei, A., G. Van Houwe, S. Nagai, I. Erb, E. van Nimwegen, and S.M. Gasser. 2009. The functional importance of telomere clustering: global changes in gene expression result from SIR factor dispersion. *Genome Res*. 19:611-625.
Talbert, P.B., and S. Henikoff. 2010. Histone variants--ancient wrap artists of the epigenome. *Nat Rev Mol Cell Biol*. 11:264-275.

Tan-Wong, S.M., H.D. Wijayatilake, and N.J. Proudfoot. 2009. Gene loops function to maintain transcriptional memory through interaction with the nuclear pore complex. *Genes Dev*. 23:2610-2624.

Towbin, B., P. Meister, B.L. Pike, and S.M. Gasser. 2010. Repetitive transgenes in C. elegans accumulate heterochromatic marks and are sequestered at the nuclear envelope in a copy number- and lamin- dependent manner *Cold Spring Harb Symp Quant Biol*. in press.

Trinklein, N.D., J.I. Murray, S.J. Hartman, D. Botstein, and R.M. Myers. 2004. The role of heat shock transcription factor 1 in the genome-wide regulation of the mammalian heat shock response. *Mol Biol Cell*. 15:1254-1261.

van Steensel, B. 2011. Chromatin: constructing the big picture. *Embo J*. 30:1885-1895.

Vergnes, L., M. Peterfy, M.O. Bergo, S.G. Young, and K. Reue. 2004. Lamin B1 is required for mouse development and nuclear integrity. *Proc Natl Acad Sci U S A*. 101:10428-10433.

Visser, A.E., F. Jaunin, S. Fakan, and J.A. Aten. 2000. High resolution analysis of interphase chromosome domains. *Journal of cell science*. 113 (Pt 14):2585-2593.

Vuister, G.W., S.J. Kim, A. Orosz, J. Marquardt, C. Wu, and A. Bax. 1994. Solution structure of the DNA-binding domain of Drosophila heat shock transcription factor. *Nat Struct Biol*. 1:605-614.

Wang, Z., C. Zang, J.A. Rosenfeld, D.E. Schones, A. Barski, S. Cuddapah, K. Cui, T.Y. Roh, W. Peng, M.Q. Zhang, and K. Zhao. 2008. Combinatorial patterns of histone acetylations and methylations in the human genome. *Nat Genet*. 40:897-903.

Woolcock, K.J., R. Stunnenberg, D. Gaidatzis, H.R. Hotz, S. Emmerth, P. Barraud, and M. Buhler. 2012. RNAi keeps Atf1-bound stress response genes in check at nuclear pores. *Genes Dev*. 26:683-692.

Wyce, A., T. Xiao, K.A. Whelan, C. Kosman, W. Walter, D. Eick, T.R. Hughes, N.J. Krogan, B.D. Strahl, and S.L. Berger. 2007. H2B ubiquitylation acts as a barrier to Ctk1 nucleosomal recruitment prior to removal by Ubp8 within a SAGA-related complex. *Mol Cell*. 27:275-288.

Xiao, H., O. Perisic, and J.T. Lis. 1991. Cooperative binding of Drosophila heat shock factor to arrays of a conserved 5 bp unit. *Cell*. 64:585-593.

Yao, J., M.B. Ardehali, C.J. Fecko, W.W. Webb, and J.T. Lis. 2007. Intranuclear distribution and local dynamics of RNA polymerase II during transcription activation. *Mol Cell*. 28:978-990.

Yoshida, T., K. Shimada, Y. Oma, V. Kalck, K. Akimura, A. Taddei, H. Iwahashi, K. Kugou, K. Ohta, S.M. Gasser, and M. Harata. 2010. Actin-related protein Arp6 influences H2A.Z-dependent and -independent gene expression and links ribosomal protein genes to nuclear pores. *PLoS Genet.* 6:e1000910.

Yuan, G.C., Y.J. Liu, M.F. Dion, M.D. Slack, L.F. Wu, S.J. Altschuler, and O.J. Rando. 2005. Genome-scale identification of nucleosome positions in S. cerevisiae. *Science*. 309:626-630.

Zlatanova, J., and A. Thakar. 2008. H2A.Z: view from the top. *Structure*. 16:166-179.

Chapter 2: *hsp-16* promoter drives nuclear pore association

The work presented in this experimental section is published in the Journal of Cell Biology (JCB) with the title *Promoter- and RNA polymerase II-dependent* hsp-16 *gene association with nuclear pores in* Caenorhabditis elegans*.* **Sabine Rohner**, Véronique Kalck, Xuefei Wang, Kohta Ikegami, Jason D. Lieb, Susan M. Gasser, Peter Meister.

Author contributions: SR, SMG and PM designed the experiments and interpreted the results except for the ChIP data (Figure 4), that were designed, performed and interpreted by XW, KI and JDL. SR, VK and PM performed all the other experiments. SR, SMG and PM wrote the manuscript, PM and SMG supervised the work.

Promoter- and RNA polymerase II–dependent *hsp-16* gene association with nuclear pores in *Caenorhabditis elegans*

Sabine Rohner,[1,2] Veronique Kalck,[1] Xuefei Wang,[3] Kohta Ikegami,[3] Jason D. Lieb,[3] Susan M. Gasser,[1,2] and Peter Meister[1]

[1]Friedrich Miescher Institute for Biomedical Research, CH-4058 Basel, Switzerland
[2]Faculty of Natural Sciences, University of Basel, CH-4056 Basel, Switzerland
[3]Department of Biology, University of North Carolina at Chapel Hill, Chapel Hill, NC 27599

Some inducible yeast genes relocate to nuclear pores upon activation, but the general relevance of this phenomenon has remained largely unexplored. Here we show that the bidirectional *hsp-16.2/41* promoter interacts with the nuclear pore complex upon activation by heat shock in the nematode *Caenorhabditis elegans*. Direct pore association was confirmed by both super-resolution microscopy and chromatin immunoprecipitation. The *hsp-16.2* promoter was sufficient to mediate perinuclear positioning under basal level conditions of expression, both in integrated transgenes carrying from 1 to 74 copies of the promoter and in a single-copy genomic insertion. Perinuclear localization of the uninduced gene depended on promoter elements essential for induction and required the heat-shock transcription factor HSF-1, RNA polymerase II, and ENY-2, a factor that binds both SAGA and the THO/TREX mRNA export complex. After induction, colocalization with nuclear pores increased significantly at the promoter and along the coding sequence, dependent on the same promoter-associated factors, including active RNA polymerase II, and correlated with nascent transcripts.

Introduction

Increasing evidence argues that the organization of the genome within the nucleus depends on sites of chromosomal anchorage at the inner face of the nuclear envelope (NE; Akhtar and Gasser, 2007; Kind and van Steensel, 2010). This occurs through heterochromatin binding to the stabilizing meshwork of nuclear lamin and associated proteins, or in some cases, such as stress-induced genes in yeast, with nuclear pores (for reviews see Dieppois and Stutz, 2010; Taddei et al., 2010; Egecioglu and Brickner, 2011). Indeed, the visualization of chromatin within the nucleus by electron microscopy has revealed a nonhomogeneous distribution of chromatin (Heitz, 1928). Generally, dark staining heterochromatin that fails to incorporate labeled UTP clusters at the NE, whereas light-staining, transcriptionally competent chromatin is internal (Visser et al., 2000; Rouquette et al., 2009). Closer observation showed, however, that the silent heterochromatic domains are excluded from nuclear pores, which suggests that active chromatin might bind the nuclear pore complex (NPC). Consistently, screens for yeast genes recovered with inner nuclear pore basket components detected both stress-induced genes and ribosomal protein genes (Brickner and Walter, 2004; Casolari et al., 2004; Cabal et al., 2006; Dieppois et al., 2006; Taddei et al., 2006; Yoshida et al., 2010). Furthermore, in both budding yeast and *Drosophila melanogaster*, the boundary or insulator elements that separate active from inactive chromatin were associated with NPC proteins (Ishii et al., 2002; Kalverda and Fornerod, 2010).

The pore association of activated yeast genes contrasts with the positioning of developmentally regulated genes in worms, flies, and human cells. The latter shift to internal sites upon

Correspondence to Susan M. Gasser: susan.gasser@fmi.ch

P. Meister's present address is Institute of Cell Biology, University of Bern, CH-3012 Bern, Switzerland.

Abbreviations used in this paper: ChIP, chromatin immunoprecipitation; chr, chromosome; DSIF, DRB sensitivity–inducing factor; HS, heat shock; HSAS, HS-associated site; HSE, HS element; HSF-1, HS transcription factor 1; NE, nuclear envelope; NPC, nuclear pore complex; pol, polymerase; qPCR, quantitative PCR; rDNA, ribosomal DNA; SAGA, Spt-Ada-Gcn-Acetyltransferase; SR-SIM, super-resolution structured illumination microscopy; tel, telomere; TSS, transcription start site; WT, wild type.

The Rockefeller University Press $30.00
J. Cell Biol. Vol. 200 No. 5 589–604
www.jcb.org/cgi/doi/10.1083/jcb.201207024

induction or shift to the nuclear lamina upon tissue-specific repression (for review see Meister et al., 2011). In mammalian cultured cells, the heat shock (HS) gene *Hsp70* localized preferentially to internal nuclear speckles upon activation (Hu et al., 2010), whereas the *Hsp70* gene in cultured *Drosophila* Schneider 2 (S2) cells was perinuclear (Kurshakova et al., 2007). Similarly, the up-regulated X chromosome in male flies is pore associated (for review see Akhtar and Gasser, 2007). Given the diversity of these results, it has remained unclear whether mechanisms that tether expressed genes at nuclear pores are conserved.

One common feature of NPC-bound genes in yeast is their response to stressful conditions (Brickner and Walter, 2004; Casolari et al., 2004; Cabal et al., 2006; Dieppois et al., 2006; Taddei et al., 2006). On a molecular level, it appears that Sus1, a protein present both in the histone acetylation and de-ubiquitination complex called SAGA (Spt-Ada-Gcn-Acetyltransferase) and in the TREX-2 (transcription and mRNA export linking) complex, is implicated in pore association (García-Oliver et al., 2012). Sus1 binds directly the nuclear pore protein Nup1 and anchors TREX-2 to the NPC. This mediates gene recruitment upon transcriptional activation and facilitates mRNA processing (García-Oliver et al., 2012). The peripheral anchoring of *Hsp70* in *Drosophila* S2 cells also requires E(y)2/ENY-2, the Sus1 homologue, which colocalizes weakly with nucleoporins, and Xmas2, the homologue of TREX-2 subunit Sac3 (Kurshakova et al., 2007). This suggested, but did not prove, that pore association is linked to mRNA processing or export. Whether the NPC regulates either mRNA synthesis or maturation remained unclear.

Here we explore the link between stress-induced gene activation and subnuclear gene positioning in an intact organism by tracking the essential heat-responsive locus *hsp-16.2* in *Caenorhabditis elegans.* The *hsp-16.2* gene is one of four related HS genes found in two clusters of two and four genes on chromosome V (chr V). The smaller cluster contains divergently transcribed *hsp-16.41* and *hsp-16.2*, whose expression level is 14-fold that of the homologous gene in the larger cluster (Stringham et al., 1992). The common promoter region of 394 bp contains two HS elements (HSEs; Fernandes et al., 1994; Trinklein et al., 2004; Guertin and Lis, 2010), which bind the conserved HS transcription factor 1 (HSF-1). HSF-1 is essential for *hsp-16.2* activation (Hajdu-Cronin et al., 2004). The *hsp-16.2* promoter contains a second HS-associated site (HSAS), with no known ligand, which improves expression in transgenic arrays if the distal HSE is absent (GuhaThakurta et al., 2002).

The promoter-associated changes that correlate with *Hsp70* activation are well characterized, particularly in *Drosophila*. Upon HS, HSF-1 trimerizes and binds in a cooperative manner to HSEs in the promoter (Xiao et al., 1991). Binding of HSF-1 affects the chromatin structure and composition by recruiting coactivators, elongation factors, histone modifying enzymes, and chaperones (for review see Guertin et al., 2010). Even without induction, the promoter is held in an open state and harbors a paused RNA polymerase II (pol II), which produces a short RNA of ∼25 nucleotides (Rougvie and Lis, 1988). Gene activation coincides with the recruitment of positive transcription elongation factor b (P-TEFb), a serine/threonine kinase that phosphorylates the carboxy-terminal domain of the pol II catalytic subunit. This phosphorylation releases paused pol II, which then productively transcribes the gene (Guertin et al., 2010). Activation leads to a rapid eviction of nucleosomes after ∼30 s in a transcription-independent manner, an event proceeded by dTip60-mediated histone H2A acetylation (Petesch and Lis, 2012).

Spatial organization analysis shows that the endogenous *hsp-16.2* locus in *C. elegans*, like transgenes that carry only the *hsp-16.2* promoter, are at or near the NE. Super-resolution microscopy shows that upon activation, transgenes bearing the *hsp-16.2* promoter colocalize efficiently with the NPC. Thus, peripheral positioning requires both HSE and HSAS elements before induction, but either is sufficient after HS. Importantly, both HSF-1 and active pol II are essential for perinuclear anchoring both before and after induction. We propose that this stress-activated promoter autonomously directs chromatin to the nuclear pore, where continued association correlates with the abundance of engaged RNA polymerases.

Results

Repetitive *hsp-16.2* promoter arrays are peripherally retained upon transcriptional induction

By studying arrays bearing developmentally regulated promoters in *C. elegans*, we have shown that the activation of tissue-specific promoters leads to their relocation toward the nuclear interior (Meister et al., 2010b). We asked whether a stress-induced promoter does the same, using a worm strain homozygous for a large integrated gene array that expresses cytoplasmic GFP under control of the *hsp-16.2* promoter (Link et al., 1999). The strain of interest carries a second large gene array expressing GFP-lacI from the constitutive *baf-1* promoter (Meister et al., 2010b). GFP-lacI binds to *lacO* sites on both integrated constructs, allowing live imaging of array position. Given that *baf-1*::*gfp-lacI* expression is insensitive to temperature shift (Fig. S1), it serves as an internal control for quantitation.

Before HS (10 min at 34°C), the four integrated gene arrays were localized at the NE (Meister et al., 2010b; Towbin et al., 2010; Fig. 1, B and E, before HS). The *hsp-16.2* array, which is slightly larger than the control array in the absence of HS (1.8-fold volume; Fig. 1, E and F), expanded visibly and immediately upon temperature shift to occupy 2.6-fold of the control array volume (Fig. 1, C, E, and F). We confirmed that the expanded array contained the *hsp-16.2* promoter by repeating this in worms in which only the *hsp-16.2* promoter array carries *lacO* sites (Fig. S1 A). The observed array unfolding resembles that reported during induced expression of array-borne genes in cultured mammalian cells (Tumbar et al., 1999; Hu et al., 2009). However, we note that the expanded HS-induced array did not shift inwards, but rather unfolded along the inner NE (Fig. 1 D). Gene induction and array decondensation were correlated, as both were ablated in a temperature-sensitive *hsf-1* mutant (*hsf-1(sy441)*; Hajdu-Cronin et al., 2004; Figs. 1 F and S1 B).

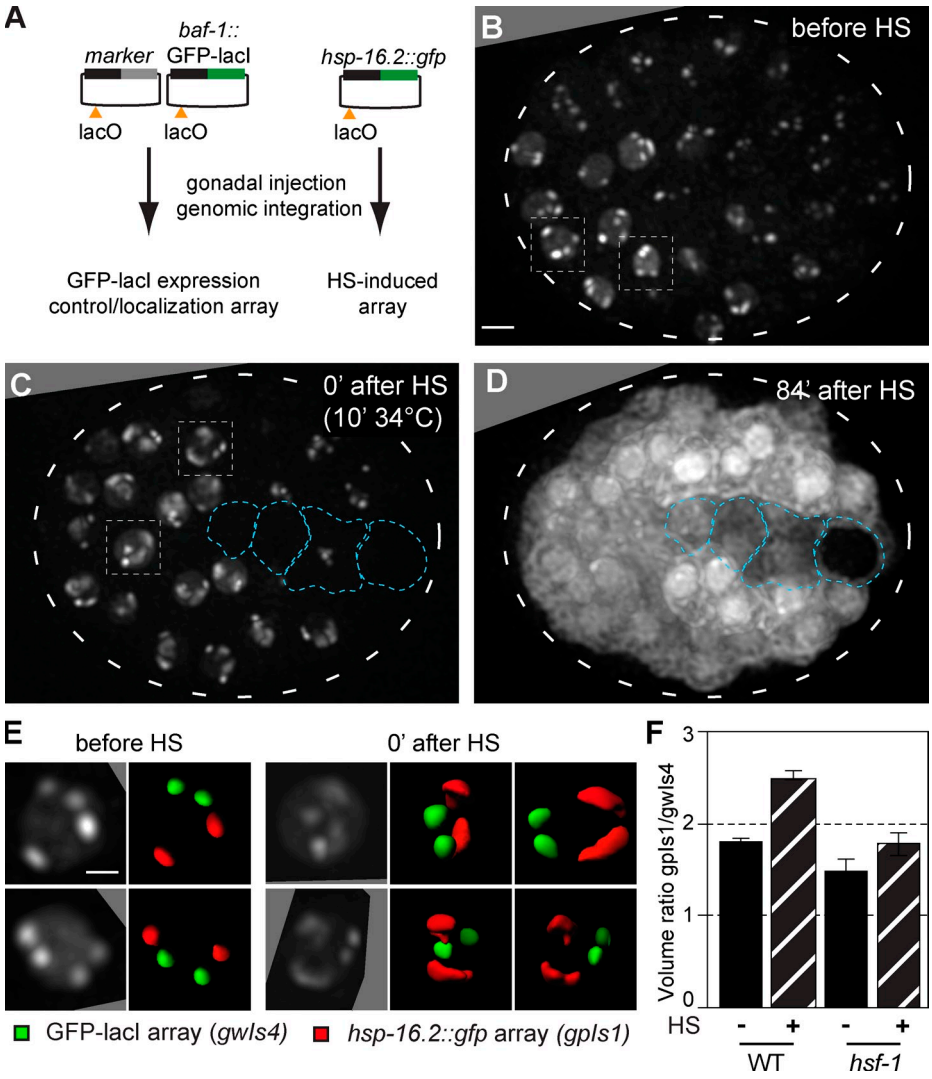

Figure 1. **HS-induced transcription leads to peripheral decondensation of large, HS-inducible arrays.** (A) Plasmids used to create large arrays by gonadal injection, bearing either *baf-1*::GFP-lacI with a muscle-specific marker (*gwIs4*) or the *hsp-16.2* promoter driving GFP (*gpIs1*), and a single *lacO* site per plasmid. Arrays contain 250–500 plasmid copies. (B) Fluorescence from an embryo of a strain carrying both *gwIs4* and *gpIs1* is shown, before HS induction. Four spots reflecting the large integrated gene arrays are located at the nuclear periphery (Meister et al., 2010b; Towbin et al., 2012). Boxed nuclei are enlarged in E. See Fig. S1. Bar, 5 µm. (C) Fluorescence from the same embryo in B after 10 min at 34°C. Boxed nuclei, enlarged in E, show decondensation of two of the arrays. Blue encircled nuclei do not respond to HS. (D) Pervasive cytoplasmic fluorescence from the same embryo in B and C captured 84 min after HS, showing *hsp-16.2::gfp* induction from the *gpIs1* array. Entire embryos are encircled by broken lines. (E) Enlarged nuclei from the embryo in B and C, with two 90° rotations for C. Array volume rendering shows no shift in subnuclear localization of *gwIs4* (green) or *gpIs1* (red), decondensed at 0 min after HS. Bar, 2 µm. (F) Array volume was quantified using the GFP-lacI signals in WT and *hsf-1* mutant worms, presented as the ratio of *gwIs4* and HS-activated *gpIs1* before and 0 min after HS (WT; n = 100, 11; *hsf-1* mutant; n = 3, 6). Error bars indicate mean ± SEM.

The endogenous *hsp-16.2* locus is efficiently recruited to the NE upon activation

The fact that HS-responsive arrays remain peripheral after induction could mean either that activation enhances the association or that *hsp-16.2* induction cannot overcome heterochromatin tethering (Meister et al., 2010b; Towbin et al., 2012). We therefore analyzed the positioning of the endogenous *hsp-16.2* locus in wild-type (WT) *C. elegans* embryos before and after HS by FISH. The endogenous *hsp-16.2* gene is found next to *hsp-16.41* on the left arm of chr V, 1.8 Mb from the left telomere. Genome-wide lamin-DAM-ID (Towbin et al., 2012; Fig. 2 A) and LEM-2 chromatin immunoprecipitation (ChIP) analysis (Gerstein et al., 2010; Ikegami et al., 2010) both showed an enrichment of the terminal 4–5 Mb of chr V at the nuclear lamina. To determine the subnuclear position of the *hsp-16.2* locus more precisely, we turned to quantitative 3D microscopy.

We scored the position of the endogenous *hsp-16.2* locus before and after HS (10 min at 34°C), relative to the edge of the DAPI-stained nucleus, in embryos of 50–150 cells. Within 3D confocal stacks of images, we located optical sections with the strongest *hsp-16.2* FISH signals, divided each focal plane into three zones of equal surface, and scored the FISH signals relative to these zones (Fig. 2 B; Meister et al., 2010a). Even before HS, the *hsp-16.2* locus showed a significant enrichment in outermost zone 1 (Fig. 2 C). After induction, the *hsp-16.2* locus became more peripheral: zone 1 values increased from 44% to

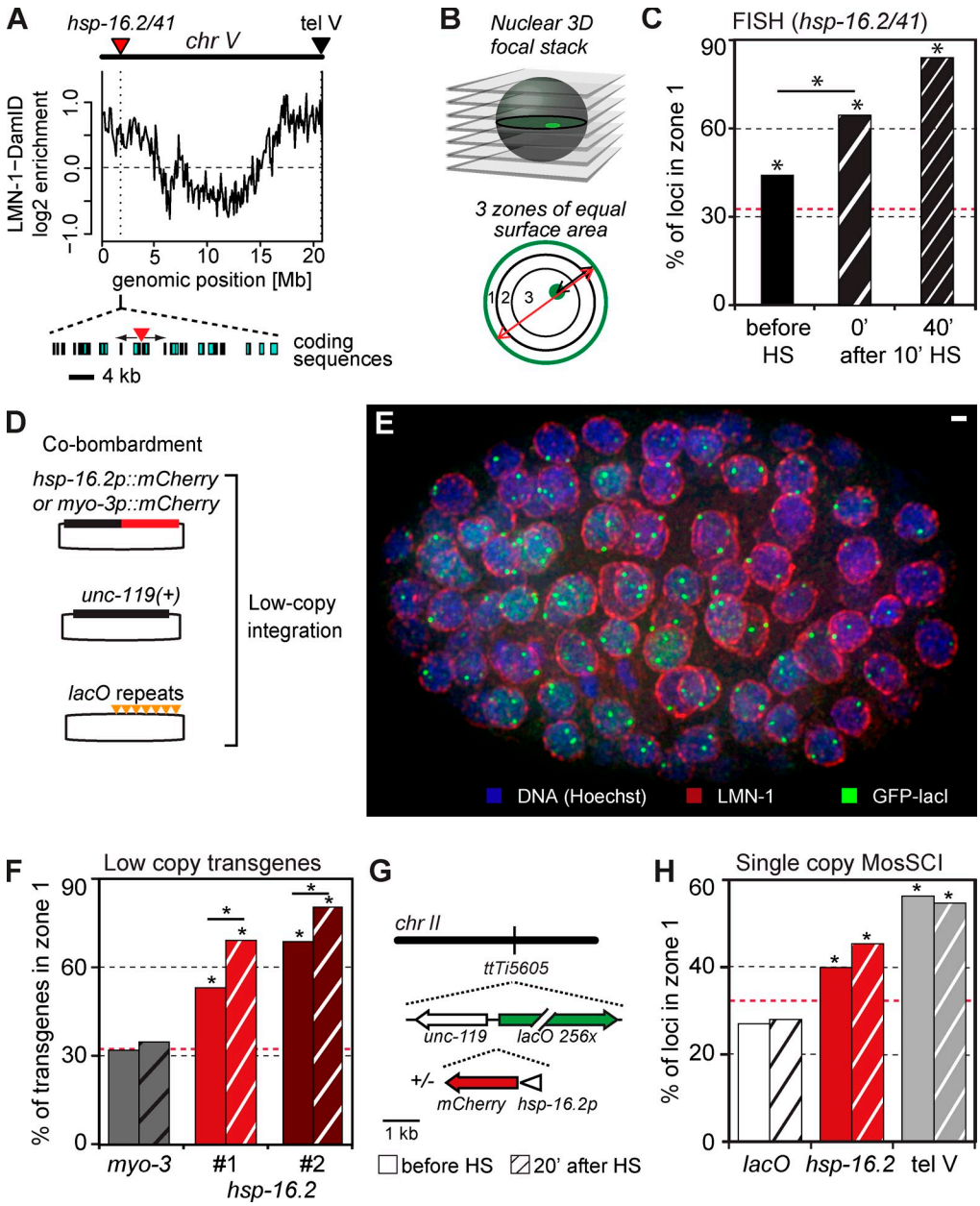

Figure 2. **The *hsp-16.2* promoter is sufficient to anchor chromatin at the nuclear periphery.** (A) Sketch shows the *hsp-16.2/41* locus on chr V left arm (red triangle), 1.8 Mb from the telomere, and the MosSCI-inserted *lacO* repeat (tel V; black triangle), at *ttTi9115*, 170 kb from TG repeats (Towbin et al., 2012). Below is LMN-1-Dm-ID data showing terminal 4–5 Mb enriched for lamin association (Towbin et al., 2012). An expanded view of coding sequences shows the divergent *hsp-16.2* and *hsp-16.41* genes. (B) Quantitation of radial positioning of endogenous loci and GFP-lacI–tagged transgenes, as described in Materials and methods. Random localization = 33% in each zone. (C) The endogenous *hsp-16.2/41* locus is enriched in zone 1 in early embryos and becomes more enriched after HS. FISH signal positions were quantified for the *hsp-16.2* locus as in B. Only zone 1 values are shown (n = 229, 293, 281; $P < 0.01$ vs. random distribution for all). Red broken lines indicate a 33% or random distribution of the foci against which all values are compared. Asterisks indicate distributions significantly different from random, or different between indicated conditions. (D) Plasmids used to create small bombarded transgenes (tg). *mCherry* is driven by either the *hsp-16.2* or the muscle-specific *myo-3* promoter, co-bombarded with an array of 256 *lacO* sites and the *unc-119*$^+$ marker. The copy number of the *hsp-16.2* promoter is 1 (tg #1) or 74 (tg #2; Fig. S2). (E) Maximal Z projection of a partial 3D reconstruction of a 200-cell-stage embryo (GW421, expressing GFP-lacI) carrying a *lacO*-tagged transgene *gwIs28[hsp-16.2::mCherry; 256xlacO; unc-119*$^+$*]*. The embryo is stained for GFP (anti-GFP, green), nuclear lamina (anti–LMN-1, red), and DNA (Hoechst, blue). Bar, 1 µm. (F) Quantitation of the GFP-lacI signal position for either the *myo-3* transgene, or the two *hsp-16.2* promoter–containing transgenes, as in B. Zone 1 values and asterisks are defined as in C. Hatched bars, after HS. Loci scored were (left to right) n = 275, 183, 503, 188, 226, and 200; p-values versus random = 0.47, 0.6 for *myo-3*; and $P < 10^{-10}$ for *hsp-16.2*–containing transgenes. A Fisher's exact test for significance before versus after HS for *hsp-16.2* transgenes yielded $P = 7.2 \times 10^{-6}$, 7.5×10^{-3}). (G) Sketch of DNA used for MosSCI insertion at *ttTi5605* in mid–chr II: *lacO* sites and *unc-119*$^+$ were integrated with or without the *hsp-16.2* promoter driving *mCherry*. (H) Quantitation of the GFP-lacI signal for *lacO* only insertion, the ectopic *hsp-16.2::mCherry* construct at *ttTi5605*, and the MosSCI *lacO* insertion at tel V (see A). Method, bars, and asterisks are defined as in B and C. Numbers scored were (left to right) n = 117, 95, 309, 346, 213, and 204; p-values versus random = 0.17, 0.31, 0.02, 3×10^{-5}, 3×10^{-12}, and 2×10^{-10}, respectively.

65% immediately after HS, and to 84% by 40 min (Fig. 2 C). Thus, the endogenous *hsp-16.2* gene was enriched at the nuclear rim before exposure to HS, and peripheral positioning was significantly enhanced by HS induction at 34°C.

Promoter sequences are sufficient to mediate perinuclear positioning

To distinguish the relative contributions of chromosomal context, coding, and promoter sequences to gene localization, we generated small transgene arrays by microparticle bombardment that contained only the 394-bp *hsp-16.2* promoter driving the *mCherry* coding sequence, and *lacO* repeats. The *mCherry* gene contains two synthetic introns and was flanked by the *unc-54* 3′ UTR, allowing us to quantify nascent and processed transcripts, and to monitor induction by mCherry fluorescence (Fig. 2 D). We obtained two independent transgenic inserts that contained either 1 (GW421, tg #1) or 74 (GW391, tg #2) copies of the promoter, integrated among 24–88 copies of plasmid, respectively (Fig. S2). Similar small transgenes, e.g., one containing the *myo-3* promoter, were shown previously to be randomly positioned in embryonic nuclei, independent of their transcriptional status (Meister et al., 2010b). For embryos with the *hsp-16.2* promoter transgenes, we observed a significant enrichment of the array at the NE during growth at normal temperatures (Fig. 2, E and F; *hsp-16.2* tg #1 zone 1 = 50% and *hsp-16.2* tg #2 zone 1 = 69%), unlike the randomly distributed *myo-3* promoter transgene (Fig. 2, E and F). Peripheral enrichment correlated with the promoter copy number, as higher values were scored for tg #2.

After HS, the *lacO*-tagged *hsp-16.2* promoter transgenes were even more peripheral (Fig. 2 F; tg #1 = 69% and #2 = 81%; P vs. non-HS = 7×10^{-6} and 0.008, respectively), whereas the *myo-3* transgene retained its random distribution (Fig. 2 F), which is consistent with earlier results (Meister et al., 2010b). Indeed, among all transgenes tested, only ones containing the *hsp-16.2* promoter were peripherally enriched in early embryos, and this was the case both before and after HS.

Because it is not possible to control copy number or insertion site of such transgenes, we next used the MosSCI insertion system to integrate desired sequences at a specific target site by homologous recombination, namely at the *ttTi5605* locus on chr II (Fig. 2 G; Materials and methods; Frøkjaer-Jensen et al., 2008). This target site (*ttTi5605*) is randomly localized in embryonic nuclei when tagged with *lacO* sites only (Fig. 2 H, *lacO*). To test the effect of a single *hsp-16.2* promoter on localization, we integrated a single copy of the *hsp-16.2* promoter driving *mCherry*, along with the *lacO* repeats. The *hsp-16.2::mCherry* construct was now significantly enriched at the nuclear rim (39%, P = 0.02 vs. 27%, P = 0.17 for *lacO* only). After 10 min at 34°C, the proportion of *hsp-16.2*–containing loci at the nuclear periphery was 44% (before vs. after HS, P = 0.27), whereas the *lacO* alone single-site insertion remained randomly distributed (28% in zone 1). A MosSCI insertion of *lacO* repeats into a subtelomeric region on chr V (tel V, Fig. 2 A; Towbin et al., 2012) showed strong association with the nuclear periphery that was unchanged upon HS (Fig. 2 H).

In summary, the endogenous *hsp-16.2* locus is distributed nonrandomly with respect to the NE, even under noninducing conditions. Importantly, the *hsp-16.2* promoter alone is significantly peripheral when integrated randomly as a transgene, or as a targeted single-copy integration in the middle of chr II (*ttTi5605*). This argues that the promoter sequence itself drives peripheral localization, even when transcription levels are low. Promoter induction significantly increased enrichment at the nuclear rim at the endogenous locus and in the case of small transgenes ($P < 0.7 \times 10^{-5}$). Chromosomal context could well influence the efficiency of perinuclear localization: the endogenous *hsp-16.2* locus is on a distal chromosome arm that is more likely to contact the NE than the mid-chromosomal *ttTi5605* MosSCI insert. We note, however, that the *hsp-16.2* promoter drives a single transcript at the MosSCI insert, whereas at the endogenous locus there are two divergent transcripts.

Super-resolution microscopy shows colocalization of induced *hsp-16.2* transgene with NPC

In yeast, inactive genes at telomeres and silent *HM* loci contact nonpore sites at the NE, whereas stress-induced genes are enriched at NPCs (Taddei et al., 2010). To examine which NE structure binds the *hsp-16.2* promoter either before or after HS in worms, we exploited super-resolution structured illumination microscopy (SR-SIM). With its 100-nm resolving power, we could distinguish individual fluorescently tagged nuclear pores and differentiate them from the lamina (Fig. 3 A and Video 1). We scored the positioning of the GFP-lacI–bound *hsp-16.2* promoter tg #1 relative to pore and lamina staining. SR-SIM measurements yielded a mean diameter of 190 nm for an immunostained NPC, which agrees perfectly with measurements derived from structural studies, given a 15 nm size for the 1° and 2° antibodies (Strambio-De-Castillia et al., 2010). Mean NPC density was ∼3 per μm^2 or 115 per embryonic nucleus, with a GFP-LacI spot diameter of ∼300 nm, providing sufficient resolution to accurately map locus position relative to pores and lamina.

We classified the position of the peripheral *hsp-16.2* transgenes as NPC colocalizing (<50 nm between the centers of mass of nearest pore and GFP-lacI spot), touching NPC (>50 nm between centers of mass), or away from NPC and adjacent to lamina (Fig. 3, B–D). The MosSCI *lacO* insertion at the chr V telomere (Fig. 2 A, tel V) served as a control.

Before HS, 35% of all *hsp-16.2* foci were touching the NPC, while a minority were either colocalized with pores (5%) or adjacent to the lamina (18%; Fig. 3 E). After HS, 74% of *hsp-16.2* transgene foci were peripheral, of which 53% were colocalized with the NPC and 12% were touching the NPC, whereas a small fraction remained adjacent to lamins (Fig. 3 E, after HS). In contrast, the tel V control locus, despite being strongly perinuclear, showed no favored distribution either before or after HS (Fig. 3 E). Thus, induced *hsp-16.2* promoter within the transgene is preferentially associated with nuclear pores.

ChIP confirms preferential *hsp-16.2* promoter association with nuclear pores

To confirm that the endogenous *hsp-16.2* locus and the MosSCI *hsp-16.2* promoter insertion also prefer a pore over the nuclear

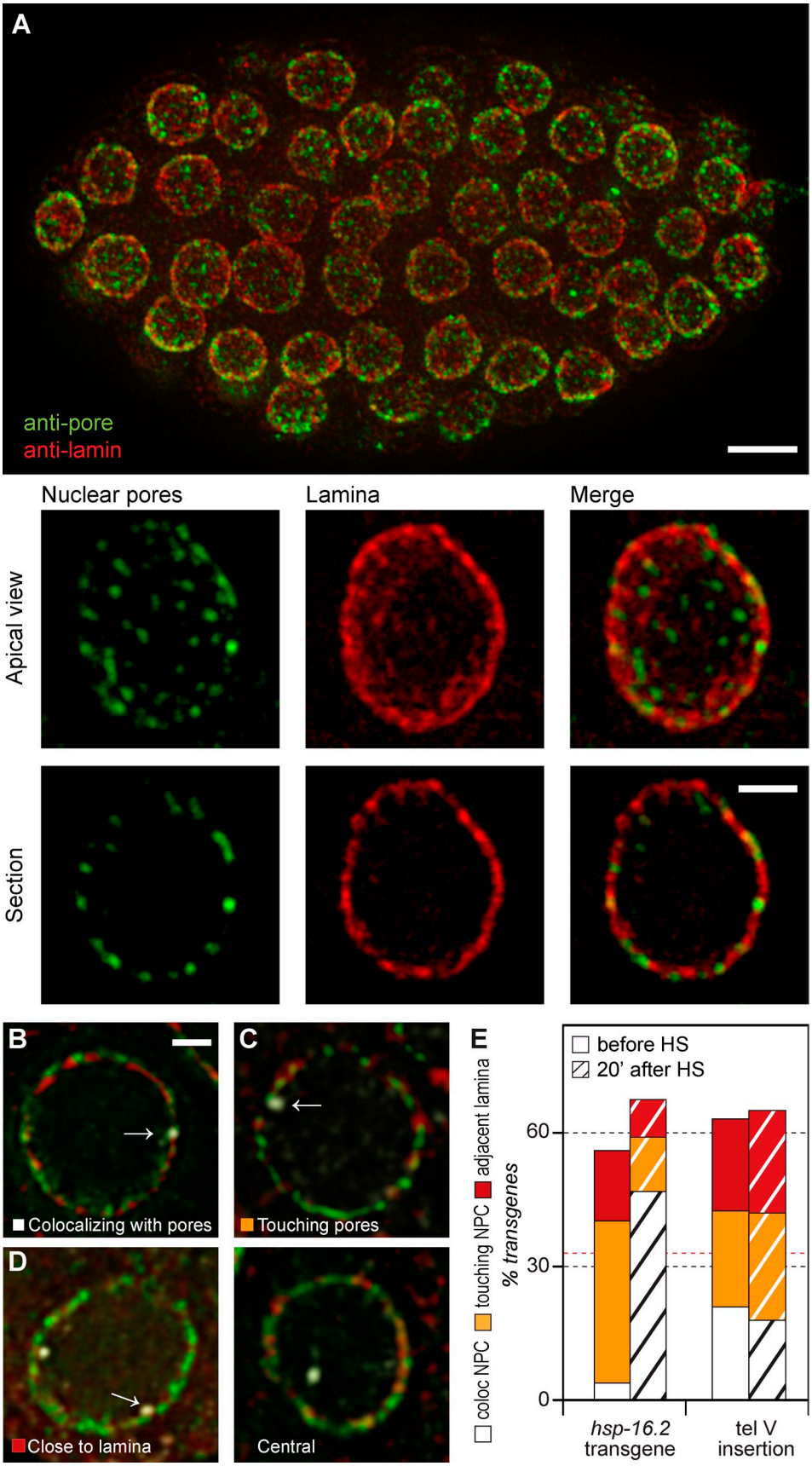

Figure 3. ***hsp-16.2* transgenes colocalize with pores after HS, and are near pores before.** (A) SR-SIM of WT worm embryo immunostained with rabbit anti–LMN-1 (*Ce* lamin; red) and anti-nucleoporin FG repeat (mAb414; green). See Video 1 for 3D imaging. Below are higher magnifications of an apical and a mid-nuclear view with separated channels. (B–D) Single mid-nucleus focal planes from SR-SIM, showing *hsp-16.2* tg1 localization by GFP-lacI signal

lamina, we performed ChIP with antibodies against NPP-13, a pore protein located in the intramembrane domain of the NPC (Nic96 in yeast, Nup93 in mammals), and LEM-2, a lamin-associated protein (Ikegami et al., 2010). Quantitative PCR (qPCR) confirms the association of these proteins with the endogenous *hsp-16.2* locus (Fig. 4 A, en), as well as the single-copy *hsp-16.2* promoter insertion at *ttTi5605* (Fig. 2 A, ec; Fig. 2 G and Fig. 4 A). Unrelated loci were used to normalize PCR values among the biological ChIP replicates (ctrl1) and to provide a non–HS-responsive control (ctrl2). These two loci were previously characterized as not interacting with the NPC (unpublished data; Fig. 4 C).

We note that the probes nearest the transcription start sites (TSSs) at the ectopic MosSCI locus (ec1), the endogenous *hsp-16.2* (en1), or the *hsp-16.41* promoter (en2) failed to cross-link efficiently to NPP-13, either before or after HS. This may be caused by interference in DNA–pore contact by holo–pol II binding. However, the promoter probe further upstream (ec2) yielded a strong enrichment for NPP-13 after HS within the *hsp-16.2* MosSCI insertion (Fig. 4 B, compare ec1 with ec2). At the endogenous locus, the association of both en1 and en2 with LEM-2 dropped after HS (Fig. 4 B), which is consistent with the SR-SIM localization data presented in Fig. 3.

Given the poor ChIP efficiency for NPP-13 with the promoter probes used in Fig. 4 A, we extended ChIP analysis along the coding sequence, and to additional sites in the promoters of both the endogenous locus and the *hsp-16.2::mCherry* MosSCI insertion. In Fig. 4 C, we compared NPP-13 recovery before HS (open diamond) and 10 min after HS (closed squares) and normalized enrichment to the ctrl1 sequence. At both sites we observed a small but significant enrichment for NPP-13 after HS, and the association spread along the coding sequence (Fig. 4 C). The *hsp-16.2* MosSCI insertion has particularly strong NPP-13 binding at the distal end of the promoter after HS, confirming the results shown in the preceding paragraph, whereas NPP-13 enrichment was low at the TSS of all constructs analyzed. The presence of NPP-13 along the gene body after HS suggests that the transcribing gene perhaps becomes exposed to contact the NPC. In summary, SR-SIM and ChIP results indicate that before HS, the *hsp-16.2* promoter is near, but does not colocalize with the NPC, whereas after HS, the promoter directly interacts with the NPC, as does the 3′ end of each transcribed gene.

Endogenous *hsp-16.2* and the MosSCI *hsp-16.2* insertion show similar induction kinetics

To validate the use of the MosSCI-integrated *hsp-16.2* promoter, we analyzed its kinetics of induction alongside those of the endogenous locus by analyzing levels of either nascent (pre-mRNA) or spliced transcripts during HS and for 40 min after return to 22°C. Unspliced (pre-mRNA) was monitored by real-time PCR, using primers that generate a unique intron–exon junction-spanning product. Values are plotted relative to *its-1*, a transcribed spacer in ribosomal DNA (rDNA), which does not fluctuate upon HS. Both unspliced *hsp-16.2* and *mCherry* transcripts (*hsp-16.2* promoter-driven) showed an immediate and proportionate increase after HS (Fig. 5 A). Nascent transcripts peaked 1 min after return to 22°C, which suggested induced rapid transcriptional shutoff. Yet significant amounts of unprocessed transcript persisted for 20–40 min after induction, which is consistent with the persistent NPC anchorage observed at both endogenous and transgenic loci after HS (Figs. 2 and 3).

The appearance and accumulation of spliced mRNA occurred 10–20 min after HS for both loci, with a slight delay for the *mCherry* mRNA, which has two introns instead of one. Spliced products continue to accumulate for 40 min after HS-induced transcription for both transcripts. We conclude that induction kinetics and processing are very similar for the endogenous gene and the MosSCI insertion (Fig. 5 A), and that NPC association correlates with the timing of transcript elongation and processing.

Two different pathways recruit the *hsp-16.2* promoter at the nuclear periphery

Having shown that the *hsp-16.2* promoter is sufficient for both rapid induction and relocation of the locus to the NPC, we checked whether both are controlled by the same promoter elements. The bidirectional endogenous *hsp-16.2* promoter drives transcription of both *hsp-16.2* and *hsp-16.41*. The promoter contains two HSEs, flanking the HSAS, which has no known ligand (Fig. 5 B). Deletion analysis and induction of high copy number ectopic arrays indicated that the proximal HSE site was most important for transcription, whereas loss of both HSE sites abolished transcription (GuhaThakurta et al., 2002). In addition, mutation of HSAS decreased reporter gene transcription supported by the distal HSE site.

We asked whether mutation of the HSE or HSAS sites would influence *hsp-16.*2 promoter-driven subnuclear localization. *lacO*-tagged single-copy reporters with modified *hsp-16.2* promoters were introduced into an otherwise identical chromatin environment by MosSCI-mediated recombination at the *ttTi5605* locus. Confirming the observations in Figs. 2–4, the MosSCI *hsp-16.2* promoter shifted the *ttTi5605* locus to the nuclear periphery in 40% of the cells before HS (Fig. 5 C). After HS, NE association increased to 44%. Mutation of either HSAS or HSE elements (Fig. 5, B and C), or both, led to a random distribution before HS (Fig. 5 C; zone 1 = 33% for $HSAS^{mt}$, 32% for $HSE1/2^{mt}$, and 31% for $HSAS^{mt}$ $HSE1/2^{mt}$). Intriguingly, when the same constructs were monitored 20 min after HS, the locus was significantly peripheral despite loss of HSAS or HSE consensuses (Fig. 5 C; zone 1 = 45% for $HSAS^{mt}$ and 46% for $HSE1/2^{mt}$).

(white) relative to LMN-1 (red) or NPC (green). Bar, 1 µm. (E) Scoring of *hsp-16.2* tg #1 and MosSCI insertion tel V before and after HS (hatched), as in B–D. White, colocalizing with NPC (pore); orange, touching NPC; red, adjacent to lamina. Non-peripheral transgenes are not indicated. The number of *hsp-16.2* tg counted, *n* colocalizing with NPC, *n* touching NPC, and *n* adjacent to LMN-1 were as follows. no HS, *n* = 197, 10, 68, and 35; and after HS, *n* = 199, 106, 23, and 18. For tel V, numbers were as follows. no HS, *n* = 215, 45, 46, 44; and after HS (*n* = 184, 33, 44, 42. The red line is defined as in Fig. 2. Bars: (A, top) 10 µm; (A, bottom) 3 µm; (B–D) 1 µm.

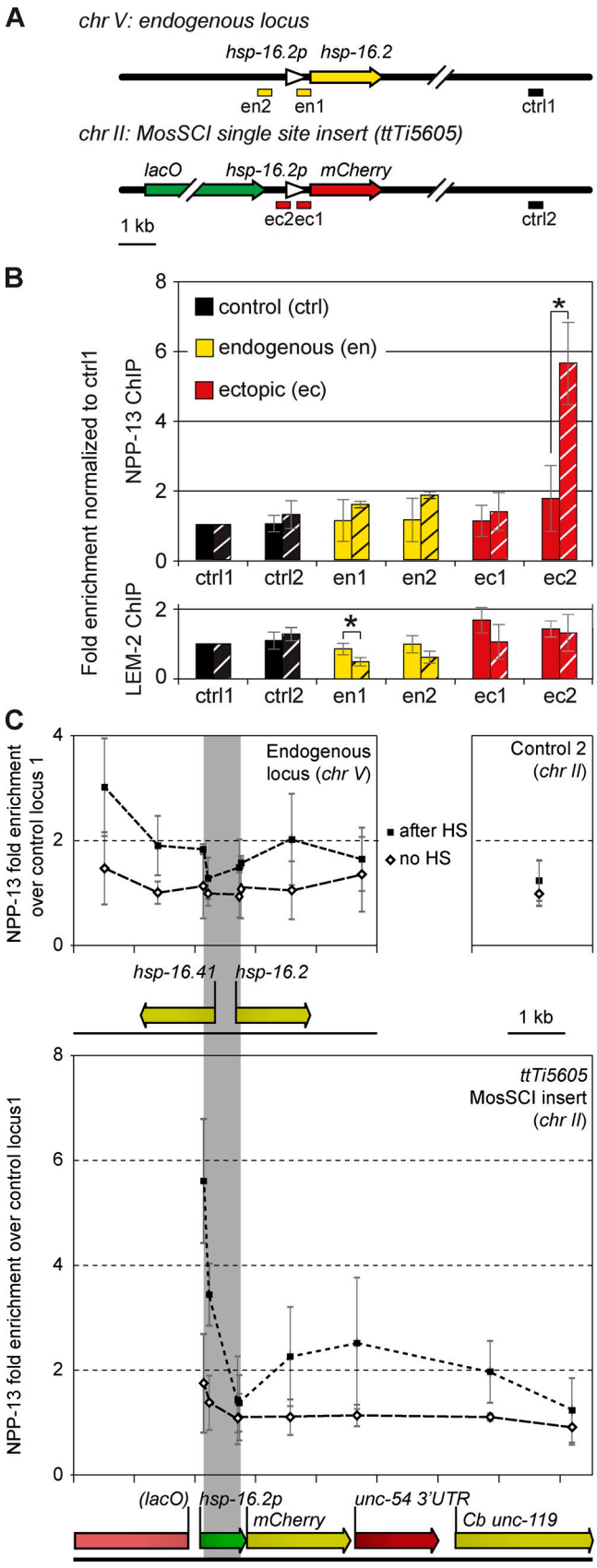

Figure 4. **NPC interaction at endogenous *hsp-16.2* and at the MosSCI–*hsp-16.2* promoter insert increases after HS.** (A) Sketch of the endogenous *hsp-16.2* locus (top, chr V) and the ectopic MosSCI insert (bottom, chr II) of *hsp-16.2::mCherry* at *ttTi5605*, showing probes used for qPCR (en1 and -2, endogenous; ec1 and -2, MosSCI insert). Probes en1, en2, and ec1 are near TSS; control loci ctrl1 and ctrl2 do not to interact with NPC or LMN-1. crtl1 is used for normalization and ctrl2 is not HS-inducible. All ChIP was performed in triplicate on a single strain; see Materials and methods for quantitation. (B) NPP-13 (top) and LEM-2 (bottom) ChIP enrichment of the probes in A, normalized to ctrl1. Values are shown before (unhatched) and 10 min after (hatched) HS. Asterisks indicate statistically significant change. (C) Additional qPCR probes were used to monitor ChIP enrichment at the endogenous *hsp-16.2* and MosSCI *hsp-16.2* promoter integration, before (Δ) and after HS (■). Loci are aligned (gray column). ctrl2 normalized to ctrl1 reflects no HS response. Error bars indicate mean ± SEM.

Loss of all three sites, however, ablated NE association (Fig. 5 E; 32% for HSAS^{mt} HSE1/2^{mt}). In conclusion, before HS, both HSAS and HSE sites are used to position the *hsp-16.2* promoter near the periphery, whereas after HS either the HSAS or HSE sequence suffices.

To test whether relocation correlates with expression efficiency, we performed real-time PCR on reverse-transcribed RNA, extracted from the strains bearing mutant and WT *hsp-16.2* promoters, before and after HS. Real-time PCR values are expressed relative to those of *its-1* (Fig. 5 D; for an agarose gel of amplicons, see Fig. S3). HS robustly induces the WT promoter-driven *mCherry*, with the same kinetics as the endogenous *hsp-16.2* mRNA (Fig. 5 A), although mCherry protein is only visible 80 min after HS (Fig. S4). Mutation of the HSE sites compromises mCherry expression (Fig. 5 D), whether or not the HSAS is intact. There is, nonetheless, a very low level of nascent and spliced transcript detectable in the HSE mutant (Figs. S3 and S4 A), even though induction is compromised and mCherry fluorescence is not detected.

When the HSAS site alone is mutated, leaving functional HSE sites, the expression level of *mCherry* is reduced ~10-fold (Fig. 5 D), yet spliced transcript could be detected after 40 min (Fig. S3) and mCherry fluorescence could be detected by 120 min (Fig. S4 A). This argues that HSAS contributes to full activation of *hsp-16.2*, even in the presence of HSE sequences. Given that HSAS is needed for peripheral positioning before induction, NE positioning before HS correlates with maximal activation.

After HS, the NPC localization of the *hsp-16.2* promoter does not require induced RNA levels because promoters that lack the HSE sites (no increased mRNA) or the HSAS site (increased mRNA) support similar recruitment to the NE upon HS (Fig. 5, C and D). The HSAS element may contribute to NPC binding through a factor that contributes to activation, but which is insufficient for induced gene expression. In contrast, HSE elements support both HS-induced transcription and relocation in the absence of HSAS, most probably through HSF-1 and pol II recruitment.

Peripheral anchoring of the *hsp-16.2* promoter depends on HSF-1

We next tested whether HSF-1 is needed for peripheral positioning (Figs. 1 and 5 E). We used *hsf-1(RNAi)* on worms bearing the *lacO*-tagged *hsp-16.2* transgene. Upon depletion of HSF-1 in embryos of RNAi-treated worms, both before and

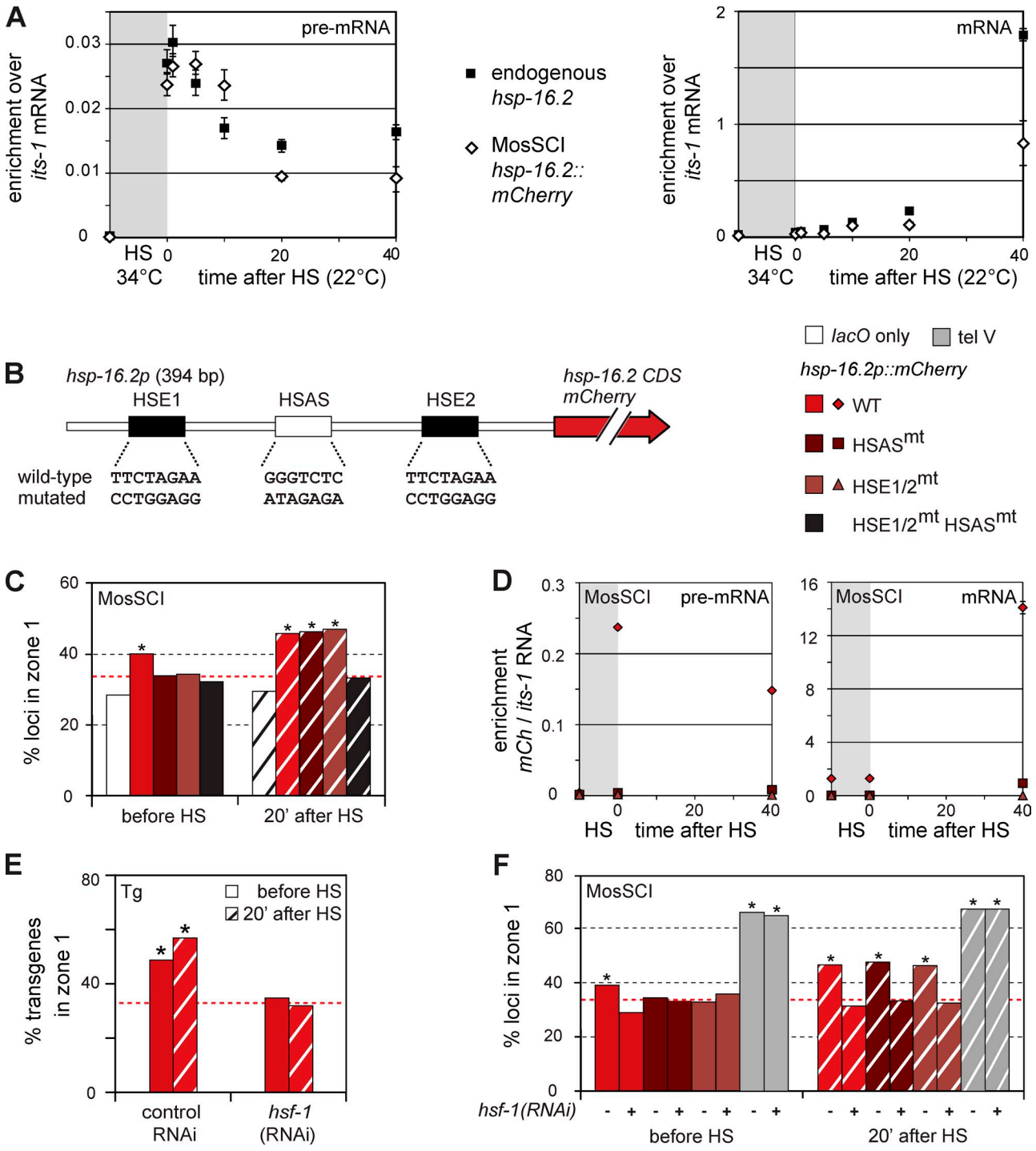

Figure 5. **HSE and HSAS sequences are necessary to anchor *hsp-16.2* at the nuclear rim.** (A) Nascent (left) and spliced (right) RNA levels of *hsp-16.2* (◇) and *mCherry* (■) before and at six time points after HS for the indicated loci. Values are normalized to *its-1*, a transcribed rDNA spacer. (B) Scheme of the *hsp-16.2/41* promoter, containing two HSF-1 binding sites, HSE1 and HSE2, on either side of the HSAS sequence, with *hsp-16.2* or *mCherry* transcription driven toward the right. Changes in mutated versions of HSE1, HSAS, or HSE2 are shown below the sketch. (C) Quantitation of subnuclear positions of the GFP-lacI signal for the MosSCI insertion of WT or mutated *hsp-16.2* promoters; color-coded as in B. Zone 1 values, bar labels, and asterisks are defined as in Fig. 2 (B and C). Cell numbers were (left to right) n = 117, 309, 367, 339, 306, 95, 346, 329, 347, and 249. P-values versus random = 0.17, 0.02, 0.80, 0.73, 0.33, 0.31, 3×10^{-5}, 1×10^{-6}, 1×10^{-6}, and 0.59, respectively. (D) Nascent and spliced RNA levels of *mCherry* driven from WT or mutated *hsp-16.2* promoters at MosSCI insertion, normalized to *its-1*. Values are shown for HSE1/2^{mt}, HSAS^{mt}, and WT, color-coded as in B. (E) HSF-1 is essential for peripheral targeting of the *hsp-16.2* tg #1 both before and after HS. Quantification of positions of the GFP-lacI signal for progeny from control RNAi or *hsf-1* RNAi fed adult progeny as in Fig. 2 B. Zone 1 scoring, asterisks, and hatching are defined the same as in Fig. 2 (B and C). Numbers counted were (left to right) n = 681, 704, 281, and 244. P-values versus random = 3×10^{-4}, 3×10^{-7}, 0.16, and 0.07, respectively. (F) Quantitation of GFP-lacI focus position for WT or mutated *hsp-16.2* promoter MosSCI inserts (coded as in B) and the *lacO*-tagged insert tel V in progeny of *hsf-1* RNAi fed adults. Scoring, asterisks, and hatching are as in Fig. 2 (B and C). Loci counted were (left to right) n = 309, 209, 367, 209, 339, 227, 95, 198, 346, 210, 329, 242, 347, 204, 91, and 209. P-values versus random = 0.02, 0.16, 0.80, 0.54, 0.73, 0.92, <0.01, <0.01, 3×10^{-5}, 0.56, 1×10^{-6}, 0.88, 1×10^{-6}, 0.86, <0.01, and <0.01, respectively.

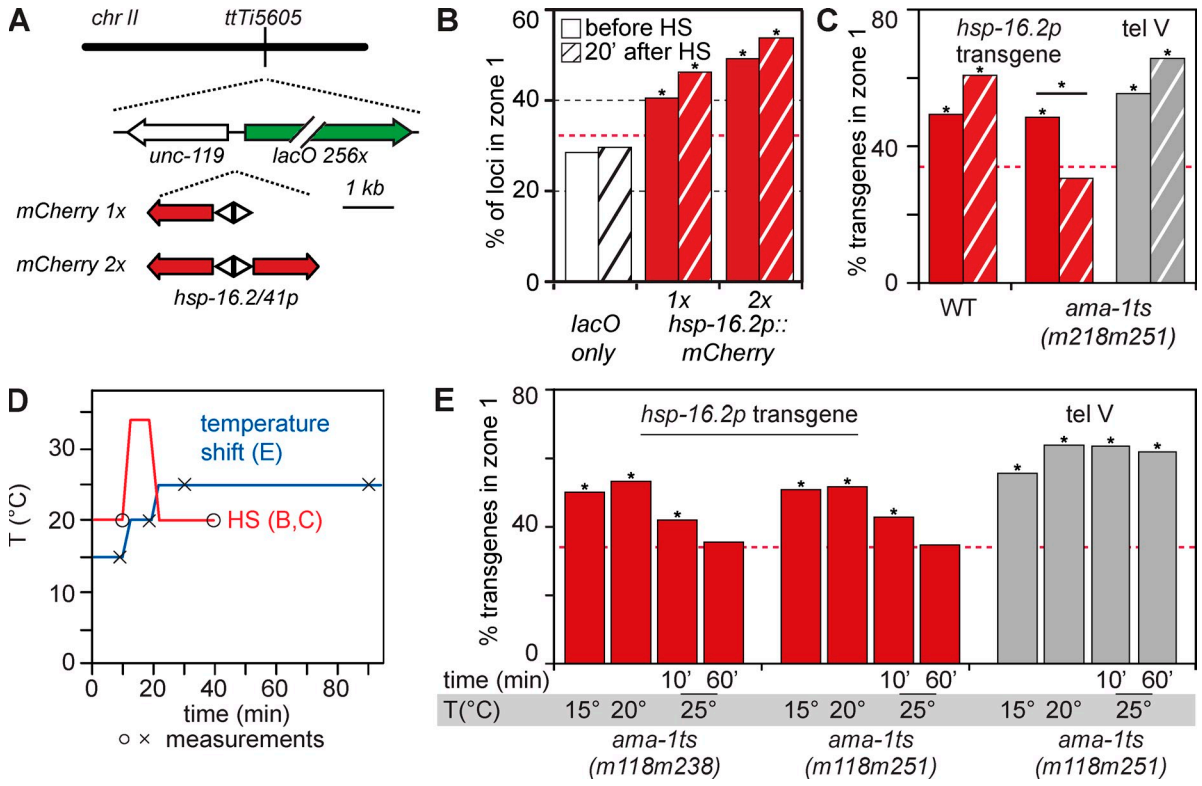

Figure 6. **Active RNA pol II is necessary for peripheral anchoring of the *hsp-16.2* promoter.** (A) MosSCI insertion at *ttTi5605* of the *hsp-16.2* promoter driving either one or two *mCherry* genes as indicated. The top shows control lacking the *hsp-16.2* promoter. (B) Quantitation of the GFP-lacI position for *lacO*-only control and uni- or bidirectional *hsp-16.2* promoter constructs (A). Scoring, zone 1 plotting, asterisks, and hatching are the same as in Fig. 2 (B and C). Loci counted were (left to right) n = 117, 95, 309, 346, 232, and 246. P-values versus random = 0.17, 0.31, 0.02, 3×10^{-5}, 7×10^{-7}, and 3×10^{-11}, respectively; for 1× versus 2× genes, both with and without HS, $P < 0.05$. (C) A thermosensitive (ts) mutation in RNA pol II AMA-1 impairs anchoring of the *hsp-16.2* tg #1. GFP-lacI signal positions in WT or *ama-1(m218m251)* embryos were scored and zone 1 values were plotted before and 20 min after HS (hatched), as in Fig. 2 (B and C). The *lacO*-tagged tel V insert in the same *ama-1*^{ts} background shows the opposite effect upon AMA-1 inactivation (HS). Loci counted were (left to right) n = 309, 346, 179, 96, 155, and 155. P-values versus random = 0.02, 3×10^{-5}, 6×10^{-5}, 0.39, 2×10^{-9}, and $<10^{-10}$, respectively. (D) Scheme of HS kinetics (red indicates samples in B and C) showing gradual temperature increase (E) testing *ama-1*^{ts} mutants for the *hsp-16.2* tg1 position. At × and ○, images were taken and quantified. (E) Progressive temperature increase in the indicated *ama-1* mutants releases *hsp-16.2* tg #1 without HS. Locus scoring, zone 1, and asterisks are the same as in Fig. 2 (B and C). Loci counted were (left to right) n = 186, 217, 208, 167, 199, 210, 256, 274, 85, 123, 76, and 39. P-values versus random = 6×10^{-6}, 1×10^{-8}, 0.02, 0.70, 4×10^{-6}, 3×10^{-7}, 0.01, 0.93, 2×10^{-5}, 1×10^{-12}, 3×10^{-8}, and 2×10^{-4}, respectively.

after HS, the *hsp-16.2* transgene was released from the nuclear rim (Fig. 5 E; 35% and 32% for *hsf-1* RNAi, vs. 50% and 55% control RNAi; n and p-values are given in the figure legend). A *myo-3* transgene showed no effect of *hsf-1* RNAi (unpublished data). We extended the analysis of *hsf-1(RNAi)* effects to the MosSCI-integrated *hsp-16.2::mCherry* construct. For the MosSCI insert with the *hsp-16.2* promoter intact or lacking either HSAS or HSE sites, HSF-1 was necessary for the peripheral enrichment scored either before or after HS (Fig. 5 F). As expected, *hsf-1(RNAi)* had no effect on the tagged tel V locus (Fig. 5 F). We conclude that HSF-1 binding to the *hsp-16.2* promoter is necessary for perinuclear localization, both before and after HS. This argues that NPC anchoring through the HSAS site after HS also depends on HSF-1, even though HSF-1 does not bind HSAS directly.

RNA pol II is essential for peripheral anchoring by the *hsp-16.2* promoter

Given that HSF-1 is necessary for pol II–dependent elongation, we next tested the role of pol II itself in NPC anchoring of the *hsp-16.2* promoter. To see if bidirectional transcription contributes to peripheral anchoring, we added a second *mCherry* gene between the promoter and the *lacO* sites at the MosSCI *ttTi5605* locus (Fig. 6 A). Peripheral localization increased significantly both before and after HS due to insertion of a second ORF (39% vs. 49% before HS and 44% vs. 53% after HS; Fig. 6 B). Thus, by doubling the amount of pol II bound (or the number of transcripts possible), we increased peripheral anchoring, both before and after HS.

To see if pol II itself was involved in the anchorage, we used two previously characterized thermo-sensitive alleles of the pol II large subunit, *ama-1(m118m238)* and *ama-1(m118m251)*. These mutations are in the catalytic subunit and appear to trigger pol II dissociation either because of loss of template binding (*m118m238* [C777Y, G1406R]) or to the disruption of contacts between AMA-1 and RPB-2, two core subunits of pol II (*m118m251* [C777Y, A364V]; Bowman et al., 2011). Animals homozygous for either mutation develop normally at 15–20°C, but arrest early in development at 25°C. At permissive temperature, *ama-1* mutants containing the *hsp-16.2* tg #1 support NE association, as in WT animals (Fig. 6 C, *ama-1ts*). However, after 10 min at 34°C, the *hsp-16.2* transgene

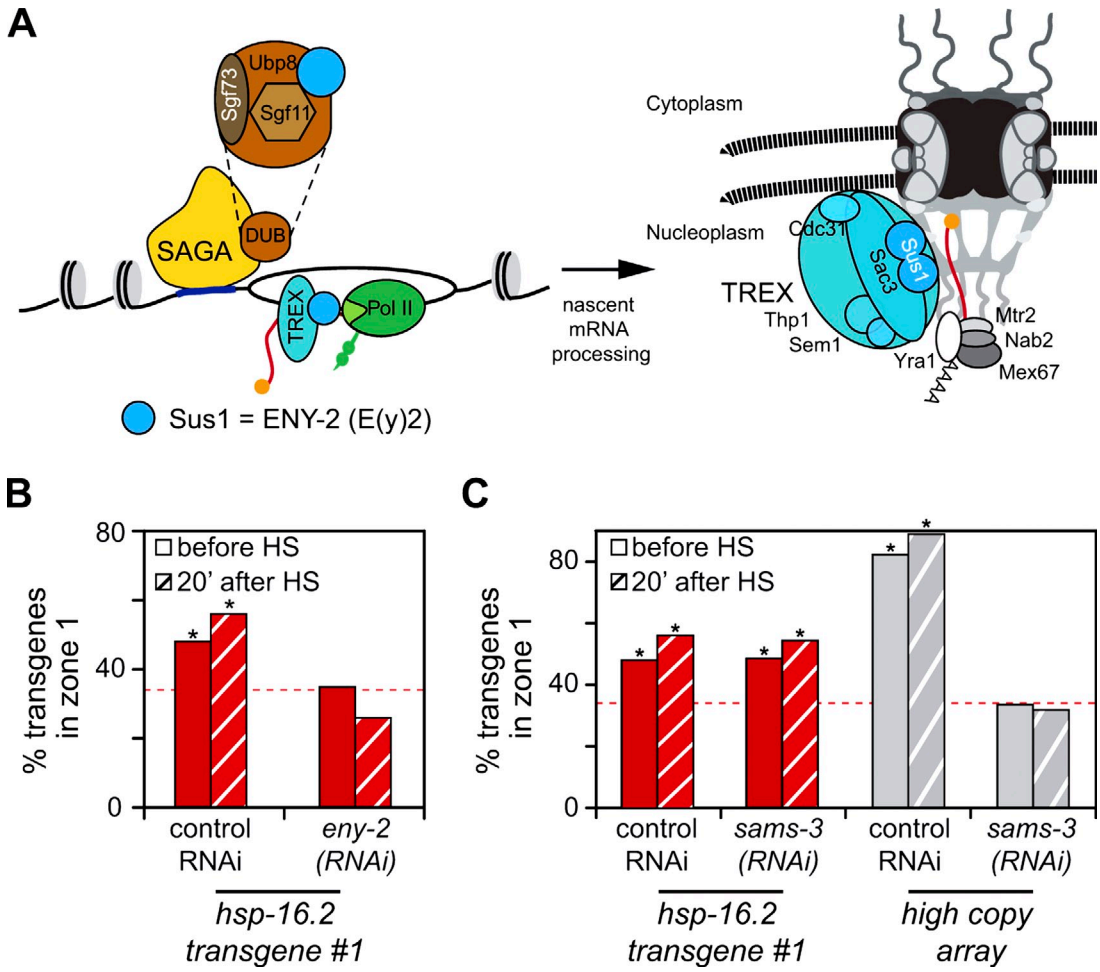

Figure 7. **The SAGA and THO/TREX component ENY-2 is required for peripheral positioning of *hsp-16.2* promoter.** (A) Sketch of budding yeast SAGA and THO/TREX complexes with yeast names (García-Oliver et al., 2012). The yeast subunit Sus1 (ENY-2, formerly e(y)2 in flies and T01C3.2 in worms) is present in both complexes (blue circle) and binds the nuclear basket. Other equivalents are Xmas-2 (*Sc*Sac3) and DSS1 (*Sc*Sem1). (B) Quantitation of *hsp-16.2* transgene 1 position in progeny from control RNAi or *eny-2(RNAi)* fed adults, scored before and after HS. Scoring, zone 1, asterisks, and hatched bars are as in Fig. 2 (B and C). Loci counted were (left to right) n = 681, 704, 157, and 157. P-values versus random = 3×10^{-4}, 3×10^{-7}, 0.65, and 0.55, respectively. (C) Peripheral position of *hsp-16.2* promoter tg #1 is unaffected by *sams-3* RNAi, unlike the heterochromatic *myo-3* array, GW76. GFP-lacI signals were scored in progeny of control RNAi or *sams-3* RNAi fed worms. Scoring, zone 1 plotting, and hatching are as in Fig. 2 (B and C). Loci counted were (left to right) n = 681, 704, 298, and 270. P-values versus random = 3×10^{-4}, 3×10^{-7}, 2×10^{-8}, and 2×10^{-13}, respectively.

became randomly distributed within the nucleus of mutant embryos (Fig. 6 C, WT vs. *ama-1ts*). This was not caused by a general release of chromatin from the NE, as the control tel V locus remains enriched in zone 1 upon pol II inactivation (Fig. 6 C, tel V). Engaged and active pol II is specifically involved in *hsp-16.2* transgene anchoring. Strikingly, even transient inactivation of pol II leads to release from the NPC.

Given that there is basal transcription of *hsp-16.2* under noninducing conditions (Fig. S3) and that the transgenes are peripherally enriched before HS induction, we examined whether progressive inactivation of pol II (AMA-1) by a step-wise temperature increase would ablate *hsp-16.2* transgene association with the NE. To test this, we took embryos from two *ama-1ts* mutant strains at a permissive temperature and increased the temperature while imaging (Fig. 6 D). Results are similar for both mutants: whereas *hsp-16.2* transgenes are enriched at the NE at a permissive temperature (15° or 20°C; Fig. 6 E), transgenes progressively lose their peripheral attachment after 10 min at 25°C, and are randomly distributed by 60 min (Fig. 6 E). In contrast, the peripherally located tel V insert was unaffected by temperature shift (Fig. 6 E). We conclude that enzymatically active pol II, either paused or actively transcribing, is necessary to anchor noninduced or induced *hsp-16.2* promoters to the NPC.

THO/TREX and anchoring and mRNA export complex factor ENY-2 bridges *hsp16.2* to NPC

Several complexes that stimulate both elongation and mRNA packaging and export are associated with engaged pol II. One such is the THO/TREX complex (García-Oliver et al., 2012; Fig. 7 A), which is implicated in the NPC anchoring of several yeast inducible genes and the *Drosophila Hsp70* cluster. Anchoring requires the *S. cerevisiae* Sus1 or *Drosophila* E(y)2/ENY2 subunit (Rodríguez-Navarro et al., 2004; Kurshakova et al., 2007; Kopytova et al., 2010), which has affinity for proteins of the inner nuclear pore basket (Kurshakova et al., 2007).

We examined the peripheral localization of the *hsp-16.2* transgenes before and after HS after *eny-2(RNAi)*. Indeed, *hsp-16.2*

transgene enrichment in zone 1 was lost without ENY-2 (Fig. 7 B, before HS, 35% vs. 44% for control RNAi), and HS treatment did not restore or improve NPC association (26% in zone 1 for *eny-2(RNAi)* vs. 56% for control RNAi; Fig. 7 B). In contrast, *eny-2(RNAi)* had no significant effect on *myo-3* transgene localization (unpublished data). Furthermore, *eny-2(RNAi)* delayed the appearance of mCherry fluorescence from 80 to 120 min after HS (Fig. S4), which is consistent with a profound effect on HS gene induction, processing, or export. We conclude that ENY-2 is essential both for anchoring the *hsp-16.2* transgene to NPCs and for maximum induction from the *hsp-16.2* promoter.

The *hsp-16.2*–NPC anchoring is distinct from the histone H3K9 methylation-dependent anchoring of heterochromatin, which is ablated by *sams-3(RNAi)* (Towbin et al., 2012). Down-regulation of S-adenosyl methyltransferases releases large heterochromatic arrays from the NE, but had no effect on the subnuclear distribution of the *hsp-16.2* transgene (Fig. 7 C).

Discussion

Several hypotheses have attempted to explain the logic of tethering highly transcribed genes at nuclear pores. Initially, Blobel proposed that targeting genes to pores would spatially facilitate mRNA export to distinct cytoplasmic domains in asymmetric cells, the so-called "gene gating" hypothesis (Blobel, 1985). Alternatively, pore-proximal localization was proposed to establish an epigenetic state that confers a transcriptional memory, facilitating reactivation of stress-inducible genes (Brickner et al., 2007). Other results suggested that the NPC could influence the fine-tuning of mRNA levels (for review see Akhtar and Gasser, 2007) or the degradation of nascent transcripts (Woolcock et al., 2012). Here we implicate specific promoter sequences and the trans-activator HSF-1 in the positioning of both the uninduced and induced *C. elegans hsp-16.2* gene at nuclear pores. We rule out chromosomal context and gene-specific intron or 3′ UTR sequences as major determinants of NE binding, and show instead that promoter-bound pol II, but not abundant mRNA, is essential for gene positioning.

The physiological significance of pore-proximal gene positioning has been tested in yeast, yet no function has been shown to be universally relevant (for reviews see Akhtar and Gasser, 2007; Dieppois and Stutz, 2010; Kind and van Steensel, 2010; Egecioglu and Brickner, 2011). In budding yeast, interaction with the NE was essential for maximal transcriptional activity of an inducible subtelomeric gene (Taddei et al., 2006), and the NPC tethering of nontelomeric genes facilitated derepression in the absence of activating factors (Brickner and Walter, 2004). However, in other cases such as ribosomal protein genes, *HSP104*, and some *GAL* loci, steady-state levels of mRNA were higher when genes were released from pores (Dieppois et al., 2006; Yoshida et al., 2010; Green et al., 2012). Similarly, transcripts of heat-induced fission yeast genes were kept low by the action of pore-associated Dicer (Woolcock et al., 2012). This diversity of phenotypes linked to gene–pore interaction most likely reflects locus-specific differences in their modes of activation, or in pathways of processing and export.

In metazoans, the association of the X chromosome in male flies contributes to the up-regulation of mRNAs (for review see Akhtar and Gasser, 2007), whereas the *Drosophila HSP70* locus was found near the NE both before and after HS in cultured S2 cells (Kurshakova et al., 2007). The down-regulation of E(y)2/ENY2 led to the release of *HSP70* from the NE of S2 cells, and reduced mRNA by ∼50% (Kurshakova et al., 2007), although in fly imaginal discs the same locus was not uniformly peripheral (Yao et al., 2007). These results suggest, but do not prove, that NPC association correlates with control over mature mRNA levels in metazoan cells.

Intriguingly, transcription of yeast *INO1* and *GAL1* was not required either for the establishment or maintenance of their perinuclear positioning (Schmid et al., 2006; Brickner et al., 2007). Analogously, the induced ectopic *C. elegans hsp-16.2* promoter was strongly enriched at the NE in the absence of HSF-1 binding sites, although the production of full-length mRNA was significantly impaired (Fig. 5, C and D). The perinuclear positioning of the *hsp-16.2* promoter is nonetheless sensitive to the loss of functional pol II both before and after HS. Reconciling these results, we propose that either a paused polymerase, or short pol II–dependent transcripts, drive association of *C. elegans* genes with the NPC.

The *hsp-16.2* promoter autonomously determines perinuclear localization

By inserting a 394-bp *hsp-16.2* promoter, either as a low-copy number array or as a single-copy MosSCI insert, we found that perinuclear positioning is intrinsic to the promoter sequence. No sequence was shown to drive positioning of the *Drosophila Hsp70* locus (Kurshakova et al., 2007), whereas in yeast, a short "DNA zip code" called gene recruitment sequence I (GRS-I) led to NPC association when inserted ectopically (Ahmed et al., 2010). Intriguingly, at the endogenous yeast *INO1* locus, pore targeting required an inositol-dependent event, which suggests that a change in either transcription factor affinity or in surrounding sequences can alter the positioning of the uninduced locus (Ahmed et al., 2010).

In our case, HSF-1 down-regulation, as well as conditional mutations that trigger pol II release from the template, impaired NE localization both before and after HS (Figs. 5 and 6). We propose that the recruitment of additional factors upon HS allows a HSE-deficient promoter to confer perinuclear localization but not to support induced gene expression. A similar situation may occur in budding yeast, where relocalization of GRS-I–containing promoters required transcriptional induction and binding of Put3, an activating transcription factor (Ahmed et al., 2010; Brickner et al., 2012). At *hsp.16.2*, the relevant factor is likely to be the NPC-binding Sus1 homologue, ENY-2, part of SAGA and THO/TREX (Fig. 8).

Our ability to exploit well-characterized ts mutants of the large pol II RPB1 subunit (AMA-1 in worms) allowed us to show that functional pol II is essential for NE positioning of *hsp-16.2*. Loss of template binding (*m118m238* [C777Y, G1406R]) or loss of interaction between the two core subunits AMA-1 and RPB-2 (*m118m251* [C777Y, A364V]; Bowman et al., 2011) compromise the perinuclear enrichment of the *hsp-16.2* promoter both before and after HS. Consistent with the notion that pol II is engaged at an uninduced *hsp-16.2* promoter,

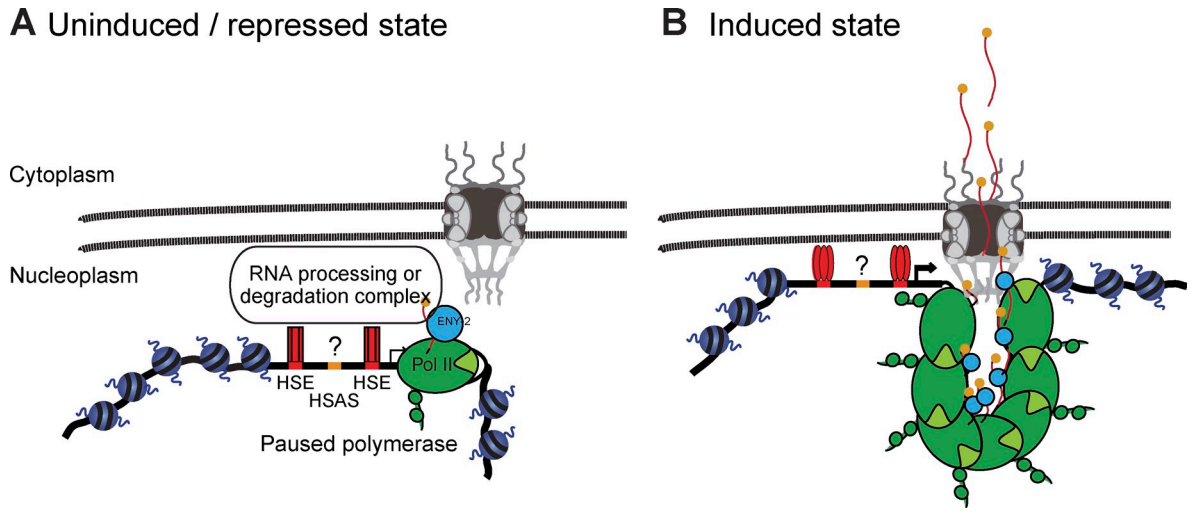

Figure 8. **Model of *hsp-16.2* positioning in relation to NPC before and after stress induction.** Model based on the results presented, proposing that *hsp-16.2* binds nuclear pores before and after HS in a similar manner, except that before HS nascent RNA is degraded and after HS it is efficiently spliced and exported. See text for details.

genome-wide mapping revealed endogenous *hsp-16.2* transcripts under normal embryonic growth conditions (www.modencode.org), which we confirmed by RT-PCR of *hsp-16.2* promoter-driven *mCherry* transcripts (Fig. S3). ModEncode ChIP data (www.modencode.org) suggest the presence of pol II along the entire *hsp-16.2* gene before HS, with enrichment of its unphosphorylated form in the promoter. Small RNAs were detected at the 5′ end of the gene, arguing that pol II may be stalled or nonproductively engaged at the *hsp-16.2* promoter. These results suggest the presence of engaged pol II before HS. However, the *hsp-16.2p::mCherry* reporter is peripheral before HS, with extremely low levels of spliced *mCherry* mRNA (Fig. S3), and some mutant promoters supported relocation (HSE^{mt}) without supporting induced transcription (Fig. 5). Thus, processed mRNA (as opposed to engaged pol II) is unlikely to be the critical link to the NE.

In *Drosophila* and other organisms, paused pol II is found 30–50 bp away from the *HSP70* TSS (Levine, 2011). Two complexes, negative elongation factor (NELF) and DRB sensitivity–inducing factor (DSIF) bind the nascent transcript, and DSIF is phosphorylated by P-TEFb, a cyclin/Cdk complex, to release paused pol II (Levine, 2011). There is no reported homologue of NELF in *C. elegans* (Baugh et al., 2009), but the *C. elegans* DSIF homologue has been shown to repress transcription of *hsp-16.2* (Shim et al., 2002). From our studies, we conclude that perinuclear anchoring of the uninduced *hsp-16.2* is mediated by a complex based either on engaged pol II or on the unprocessed mRNA itself, and that factors associated with an engaged pol II, such as the ENY-2–containing THO/TREX complex or SAGA-associated DUB, are likely tethers (Fig. 8). Consistently, loss of ENY-2 correlated with loss of peripheral enrichment of the *hsp-16.2* transgene.

Strong colocalization of the *hsp-16.2* promoter with NPC after induction

Our study demonstrates by super-resolution microscopy that after HS induction, the majority of *hsp-16.2* transgenes colocalize with the NPC, whereas before HS the same transgene is near but not overlapping with nuclear pores (Fig. 3). Similarly, ChIP results show enriched pore association, and a drop in LEM-2 association, after HS. Thus, gene induction coincides with a shift of the *hsp-16.2* promoter from a site near pores to direct NPC colocalization, where it remains even after a return to 22°C. This is consistent with two related modes of association, both dependent on pol II, but one being enhanced by nascent transcript.

Rapid induction and rapid repression: the dual function of nuclear pores?

Locus retention at the pore after HS, despite a return to 22°C, could also reflect a process that either degrades or delays processing of the induced mRNA, triggered by the return to non-HS conditions. Indeed, NPC association may promote both message processing and export, as well as degradation, depending on the transcription factors bound to the promoter, and perhaps their phosphorylation status. It is noteworthy that in mammalian cells, c-Myc appears to regulate not only induction of c-Myc regulated genes, but also the stability of the resulting mRNA in the cytoplasm (Rounbehler et al., 2012).

Based on recent results in fission yeast (Woolcock et al., 2012), we propose that pol II– and mRNA-mediated association of stress-inducible genes with nuclear pores has evolved to control genes that require rapid induction, rapid repression, and efficient clearance of unwanted mRNA once conditions change. In *S. pombe*, a set of divergently transcribed heat-induced genes were seen to be repressed cotranscriptionally by the RNAi machinery (Woolcock et al., 2012). Intriguingly, at least some of these genes are targeted to the NPC for induction, and remain there after the shift back to noninducing conditions (Woolcock et al., 2012). RNA degradation, or simply impaired processing of unspliced mRNAs, may be used to down-regulate temperature-induced genes once the stress is no longer present. It will be interesting to test whether enzymes that control splicing or co-transcriptional RNA degradation also contribute to the persistent NPC localization of HS-induced genes in *C. elegans*.

Materials and methods

Transgenic strains and molecular biology

Standard *C. elegans* culture conditions and crossing procedures were used. Unless otherwise stated, worms were maintained at 22.5°C. GFP-lacI was expressed from *gwIs39[baf-1::GFP-lacI; vit-5::GFP]*. For strains bearing more than one large array, integrations were performed separately and backcrossed to WT worms before crossing strains. A full strains list is available in Table S1. Note that although a blastP of T01C3.2 against fly or human protein databases does not detect ENY2, the *Brugia malayi* homologue of T01C3.2 detects ENY2 in both flies and mammals (WormBase).

Cloning of *hsp-16.2p::mCherry* constructs

The *hsp-16.2* WT promoter construct driving *mCherry* expression was obtained by replacing GFP in pPD49.78 by *WmCherry*. *hsp-16.2* promoter constructs containing mutations in HSE or HSAS sites were created by replacing the promoter in pPD49.78 with the mutated promoters described in GuhaThakurta et al. (2002). Specifically, the original sequence of HSE (5′-TTCTAGAA-3′) was replaced by 5′-CCTGGAGG-3′, and the original HSAS sequence (5′-GGGTCTC-3′) was replaced by 5′-ATAGAGA-3′. Insertion of *lacO* repeats at *ttTi5605* (middle of chr II) was achieved by cloning the repeats from pSR1 (Rohner et al., 2008) into pCJ151 (Frøkjaer-Jensen et al., 2008). To insert *hsp-16.2::mCherry* constructs at *ttTi5605*, *hsp-16.2::mCherry* fusions (WT or mutated promoter versions) were inserted in pCFJ151-*lacO*. For the bidirectional promoter construct, the *mCherry* coding sequence was obtained by PCR and was inserted in appropriately digested pPD49.78-*mCherry*. Insertion of *lacO* repeats on tel V was achieved using *Mos* insertion *ttTi9115* (right arm of chr V). The *myo-3::mCherry* promoter fusion used is described in Meister et al. (2010b).

Small transgenes were obtained by microparticle co-bombardment of *hsp-16.2::mCherry* with a *lacO* repeat construct (pSR1) (Rohner et al., 2008) and the *unc-119* rescuing construct (Fig. 2 D). In brief, worms were bombarded with micrometer-sized gold beads loaded with DNA. Bombardment leads to the formation of small-sized transgenes containing 10–100 cointegrated plasmids (Praitis, 2006). Strains were backcrossed to *unc-119(ed3)* III parents after integration. MosSCI strains were obtained according to the method of Frøkjaer-Jensen et al. (2008), a method based on homologous recombination targeted to transposon sites, through either a direct or indirect method.

FISH

For the single-gene FISH, cosmid F36H9 and a plasmid covering *hsp-16.2* were labeled with Alexa Fluor 555 and Alexa Fluor 647, respectively, using the FISHTag kit (Invitrogen). FISH was performed as follows: embryos from bleached worms were fixed for 5 min in 2% PFA and spread on poly-L-lysine–coated slides. They were freeze-cracked on dry ice before 2 min of dehydration in 100% ethanol. Slides were washed in SSC, treated with RNase, and dehydrated progressively in 70%, 85%, 95%, and 100% ethanol, then air-dried for 5 min. The sample was denatured with heat after probe addition. Probe and samples were incubated overnight at 37°C before stringent washes in SSC buffers. Samples were DAPI-stained quickly before mounting in ProLong Gold antifade (Invitrogen). Image acquisition was performed at room-temperature on a widefield microscope (DeltaVision; Olympus IX70) with a UPlan-SApochromat 100×/1.4 NA UIS2 oil objective lens, a charge-coupled device (CCD) camera (HQ CoolSNAP; Photometrics), and SoftWoRx software (Fig. 2 C). Samples were deconvolved using the multidimensional deconvolution software Huygens (Scientific Volume Imaging), and position scoring relative to nuclear periphery was determined with ImageJ software (National Institutes of Health) using the Point Picker plugin (http://bigwww.epfl.ch/thevenaz/pointpicker). This experiment was performed twice.

Immunofluorescence staining for SIM

For immunostaining, embryos were fixed for 5 min in 2% PFA before freeze-cracking, followed by dehydration in −20°C 100% ethanol. After three washes in PBS and 0.25% Triton X-100 (PBS-T), slides were blocked in PBS-T 0.5% BSA before 1 h of incubation with primary antibody (mAB414 [ab24609; Abcam]; anti–LMN-1 [a gift of Y. Gruenbaum, The Hebrew University of Jerusalem, Jerusalem, Israel]; or anti-GFP [D153_3; MBL]) at RT. After three washes with PBS-T, samples were incubated for 1 h with secondary antibodies (Alexa Fluor 488 anti–rabbit and Alexa Fluor 555 anti–mouse [Fig. 3 A], or Alexa Fluor 488 anti–rat, Alexa Fluor 555 anti–mouse, and Alexa Fluor 647 anti–rabbit [Fig. 3, B–D]; Invitrogen) at RT before final washes and DNA staining with Hoechst 33258.

Microscopy and quantitation

Live microscopy was performed on 2% agarose pads at room temperature. For microscopy of embryos, a spinning disk multipoint confocal microscope (AxioImager M1 [Carl Zeiss] + Yokogawa CSU-22 scan head, plan-Neo-Fluar 100×/1.45 NA oil objective lens, an EM-CCD camera [Cascade II; Photometrics], and MetaMorph 7.7.2 software [Molecular Devices]) was used (Figs. 1, 2 [E, F, and H], 5 [C, E, and F], 6 [B, C, and E], and 7 [B and C]). For each picture, a stack with a z spacing of 0.2 µm was taken and deconvolved using the multidimensional deconvolution software Huygens (Scientific Volume Imaging). 3D reconstructions used Imaris software (Bitplane). For quantitative analysis of arrays, transgenes, and locus position, measurements were made with ImageJ using Point Picker, and scoring of radial positioning of endogenous loci and GFP-lacI–tagged transgenes were performed as described in Meister et al. (2010a). In brief, through-focus stacks of images are acquired at 200-nm intervals, and in the plane of the fluorescent locus, the nuclear cross section is divided in three concentric zones of equal surface area. To score spot position, the ratio of the distance from spot center to periphery (black line) over the nuclear radius (red line/2) is determined for many foci, which are binned into zones 1–3, such that a random localization would imply 33% in each zone. All scoring was performed on at least two biologically independent experiments. Significance of locus distribution relative to a random distribution was performed using a χ^2 test with a degree of freedom of 2, when an entire distribution is compared with a random distribution, whereas the significance of changes in two test conditions (e.g., zone 1 in ±HS) was determined using the Fisher's exact test. For position scoring on SR-SIM microscopy, single sections with *lacO*/GFP-lacI spots were scored relative to the NPC and lamina. The transgene position analysis (Fig. 3 E) is based on two independent experiments, scored by two independent researchers.

Z projections of embryos were done in ImageJ using maximal intensity projection. High-resolution imaging was done with a super-resolution structured illumination microscope (Elyra S.1 [Carl Zeiss], Plan-Apochromat 63×/1.4 NA objective lens, EM-CCD camera [iXon 885; Andor Technology], and ZEN Blue 2010 D software [Carl Zeiss]; Fig. 3) at RT. Processing was performed with Zen software (Carl Zeiss) and 3D reconstruction and analysis was performed with Imaris software.

The Lamin Dam-ID study shown in Fig. 2 A was performed as described previously (Towbin et al., 2012) using LMN-1-Dam-ID data from three biological replicates of WT *C. elegans* embryos.

Temperature shift experiments

For HS, the embryos or worms were shifted to 34°C for 10 min either in a slide incubator for a PCR machine or in a water bath. For gradual increase of temperature on the microscope stage, embryos from adults grown at 15°C were transferred on 2% agarose pads on a mini-stage temperature controller (CB164-V1; EMBL). Embryos were imaged at 15°C, temperature was shifted at 20°C, then at 25°C. Pictures were taken always after a 10-min incubation, and, while at 25°C, images were taken again after 1 h.

RNAi experiments

RNAi was performed by feeding on plates as described previously with minor adaptations (Timmons et al., 2001). Worms were put on the feeding plates either as L4 and left for 24 h (*hsf-1*, *eny-2*) or left for two generations on RNAi plates starting with synchronized L1s (*sams-3*). An EcoRV fragment containing 25 bp of perfect identity to GFP-LacI was removed from vector L4440 (Fire vector library) and used as a mock RNAi control.

RNA extraction and qPCR

Extraction of RNA was performed on embryos according to the WormBook protocol (Stiernagle, 2006). The RNA was purified using the RNeasy kit (catalog no. 74104; QIAGEN) including DNase treatment. Reverse transcription PCR was done with ProtoScript AMV First Strand cDNA Synthesis kit (E6550S; New England Biolabs, Inc.). Real-time qPCR was done with GoTaq qPCR Master Mix with an ABI 7500 Fast qPCR machine. Primer sequences can be found in Table S2. The data shown in Fig. 5 (A and D) were obtained by RNA extraction of two independent experiments.

ChIP-qPCR

Standard worm culture techniques were used to obtain embryos from GW615 strain in S liquid media (Stiernagle, 2006). Embryos in M9 buffer were divided into two aliquots: one aliquot was subsequently incubated in 34°C M9 buffer for 10 min (HS), while the other aliquot was incubated in 20°C M9 buffer for 10 min (non-HS). Embryos were further incubated in buffer at 25°C for 10 min and then cross-linked in 2% formaldehyde

solution. Chromatin extracts were prepared by sonicating the cross-linked embryos in FA buffer (50 mM Hepes/KOH, pH 7.5, 1 mM EDTA, 1% Triton X-100, 0.1% sodium deoxycholate, and 150 mM NaCl). ChIP was performed by incubating the chromatin extract with anti–NPP-13 or anti–LEM-2 antibodies immobilized onto Protein A–conjugated Sepharose beads (Ikegami et al., 2010). Affinity-purified rabbit polyclonal antibodies for NPP-13 (aa 667–766; SDQ4094) and for LEM-2 (aa 1–100; SDQ4051) were produced by genetic immunization at SDIX. After 12 cycles of ligation-mediated PCR amplification, the ChIP DNA was quantified using real-time PCR amplification monitored by a SYBR green dye in a PCR instrument (7900HT; Applied Biosystems). ChIP enrichment represented by an amount of ChIP DNA ([ChIP]) over an amount of input DNA ([Input]) at a given locus was calculated by: $[ChIP]/[Input] = 2^{(CT_{input} - CT_{chip})/PCR\ efficiency}$, where CT*input* and CT*chip* are Ct (threshold cycle) values for input and ChIP DNA, respectively. PCR efficiencies for primer pairs were: ctrl1, 0.998; ctrl2, 0.971; en1, 1.034; en2, 1.044; ec1, 0.951; and ec2, 1.002.

Online supplemental material

Fig. S1 shows controls for the HS induced integrated array of *hsp-16.2* promoters (Fig. 1). Fig. S2 shows quantification by real-time PCR of the number of plasmids present in the small arrays carrying *hsp-16.2::mCherry* (Fig. 2). Fig. S3 shows that PCR amplification detects *mCherry* mRNA in a reverse transcription–dependent manner. Fig. S4 shows mCherry protein detection after HS induction. Video 1 shows 3D reconstruction of WT *C. elegans* embryos stained for nuclear pores and nuclear lamina (Fig. 3). Table S1 gives an overview of *C. elegans* strains used including genetic details. Table S2 gives an overview of primers used. Online supplemental material is available at http://www.jcb.org/cgi/content/full/jcb.201207024/DC1. Additional data are available in the JCB DataViewer at http://dx.doi.org/10.10831/jcb.201207024.dv.

We thank Y. Gruenbaum for antibodies; M. Thomas, R. Arpagaus, and I. Katic for assistance; I. Katic, the *Caenorhabditis* Genetics Center, D. Riddle, and P. Sternberg for strains; C. Link for plasmids; and R. Thierry, J. Pielage, L. Gelman, and S. Bourke for microscopy support.

This work was supported by the Novartis Research Foundation and the "Fondation Suisse de Recherche sur les Maladies Musculaires."

Submitted: 3 July 2012
Accepted: 31 January 2013

References

Ahmed, S., D.G. Brickner, W.H. Light, I. Cajigas, M. McDonough, A.B. Froyshteter, T. Volpe, and J.H. Brickner. 2010. DNA zip codes control an ancient mechanism for gene targeting to the nuclear periphery. *Nat. Cell Biol.* 12:111–118. http://dx.doi.org/10.1038/ncb2011

Akhtar, A., and S.M. Gasser. 2007. The nuclear envelope and transcriptional control. *Nat. Rev. Genet.* 8:507–517. http://dx.doi.org/10.1038/nrg2122

Baugh, L.R., J. Demodena, and P.W. Sternberg. 2009. RNA Pol II accumulates at promoters of growth genes during developmental arrest. *Science*. 324:92–94. http://dx.doi.org/10.1126/science.1169628

Blobel, G. 1985. Gene gating: a hypothesis. *Proc. Natl. Acad. Sci. USA*. 82: 8527–8529. http://dx.doi.org/10.1073/pnas.82.24.8527

Bowman, E.A., D.L. Riddle, and W. Kelly. 2011. Amino acid substitutions in the *Caenorhabditis elegans* RNA polymerase II large subunit AMA-1/RPB-1 that result in α-amanitin resistance and/or reduced function. *G3 (Bethesda)*. 1:411–416. http://dx.doi.org/10.1534/g3.111.000968

Brickner, J.H., and P. Walter. 2004. Gene recruitment of the activated INO1 locus to the nuclear membrane. *PLoS Biol.* 2:e342. http://dx.doi.org/10.1371/journal.pbio.0020342

Brickner, D.G., I. Cajigas, Y. Fondufe-Mittendorf, S. Ahmed, P.C. Lee, J. Widom, and J.H. Brickner. 2007. H2A.Z-mediated localization of genes at the nuclear periphery confers epigenetic memory of previous transcriptional state. *PLoS Biol.* 5:e81. http://dx.doi.org/10.1371/journal.pbio.0050081

Brickner, D.G., S. Ahmed, L. Meldi, A. Thompson, W. Light, M. Young, T.L. Hickman, F. Chu, E. Fabre, and J.H. Brickner. 2012. Transcription factor binding to a DNA zip code controls interchromosomal clustering at the nuclear periphery. *Dev. Cell*. 22:1234–1246. http://dx.doi.org/10.1016/j.devcel.2012.03.012

Cabal, G.G., A. Genovesio, S. Rodriguez-Navarro, C. Zimmer, O. Gadal, A. Lesne, H. Buc, F. Feuerbach-Fournier, J.C. Olivo-Marin, E.C. Hurt, and U. Nehrbass. 2006. SAGA interacting factors confine sub-diffusion of transcribed genes to the nuclear envelope. *Nature*. 441:770–773. http://dx.doi.org/10.1038/nature04752

Casolari, J.M., C.R. Brown, S. Komili, J. West, H. Hieronymus, and P.A. Silver. 2004. Genome-wide localization of the nuclear transport machinery couples transcriptional status and nuclear organization. *Cell*. 117:427–439. http://dx.doi.org/10.1016/S0092-8674(04)00448-9

Dieppois, G., and F. Stutz. 2010. Connecting the transcription site to the nuclear pore: a multi-tether process that regulates gene expression. *J. Cell Sci.* 123:1989–1999. http://dx.doi.org/10.1242/jcs.053694

Dieppois, G., N. Iglesias, and F. Stutz. 2006. Cotranscriptional recruitment to the mRNA export receptor Mex67p contributes to nuclear pore anchoring of activated genes. *Mol. Cell. Biol.* 26:7858–7870. http://dx.doi.org/10.1128/MCB.00870-06

Egecioglu, D., and J.H. Brickner. 2011. Gene positioning and expression. *Curr. Opin. Cell Biol.* 23:338–345. http://dx.doi.org/10.1016/j.ceb.2011.01.001

Fernandes, M., H. Xiao, and J.T. Lis. 1994. Fine structure analyses of the *Drosophila* and *Saccharomyces* heat shock factor—heat shock element interactions. *Nucleic Acids Res.* 22:167–173. http://dx.doi.org/10.1093/nar/22.2.167

Frøkjaer-Jensen, C., M.W. Davis, C.E. Hopkins, B.J. Newman, J.M. Thummel, S.P. Olesen, M. Grunnet, and E.M. Jorgensen. 2008. Single-copy insertion of transgenes in *Caenorhabditis elegans*. *Nat. Genet.* 40:1375–1383. http://dx.doi.org/10.1038/ng.248

García-Oliver, E., V. García-Molinero, and S. Rodríguez-Navarro. 2012. mRNA export and gene expression: The SAGA-TREX-2 connection. *Biochim. Biophys. Acta*. 1819:555–565. http://dx.doi.org/10.1016/j.bbagrm.2011.11.011

Gerstein, M.B., Z.J. Lu, E.L. Van Nostrand, C. Cheng, B.I. Arshinoff, T. Liu, K.Y. Yip, R. Robilotto, A. Rechtsteiner, K. Ikegami, et al. 2010. Integrative analysis of the *Caenorhabditis elegans* genome by the modENCODE project. *Science*. 330:1775–1787. http://dx.doi.org/10.1126/science.1196914

Green, E.M., Y. Jiang, R. Joyner, and K. Weis. 2012. A negative feedback loop at the nuclear periphery regulates GAL gene expression. *Mol. Biol. Cell*. 23:1367–1375. http://dx.doi.org/10.1091/mbc.E11-06-0547

Guertin, M.J., and J.T. Lis. 2010. Chromatin landscape dictates HSF binding to target DNA elements. *PLoS Genet.* 6:e1001114. http://dx.doi.org/10.1371/journal.pgen.1001114

Guertin, M.J., S.J. Petesch, K.L. Zobeck, I.M. Min, and J.T. Lis. 2010. *Drosophila* heat shock system as a general model to investigate transcriptional regulation. *Cold Spring Harb. Symp. Quant. Biol.* 75:1–9. http://dx.doi.org/10.1101/sqb.2010.75.039

GuhaThakurta, D., L. Palomar, G.D. Stormo, P. Tedesco, T.E. Johnson, D.W. Walker, G. Lithgow, S. Kim, and C.D. Link. 2002. Identification of a novel cis-regulatory element involved in the heat shock response in *Caenorhabditis elegans* using microarray gene expression and computational methods. *Genome Res.* 12:701–712. http://dx.doi.org/10.1101/gr.228902

Hajdu-Cronin, Y.M., W.J. Chen, and P.W. Sternberg. 2004. The L-type cyclin CYL-1 and the heat-shock-factor HSF-1 are required for heat-shock-induced protein expression in *Caenorhabditis elegans*. *Genetics*. 168:1937–1949. http://dx.doi.org/10.1534/genetics.104.028423

Heitz, E. 1928. Das Heterochromatin der Moose. *Jahrbücher für wissenschaftliche Botanik*. 69:762–818.

Hu, Y., I. Kireev, M. Plutz, N. Ashourian, and A.S. Belmont. 2009. Large-scale chromatin structure of inducible genes: transcription on a condensed, linear template. *J. Cell Biol.* 185:87–100. http://dx.doi.org/10.1083/jcb.200809196

Hu, Y., M. Plutz, and A.S. Belmont. 2010. Hsp70 gene association with nuclear speckles is Hsp70 promoter specific. *J. Cell Biol.* 191:711–719. http://dx.doi.org/10.1083/jcb.201004041

Ikegami, K., T.A. Egelhofer, S. Strome, and J.D. Lieb. 2010. *Caenorhabditis elegans* chromosome arms are anchored to the nuclear membrane via discontinuous association with LEM-2. *Genome Biol.* 11:R120. http://dx.doi.org/10.1186/gb-2010-11-12-r120

Ishii, K., G. Arib, C. Lin, G. Van Houwe, and U.K. Laemmli. 2002. Chromatin boundaries in budding yeast: the nuclear pore connection. *Cell*. 109: 551–562. http://dx.doi.org/10.1016/S0092-8674(02)00756-0

Kalverda, B., and M. Fornerod. 2010. Characterization of genome-nucleoporin interactions in *Drosophila* links chromatin insulators to the nuclear pore complex. *Cell Cycle*. 9:4812–4817. http://dx.doi.org/10.4161/cc.9.24.14328

Kind, J., and B. van Steensel. 2010. Genome-nuclear lamina interactions and gene regulation. *Curr. Opin. Cell Biol.* 22:320–325. http://dx.doi.org/10.1016/j.ceb.2010.04.002

Kopytova, D.V., A.V. Orlova, A.N. Krasnov, D.Y. Gurskiy, J.V. Nikolenko, E.N. Nabirochkina, Y.V. Shidlovskii, and S.G. Georgieva. 2010. Multifunctional factor ENY2 is associated with the THO complex and promotes its recruitment onto nascent mRNA. *Genes Dev.* 24:86–96. http://dx.doi.org/10.1101/gad.550010

Kurshakova, M.M., A.N. Krasnov, D.V. Kopytova, Y.V. Shidlovskii, J.V. Nikolenko, E.N. Nabirochkina, D. Spehner, P. Schultz, L. Tora, and S.G. Georgieva. 2007. SAGA and a novel *Drosophila* export complex anchor efficient transcription and mRNA export to NPC. *EMBO J.* 26:4956–4965. http://dx.doi.org/10.1038/sj.emboj.7601901

Levine, M. 2011. Paused RNA polymerase II as a developmental checkpoint. *Cell*. 145:502–511. http://dx.doi.org/10.1016/j.cell.2011.04.021

Link, C.D., J.R. Cypser, C.J. Johnson, and T.E. Johnson. 1999. Direct observation of stress response in *Caenorhabditis elegans* using a reporter transgene. *Cell Stress Chaperones*. 4:235–242. http://dx.doi.org/10.1379/1466-1268(1999)004<0235:DOOSRI>2.3.CO;2

Meister, P., L.R. Gehlen, E. Varela, V. Kalck, and S.M. Gasser. 2010a. Visualizing yeast chromosomes and nuclear architecture. *Methods Enzymol.* 470:535–567. http://dx.doi.org/10.1016/S0076-6879(10)70021-5

Meister, P., B.D. Towbin, B.L. Pike, A. Ponti, and S.M. Gasser. 2010b. The spatial dynamics of tissue-specific promoters during *C. elegans* development. *Genes Dev.* 24:766–782. http://dx.doi.org/10.1101/gad.559610

Meister, P., S. Mango, and S.M. Gasser. 2011. Locking the genome: nuclear organization and cell fate. *Curr. Opin. Genet. Dev.* 21:167–174. http://dx.doi.org/10.1016/j.gde.2011.01.023

Petesch, S.J., and J.T. Lis. 2012. Activator-induced spread of poly(ADP-ribose) polymerase promotes nucleosome loss at Hsp70. *Mol. Cell*. 45:64–74. http://dx.doi.org/10.1016/j.molcel.2011.11.015

Praitis, V. 2006. Creation of transgenic lines using microparticle bombardment methods. *Methods Mol. Biol.* 351:93–107.

Rodríguez-Navarro, S., T. Fischer, M.J. Luo, O. Antúnez, S. Brettschneider, J. Lechner, J.E. Pérez-Ortín, R. Reed, and E. Hurt. 2004. Sus1, a functional component of the SAGA histone acetylase complex and the nuclear pore-associated mRNA export machinery. *Cell*. 116:75–86. http://dx.doi.org/10.1016/S0092-8674(03)01025-0

Rohner, S., S.M. Gasser, and P. Meister. 2008. Modules for cloning-free chromatin tagging in *Saccharomyces cerevisae*. *Yeast*. 25:235–239. http://dx.doi.org/10.1002/yea.1580

Rougvie, A.E., and J.T. Lis. 1988. The RNA polymerase II molecule at the 5′ end of the uninduced hsp70 gene of *D. melanogaster* is transcriptionally engaged. *Cell*. 54:795–804. http://dx.doi.org/10.1016/S0092-8674(88)91087-2

Rounbehler, R.J., M. Fallahi, C. Yang, M.A. Steeves, W. Li, J.R. Doherty, F.X. Schaub, S. Sanduja, D.A. Dixon, P.J. Blackshear, and J.L. Cleveland. 2012. Tristetraprolin impairs myc-induced lymphoma and abolishes the malignant state. *Cell*. 150:563–574. http://dx.doi.org/10.1016/j.cell.2012.06.033

Rouquette, J., C. Genoud, G.H. Vazquez-Nin, B. Kraus, T. Cremer, and S. Fakan. 2009. Revealing the high-resolution three-dimensional network of chromatin and interchromatin space: a novel electron-microscopic approach to reconstructing nuclear architecture. *Chromosome Res.* 17:801–810. http://dx.doi.org/10.1007/s10577-009-9070-x

Schmid, M., G. Arib, C. Laemmli, J. Nishikawa, T. Durussel, and U.K. Laemmli. 2006. Nup-PI: the nucleopore-promoter interaction of genes in yeast. *Mol. Cell*. 21:379–391. http://dx.doi.org/10.1016/j.molcel.2005.12.012

Shim, E.Y., A.K. Walker, Y. Shi, and T.K. Blackwell. 2002. CDK-9/cyclin T (P-TEFb) is required in two postinitiation pathways for transcription in the *C. elegans* embryo. *Genes Dev.* 16:2135–2146. http://dx.doi.org/10.1101/gad.999002

Stiernagle, T. 2006. Maintenance of *C. elegans. WormBook*. http://dx.doi.org/10.1895/wormbook.1.101.1

Strambio-De-Castillia, C., M. Niepel, and M.P. Rout. 2010. The nuclear pore complex: bridging nuclear transport and gene regulation. *Nat. Rev. Mol. Cell Biol.* 11:490–501. http://dx.doi.org/10.1038/nrm2928

Stringham, E.G., D.K. Dixon, D. Jones, and E.P. Candido. 1992. Temporal and spatial expression patterns of the small heat shock (hsp16) genes in transgenic *Caenorhabditis elegans*. *Mol. Biol. Cell*. 3:221–233.

Taddei, A., G. Van Houwe, F. Hediger, V. Kalck, F. Cubizolles, H. Schober, and S.M. Gasser. 2006. Nuclear pore association confers optimal expression levels for an inducible yeast gene. *Nature*. 441:774–778. http://dx.doi.org/10.1038/nature04845

Taddei, A., H. Schober, and S.M. Gasser. 2010. The budding yeast nucleus. *Cold Spring Harb. Perspect. Biol.* 2:a000612. http://dx.doi.org/10.1101/cshperspect.a000612

Timmons, L., D.L. Court, and A. Fire. 2001. Ingestion of bacterially expressed dsRNAs can produce specific and potent genetic interference in *Caenorhabditis elegans*. *Gene*. 263:103–112. http://dx.doi.org/10.1016/S0378-1119(00)00579-5

Towbin, B.D., P. Meister, B.L. Pike, and S.M. Gasser. 2010. Repetitive transgenes in *C. elegans* accumulate heterochromatic marks and are sequestered at the nuclear envelope in a copy-number- and lamin-dependent manner. *Cold Spring Harb. Symp. Quant. Biol.* 75:555–565. http://dx.doi.org/10.1101/sqb.2010.75.041

Towbin, B.D., C. González-Aguilera, R. Sack, D. Gaidatzis, V. Kalck, P. Meister, P. Askjaer, and S.M. Gasser. 2012. Step-wise methylation of histone H3K9 positions heterochromatin at the nuclear periphery. *Cell*. 150:934–947. http://dx.doi.org/10.1016/j.cell.2012.06.051

Trinklein, N.D., J.I. Murray, S.J. Hartman, D. Botstein, and R.M. Myers. 2004. The role of heat shock transcription factor 1 in the genome-wide regulation of the mammalian heat shock response. *Mol. Biol. Cell*. 15:1254–1261. http://dx.doi.org/10.1091/mbc.E03-10-0738

Tumbar, T., G. Sudlow, and A.S. Belmont. 1999. Large-scale chromatin unfolding and remodeling induced by VP16 acidic activation domain. *J. Cell Biol.* 145:1341–1354. http://dx.doi.org/10.1083/jcb.145.7.1341

Visser, A.E., F. Jaunin, S. Fakan, and J.A. Aten. 2000. High resolution analysis of interphase chromosome domains. *J. Cell Sci.* 113:2585–2593.

Woolcock, K.J., R. Stunnenberg, D. Gaidatzis, H.R. Hotz, S. Emmerth, P. Barraud, and M. Bühler. 2012. RNAi keeps Atf1-bound stress response genes in check at nuclear pores. *Genes Dev.* 26:683–692. http://dx.doi.org/10.1101/gad.186866.112

Xiao, H., O. Perisic, and J.T. Lis. 1991. Cooperative binding of *Drosophila* heat shock factor to arrays of a conserved 5 bp unit. *Cell*. 64:585–593. http://dx.doi.org/10.1016/0092-8674(91)90242-Q

Yao, J., M.B. Ardehali, C.J. Fecko, W.W. Webb, and J.T. Lis. 2007. Intranuclear distribution and local dynamics of RNA polymerase II during transcription activation. *Mol. Cell*. 28:978–990. http://dx.doi.org/10.1016/j.molcel.2007.10.017

Yoshida, T., K. Shimada, Y. Oma, V. Kalck, K. Akimura, A. Taddei, H. Iwahashi, K. Kugou, K. Ohta, S.M. Gasser, and M. Harata. 2010. Actin-related protein Arp6 influences H2A.Z-dependent and -independent gene expression and links ribosomal protein genes to nuclear pores. *PLoS Genet.* 6:e1000910. http://dx.doi.org/10.1371/journal.pgen.1000910

Rohner et al., http://www.jcb.org/cgi/content/full/jcb.201207024/DC1

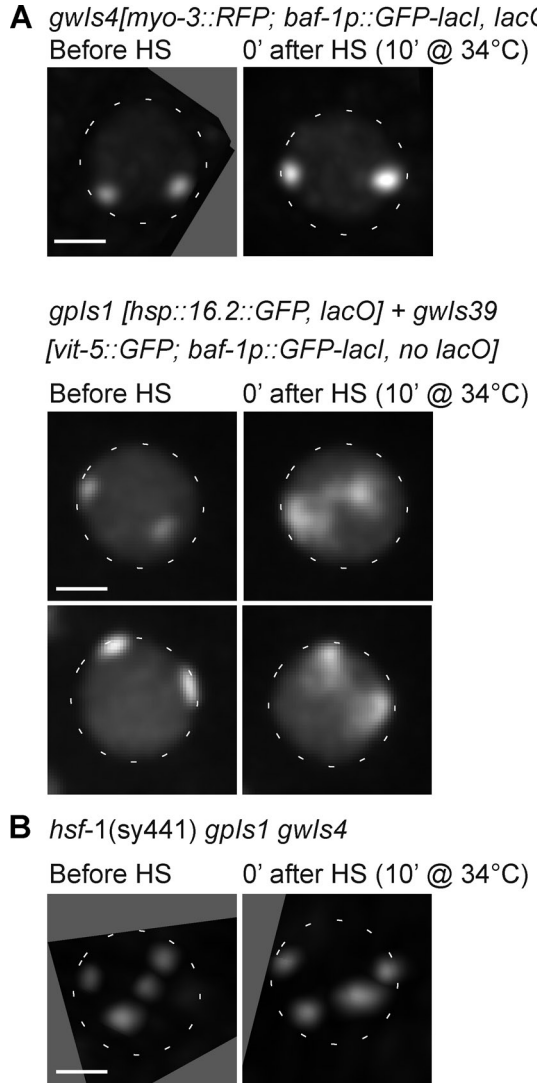

Figure S1. **Controls for the induced integrated array of *hsp-16.2* promoter.** (A) HS does not induce decondensation of a large array bearing *baf-1* promoter–driven GFP-lacI in embryos. Nuclei from an embryo of a strain carrying only the GFP-lacI–expressing array *gwIs4* are shown before and after HS. No change in array shape is observed upon HS. (B) *hsf-1(sy441)* impairs decondensation of HS-activated arrays. In a strain carrying both a GFP-lacI–expressing array (*gwIs4*) and an HS-activated array (*gpIs1*), no difference in size can be observed before and after HS. Each nucleus is encircled by a broken line. Bars, 2 µm.

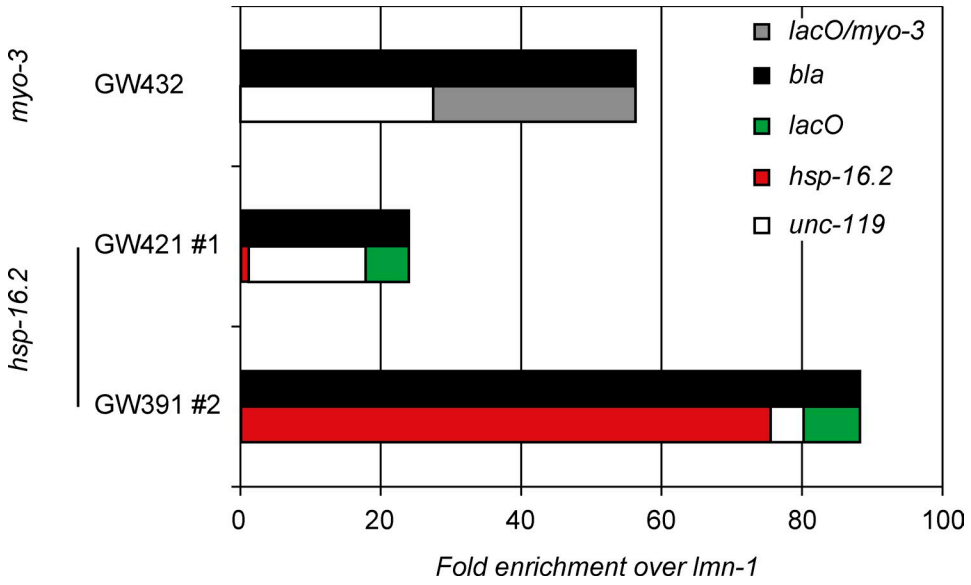

Figure S2. **Quantification by real-time PCR of the number of plasmids present in the small arrays carrying *hsp-16.2::mCherry*.** Copy numbers of plasmids found in integrated transgenes shown in Fig. 2 D were determined for *unc-119*, *hsp-16.2*, and the *bla* sequences (present in all plasmids). Normalization of PCR efficiency for *unc-119* and *hsp-16.2* was achieved using WT worms. The *lacO* copy number was calculated by subtracting the *unc-119* and *hsp-16.2* plasmid number from the total *bla* copy number.

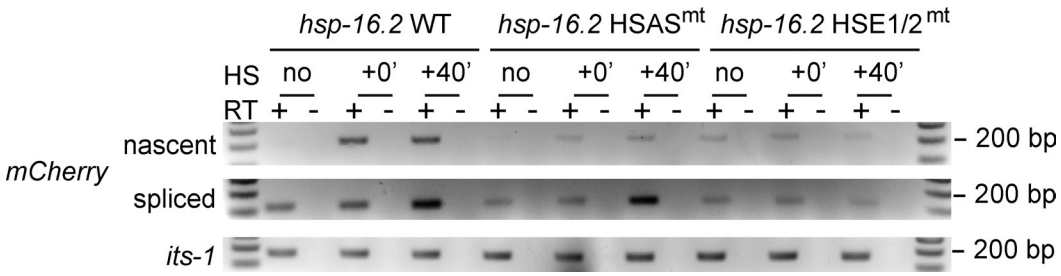

Figure S3. **PCR amplification detects *mCherry* mRNA in a reverse transcription–dependent manner.** Nascent and spliced RNAs were detected by real-time PCR of RNA driven from the indicated mutant *hsp-16.2* promoters in the MosSCI integration. The levels are extremely low when normalized to *its-1* (Fig. 5). Detection of transcripts is nonetheless possible after 30 cycles of normal PCR using primers specific for the nascent (top row) and spliced (middle row) *mCherry* RNA, performed on reverse-transcribed RNA isolated from the indicated MosSCI integration strains. Amplification from a control rDNA spacer transcript, *its-1*, is shown in the bottom row. All amplifications are dependent on reverse transcription (RT) and are therefore not caused by contaminating DNA. Amplicon signals are visible even though the levels for both nascent and spliced *mCherry* are reduced in the mutant constructs.

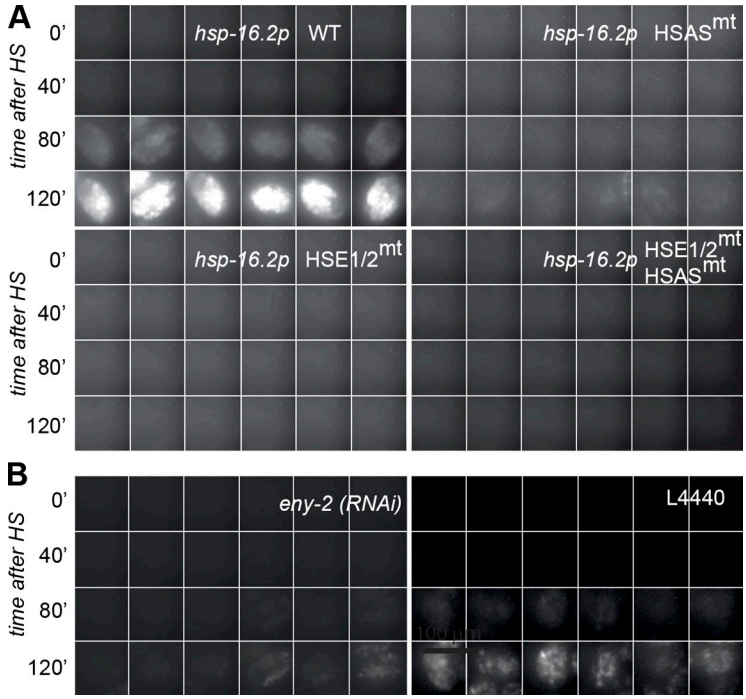

Figure S4. **mCherry protein detection after HS induction.** (A) Red fluorescence signal from mCherry protein in 24 whole embryos from worms carrying the WT or mutated *hsp-16.2* promoter MosSCI insertions driving *mCherry,* as described in Fig. 5 B and scored in Fig. 5 C. The same contrast and brightness was applied to all images. (B) mCherry red fluorescence signal from embryos of the progeny of control RNAi or *eny-2(RNAi)* fed adults as scored in Fig. 7 B. The same contrast and brightness was applied to all images.

Table S1. **Overview of *C. elegans* strains used including genetic details**

Strain name	Genotype	Arrays/transgenes
N2	*WT Bristol isolate*	
GW76	*gwIs4[myo-3::rfp baf-1::gfp-lacI let-858 3′UTR] X*	**Large array**
GW102	*gwIs4 [myo-3::rfp baf-1::gfp-lacI let-858 3′UTR] X; gpIs1[hsp-16.2::gfp]*	**Large arrays**
GW220	*gwIs4 [myo-3::rfp baf-1::gfp-lacI let-858 3′UTR] X; gpIs1[hsp-16.2::gfp] hsf-1(sy441)I*	**Large arrays**
GW391	*gwIs49[hsp-16.2::mCherry 256xLacO 4xLexA; unc-119(+)]; unc-119(ed3) III; gwIs39[baf-1::GFP-LacI::let-858 3′UTR; vit-5::GFP] III*	**Small transgene**/large array
GW421	*gwIs58[hsp-16.2::mCherry 256xLacO 4xLexA; unc-119(+)]; unc-119(ed3) III; gwIs39[baf-1::GFP-LacI::let-858 3′UTR; vit-5::GFP] III*	**Small transgene**/large array
GW432	*gwIs28[myo-3::wmCherry unc-119(+) 256 x LacO 4xLexA; unc-119(+)]; gwIs39[baf-1::GFP-LacI::let-858 3′UTR; vit-5::GFP] III; unc-119(?) III*	**Small transgene**/large array
GW440	*gwSi0[256x lacO; unc-119(+)]; gwIs39[baf-1::GFP-LacI::let-858 3′UTR; vit-5::GFP] III; unc-119(ed3) III*	**MosSCI**/large array
GW615	*gwSi3[hsp-16.2::wmCherry; 256x lacO; unc-119(+)]; gwIs39[baf-1::GFP-LacI::let-858 3′UTR; vit-5::GFP] III; unc-119(ed3) III*	**MosSCI**/large array
GW644	*gwSi5[hsp-16.2 HSE1/2^{mt}::wmCherry; 256x lacO; unc-119(+)]; gwIs39[baf-1::GFP-LacI::let-858 3′UTR; vit-5::GFP] III; unc-119(ed3) III*	**MosSCI**/large array
GW648	*gwSi9[hsp-16.2 HSAS^{mt}HSE1/2^{mt}::wmCherry; 256x lacO; unc-119(+)]; gwIs39[baf-1::GFP-LacI::let-858 3′UTR; vit-5::GFP] III; unc-119(ed3) III*	**MosSCI**/large array
GW649	*gwSi10[hsp-16.2 HSAS^{mt}::wmCherry; 256x lacO; unc-119(+)]; gwIs39[baf-1::GFP-LacI::let-858 3′UTR; vit-5::GFP] III; unc-119(ed3) III*	**MosSCI**/large array
GW597	*gwIs58[hsp-16.2::mCherry 256xLacO 4xLexA; unc-119(+)]; unc-119(ed3) III; gwIs39[baf-1::GFP-LacI::let-858 3′UTR; vit-5::GFP] II; dpy-13(e184) ama-1(m118m251) IV*	**Small transgene**/large array
GW691	*gwIs58[hsp-16.2::mCherry 256xLacO 4xLexA; unc-119(+)]; unc-119(ed3) III; gwIs39[baf-1::GFP-LacI::let-858 3′UTR; vit-5::GFP] III; dpy-13(e184) ama-1(m118m238) IV*	**Small transgene**/large array
GW692	*gwSi13[256x lacO @ ttTi9115; unc-119(+)]V; unc-119(ed3)III; gwIs39[baf-1::GFP-LacI::let-858 3′UTR; vit-5::GFP] III*	**MosSCI**/large array
GW815	*gwSi16[hsp-16.2/41::mCherry 2x]; unc-119(ed3)III; gwIs39 [baf-1::GFP-LacI::let-858 3′UTR; vit-5::GFP]III*	**MosSCI**/large array
GW820	*gwSi13[256x lacO @ ttTi9115; unc-119(+)]V; unc-119(ed3)III; gwIs39[baf-1::GFP-LacI::let-858 3′UTR; vit-5::GFP] III; dpy-13(e184) ama-1(m118m251)IV*	**MosSCI**/large array
PMW54	*gwIs39[baf-1::gfp-lacI let-858 3′UTR; vit-5::gfp] III; gpIs1[hsp-16.2::gfp]*	**Large array**/large array

Arrays indicated in bold contain *lacO* sites and make a visible spot when combined with GFP-LacI.

Table S2. **Overview of primers used**

Amplified Locus	Sequence (5′-3′)	Forward/reverse	Locus	Used for
mCherry; processed	ATTACGATGCTGAGGTGAAGAC	Forward	Transgene	qPCR on cDNA
mCherry; processed	CGATAGTGTAATCCTCGTTGTG	Reverse	Transgene	qPCR on cDNA
hsp-16.2; processed	ATCTTATGAGAGATATGGCTC	Forward	Endogenous	qPCR on cDNA
hsp-16.2; processed	TTGTTAACAATCTCAGAAGACT	Reverse	Endogenous	qPCR on cDNA
mCherry; nascent	AAGGGTGAAGAAGATAACATGG	Forward	Transgene	qPCR on cDNA
mCherry; nascent	GTCCGCCTTTAGTTACCTGA	Reverse	Transgene	qPCR on cDNA
hsp-16.2; nascent	TGAGTCTTCTGAGGTAAATAA	Forward	Endogenous	qPCR on cDNA
hsp-16.2; nascent	CATTGTTAACAATCTGAAAGC	Reverse	Endogenous	qPCR on cDNA
its-1	CCTGGTGGCTATATGCGTCT	Forward	Endogenous	qPCR on cDNA
its-1	CCGTGAAGACTTTTGGCAAT	Reverse	Endogenous	qPCR on cDNA
intergenic locus on *chr V*	CAAAAAGCGTTTTCAGCACA	Forward	Control	qPCR after ChIP
intergenic locus on *chr V*	TCTGAAGTGGGGAGCTTTGT	Reverse	Control	qPCR after ChIP
intergenic locus on *chr II*	AAGACAAACACTGCCAGAAAA	Forward	Control	qPCR after ChIP
intergenic locus on *chr II*	ATCCTTGACGCCAGTGACAT	Reverse	Control	qPCR after ChIP
hsp-16.2	GGGGATCCAGTGAGATGATT	Forward	Ectopic	qPCR after ChIP
hsp-16.2	ATGTGAGTCGCCCTCCTTTT	Reverse	Ectopic	qPCR after ChIP
hsp-16.2	TGGACGGAAATAGTGGTAAAGTG	Forward	Endogenous	qPCR after ChIP
hsp-16.2	CCTTTTGCAACAAGCAGCTC	Reverse	Endogenous	qPCR after ChIP
hsp-16.2	AAGCCAACACGCTTTGTTCT	Forward	Ectopic/endogenous	qPCR after ChIP
hsp-16.2	TCCAGTGAGTTCGTCCAAGA	Reverse	Endogenous	qPCR after ChIP
hsp-16.2	CGACTCTAGAGGATCAAGAGCA	Reverse	Ectopic	qPCR after ChIP
hsp-16.2	ATTCAGCAGATTTCTCTTCGAC	Forward	Endogenous	qPCR after ChIP
hsp-16.2	GTACGCTATCAATCCAAGGAG	Reverse	Endogenous	qPCR after ChIP
hsp-16.2	CACAAAGGGACAGTTCTGAG	Forward	Endogenous	qPCR after ChIP
hsp-16.2	TAAGATCTAGGAACATCCACAG	Reverse	Endogenous	qPCR after ChIP
hsp-16.2	CTCCTGACTCCAAACTTCTC	Forward	Endogenous	qPCR after ChIP
hsp-16.2	AACATTTCTGCCTTCTCCT	Reverse	Endogenous	qPCR after ChIP
hsp-16.2	GAACATGGATACTTGAAACGCT	Forward	Endogenous	qPCR after ChIP
hsp-16.2	GTGATGAGTTTGTCTTCTTTGG	Reverse	Endogenous	qPCR after ChIP
mCherry	GTCACTGTAACAACTCCTCC	Forward	Ectopic	qPCR after ChIP
mCherry	TTAAACATCCGGCAGATATACC	Reverse	Ectopic	qPCR after ChIP
mCherry	GGAGAAAGAGCATGTAGGA	Forward	Ectopic	qPCR after ChIP
mCherry	TCCCACAACGAGGATTACAC	Reverse	Ectopic	qPCR after ChIP
Cbunc-119	CACAACAAAGCCGACTACTC	Forward	Ectopic	qPCR after ChIP
Cbunc-119	GGGAAGGAACAAACTAGACAG	Reverse	Ectopic	qPCR after ChIP
Cbunc-119	ACCAAACCGATATGAAAGCC	Forward	Ectopic	qPCR after ChIP
Cbunc-119	AAGATACCTTGAGTGATTCCC	Reverse	Ectopic	qPCR after ChIP
lmn-1	CAAGAGAACAACAGACTCCAG	Forward	Endogenous	qPCR copy number
lmn-1	TAATAAGACCACCGCATCAG	Reverse	Endogenous	qPCR copy number
unc-119	CCACACCACCTCTAATCTCC	Forward	Endogenous/tg	qPCR copy number
unc-119	TCATTTCTCTGCGTCTTCCT	Reverse	Endogenous/tg	qPCR copy number
hsp-16.2	TGAATCAGAATATGGAGAACGG	Forward	Endogenous/tg	qPCR copy number
hsp-16.2	GACTCACATTCGGTACATGG	Reverse	Endogenous/tg	qPCR copy number
bla	ATCGTTGTCAGAAGTAAGTTGG	Forward	Tg	qPCR copy number
bla	GCCGCATACACTATTCTCAG	Reverse	Tg	qPCR copy number

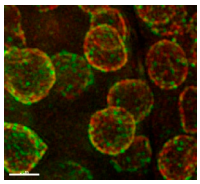

Video 1. **3D reconstruction of WT *C. elegans* embryos stained for nuclear pores and lamina.** WT *C. elegans* embryos were fixed on glass slides and immunostained for nuclear pores (Mab414; green) and nuclear lamina (anti–LMN-1; red). Images were acquired on a super-resolution structured illumination microscope (Elyra system [Carl Zeiss] with an EM-CCD camera [Andor iXon 885]), and the 3D reconstruction was performed with Zen software.

Chapter 3: Additional results

In this chapter I present preliminary data, which allows us to speculate on additional proteins and with it pathways, involved in the peripheral localisation of the *hsp-16.2* locus. I will first give a brief introduction and will then present the results and discuss them.

Background

We wanted to further examine the involvement of *trans* elements that might be linked to mRNA splicing or stability, in the peripheral anchorage of *hsp-16.2*. In this section we examine a putative splicing factor that interacts with ENY-2, as well as components of the RNAi machinery.

RSY-1 interacts with ENY-2 and is a putative splicing factor

In a genome wide interaction screen by yeast two hybrid in *C. elegans*, RSY-1 was found to interact with ENY-2, a protein that we showed to be important for peripheral localisation of *hsp-16.2* (Simonis et al., 2009). RSY-1 stands for Regulator of SYnapse formation and was, as the name indicates shown to be relevant for the formation of synapses in *C. elegans*. The loss of RSY-1 led to the formation of additional synapses (Patel and Shen, 2009). Comparing the protein sequence to sequences of other species reveals a quite high similarity to arginine /serine rich proteins in mouse and human known as splicing factors. The possible involvement in RNA processing and the fact that RSY-1 is interacting with ENY-2 encouraged us to investigate the effect of a knockout of the gene encoding RSY-1.

Components of the RNAi machinery interact with nuclear pores and control expression levels of heat inducible genes by cotranscriptional gene silencing

Studies in *Schizosaccharomyces pombe* showed that Dicer, an endoribonuclease that cuts double stranded RNA into small interfering RNA, which then cause the degradation of messenger RNA (mRNA), is localised at nuclear pores (Emmerth et al., 2010). In *C. elegans* it was shown that DCR-1 interacts with nuclear pores in the germline (Beshore et al., 2011). Very recently it was shown that a knockout of Dicer in *S. pombe* results in the up-regulation of three different heat shock genes, *hsp16*, *hsp104* and *hsp9*, in their uninduced state. The authors suggest that stress genes might be recruited to the nuclear pore complex, where they are kept poised for rapid mRNA export, but kept in check by RNAi-mediated cotranscriptional gene silencing (Woolcock et al., 2012). Similarly in S2 cells from *Drosophila*, DCR2 and AGO2, two proteins involved in the RNA interference pathway, have an influence on expression levels of the two heat shock loci *Hsp70* and *Hsp68*. Both *Hsp70* and *Hsp68* were expressed at a higher level in their uninduced state

when DCR2 or AGO2 were downregulated by RNAi. During heat shock no change in expression levels was observed which suggests that none of the two is involved in heat-shock-gene-mediated activation (Cernilogar et al., 2011). In neither of the studies the direct effect on localisation within the nucleus was tested upon disruption of the above mentioned proteins.

Recently proteins involved in the nuclear RNAi pathway in *C. elegans* have been identified. These four proteins are called Nrde-1 to 4 for Nuclear RNAi defective. First Nrde-3 was identified as an Argonaute protein that binds to siRNAs in the cytoplasm and transports them into the nucleoplasm (Guang et al., 2008). Nrde-3 recruits other Nrde factors (Nrde-1, Nrde-2, and Nrde-4) which results in a deposition of a repressive mark (H3K9) on the surrounding nucleosomes (Burkhart et al., 2011; Guang et al., 2010). If the Nrde pathway is functional, pol II will be inhibited during the elongation phase of transcription. In addition the pathway helps to regulate transcription and chromatin dynamics (Burkhart et al., 2011). We were curious to see what effect a knockdown the different Nrde factors has on localisation, since it is possible that also in *C. elegans* the RNAi machinery is interacting with the nuclear pore complex, regulates cotranscriptionally the expression of heat-inducible genes and also helps to tether them to the nuclear pore complex.

Results and discussion

RSY-1, a putative splicing factor, is important for peripheral localisation only upon heat induction

As illustrated in the previous chapter, many different proteins are involved in the tethering of *hsp-16.2* to the nuclear periphery. One of the hypotheses in the field, the gene gating hypothesis, argues that stress-inducible genes are localised at nuclear pores for a synchronised and thus more efficient co-transcriptional processing and export (Blobel, 1985). Our findings that RNA polymerase II and ENY-2, a factor involved in mRNA transport and export, are involved in the peripheral localisation of *hsp-16.2*, reinforce this theory.

To check if RSY-1 participates in the anchorage of *hsp-16.2* at the periphery, we crossed our bombardment derived *hsp-16.2* promoter mCherry fusion to a strain with a stop mutation in *rsy-1* (wy94) (Patel and Shen, 2009) and analysed the distribution of the *hsp-16.2* promoter within the nucleus, using the methodology described in the previous chapter (Figure 2B). We find that in the uninduced condition, no significant change in the percentage occurs (49% in zone one in wt RSY-1 vs 53% in zone one in RSY-1 (wy94)). However, in the induced state we find that instead of an enrichment at the nuclear envelope, we observe a near-random distribution within the nucleus (60% in zone 1 in wt *RSY-1* vs 35% in zone 1 in *rsy-1 (wy94*)) (Figure 9A).

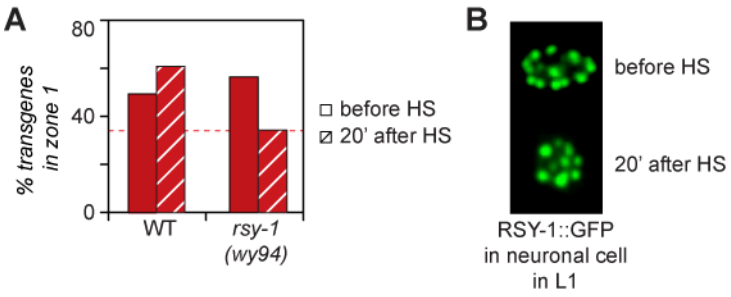

Figure 9: RSY-1 is distributed in speckle like manner and is important for peripheral localization of *hsp-16.2* only upon induction A. Quantification of *hsp-16.2* transgenes using 3-zone scoring; before HS: WT 49%; *rsy-1* (wy94) 53% (n= 142; 130); 20' after HS: WT 60%; *rsy-1* (wy94) 35% (n=191; 86); B. RSY-1::GFP expressed under a neuronal promoter (*unc-86*) in neuronal cells of the L1 stage.

Performing a BlastP to find similar proteins in other species reveals that in mouse as well as in human a serine /arginine rich splicing factor shows 37% identity (Figure 10). It is difficult to be certain that this is a functional homologue. So far we were only able to express a GFP tagged version of RSY-1 under a neuronal promoter that is only expressed from the first larval stage onwards, but the distribution pattern we see resembles the distribution pattern of splicing speckles in mammalian cells (Figure 9B and Figure 1 in (Spector and Lamond, 2011)). Taken together these results indicate that RSY-1 might be implicated in the peripheral localisation of *hsp-16.2* in a co-transcriptional processing manner. I hypothesise that only when a transcript ready for splicing is present and thus interacts with RSY-1, it is tethered via this protein to the nuclear periphery, which would explain why RSY-1 only has an impact on peripheral localisation of *hsp-16.2* upon heat induction, and not in the uninduced state.

>sp|Q8TF01.2|PNISR_HUMAN RecName: Full=Arginine/serine-rich protein PNISR; AltName: Full=PNN-interacting serine/arginine-rich protein; AltName: Full=SR-related protein; AltName: Full=SR-rich protein; AltName: Full=Serine/arginine-rich-splicing regulatory protein 130; Short=SRrp130; AltName: Full=Splicing factor, arginine/serine-rich 130; AltName: Full=Splicing factor, arginine/serine-rich 18
Length=805

GENE ID: 25957 PNISR | PNN-interacting serine/arginine-rich protein [Homo sapiens] (10 or fewer PubMed links)

Score = 55.1 bits (131), Expect = 1e-06, Method: Compositional matrix adjust.
Identities = 61/164 (37%), Positives = 84/164 (51%), Gaps = 32/164 (20%)

```
Query  270  RKKLPAWILEGLEKAEREKQKQWEKEE------KLKKAEEEKARRRAEAG-------KSK  316
            R+ LPAWI EGLEK EREKQK+ EKE     +L K +E+KA  AE G     +SK
Sbjct  229  RRTLPAWIREGLEKMEREKQKKLEKERMEQQRSQLSK-KEKKATEDAEGGDGPRLPQRSK  287

Query  317  FDSSSDEESPENEKFPVGNGKSEY------QEDDNDSEDDLEERREQFIRCVKTLMMNVL  370
            FDS  ++E  EN +  +GK      QE+ +D E  EE+ Q +  K L+  +L
Sbjct  288  FDSDEEEEDTENVE-AASSGKVTRSPSPVPQEEHSDPEMTEEEKEYQMMLLTKMLLTEIL  346

Query  371  LESSNDVIMRIIQEELREHEKLQFERKKLATAP-KIIGNSSALA  413
            L+ +++I  + ++ R       K  AP K +  SSALA
Sbjct  347  LDVTDEEIYYVAKDAHR----------KATKAPAKQLAQSSALA  380
```

Score = 33.9 bits (76), Expect = 4.1, Method: Compositional matrix adjust.
Identities = 40/146 (27%), Positives = 56/146 (38%), Gaps = 23/146 (16%)

```
Query  8    HQAQPAESVDWAQLAQQWMAMRDTDDRRAG---------NSHDFAQNHQLPWHQPRHPGP  58
            HQ  P++ +DWA LAQ W+A R+  +++       N  D +         GP
Sbjct  25   HQQDPSQ-IDWAALAQAWIAQREASGQQSMVEQPPGMMPNGQDMS---------TMESGP  74

Query  59   PAHQDW-GDWSANRDEQ--WRGPPGPSGPSGPPVYHNQGP-PRGYPPPPPQGADTWRGAP  114
            H ++ GD + NR Q W   P P   +  P P  PP      G
Sbjct  75   NNHGNFQGDSNFNRMWQPEWGMHQQPPHPPPDQPWMPPTPGPMDIVPPSEDSNSQDSGEF  134

Query  115  PPAHHGHFGPPGHHFQGPPQHFPPGP  140
            P +  F   H+F GPP +F  GP
Sbjct  135  APDNRHIFNQNNHNFGGPPDNFAVGP  160
```

>sp|A2AJT4.1|PNISR_MOUSE RecName: Full=Arginine/serine-rich protein PNISR; AltName: Full=Serine/arginine-rich-splicing regulatory protein 130; Short=SRrp130; AltName: Full=Splicing factor, arginine/serine-rich 18; AltName: Full=Splicing factor, arginine/serine-rich 18
Length=805

GENE ID: 66625 Sfrs18 | serine/arginine-rich splicing factor 18 [Mus musculus] (Over 10 PubMed links)

Score = 52.0 bits (123), Expect = 1e-05, Method: Compositional matrix adjust.
Identities = 60/164 (37%), Positives = 85/164 (52%), Gaps = 32/164 (20%)

```
Query  270  RKKLPAWILEGLEKAEREKQKQWEKEE------KLKKAEEEKARRRAEAG-------KSK  316
            R+ LPAWI EGLEK EREKQK+ EKE     +L K +E+KA  AE G     +SK
Sbjct  229  RRTLPAWIREGLEKMEREKQKKLEKERMEQQRSQLSK-KEKKATEDAEGGDGPRLPQRSK  287

Query  317  FDSSSDEESPENEKFPVGNGKSEY------QEDDNDSEDDLEERREQFIRCVKTLMMNVL  370
            FDS  ++E  EN +  V +GK      QE+ ++ E  EE+ Q +  K L+  +L
Sbjct  288  FDSDEEDEDAENLE-AVSSGKVTRSPSPAPQEEHSEPEMTEEEKEYQMMLLTKMLLTEIL  346

Query  371  LESSNDVIMRIIQEELREHEKLQFERKKLATAP-KIIGNSSALA  413
            L+ +++I  + ++ R       K  AP K +  SSALA
Sbjct  347  LDVTDEEIYYVAKDAHR----------KATKAPAKQLAQSSALA  380
```

Score = 34.3 bits (77), Expect = 3.1, Method: Compositional matrix adjust.
Identities = 40/146 (27%), Positives = 56/146 (38%), Gaps = 23/146 (16%)

```
Query  8    HQAQPAESVDWAQLAQQWMAMRDTDDRRAG---------NSHDFAQNHQLPWHQPRHPGP  58
            HQ  P++ +DWA LAQ W+A R+  +++       N  D +         GP
Sbjct  25   HQQDPSQ-IDWAALAQAWIAQREASGQQSIVEQPPGMMPNGQDMS---------AMESGP  74

Query  59   PAHQDW-GDWSANRDEQ--WRGPPGPSGPSGPPVYHNQGP-PRGYPPPPPQGADTWRGAP  114
            H ++ GD + NR Q W   P P   +  P P  PP      G
Sbjct  75   NNHGNFQGDSNFNRMWQPEWGMHQQPPHPPPEQPWMPPAPGPMDIVPPSEDSNSQDSGEF  134

Query  115  PPAHHGHFGPPGHHFQGPPQHFPPGP  140
            P +  F   H+F GPP +F  GP
Sbjct  135  APDNRHIFNQNNHNFGGPPDNFAVGP  160
```

Figure 10: Results of a BlastP of RSY-1 to identify homologue proteins in other species

In a next step we would like to find out if RSY-1 has a splicing activity by comparing pre-mRNA and processed RNA levels in the strain carrying the RSY-1 (wy94) stop mutation. Another interesting question is how RSY-1 is distributed within the nucleus of embryos and if it is interacting with nuclear pores.

Knockdown of DCR-1 and components of the Nrde pathway results in random distribution of *hsp-16.2*

As mentioned above, knockout of Dicer results in the up-regulation of three different heat shock genes in *S. pombe* (Woolcock et al., 2012). Since it has been shown before in *S. pombe* (Emmerth et al., 2010) as well as in *C. elegans* germline (Beshore et al., 2011), that Dicer localises at the nuclear pore complex, we were interested to see if knockdown of DCR-1 or of three other factors that are part of the RNAi machinery has an influence on nuclear localisation of *hsp-16.2*. After several generations of RNAi against *dcr-1*, *nrde-1*, *nrde-2* and *nrde-3*, an almost random localisation of *hsp-16.2* occurs both before (% in zone 1: mock RNAi 48%; *dcr-1* 41%; *nrde-1* 35%; *nrde-2* 39%; *nrde-3* 35%) and after heat-shock induction (% in zone 1: mock RNAi 56%; *dcr-1* 44%; *nrde-1* 30%; *nrde-2* 38%; *nrde-3* 32%) (Figure 11). This gives us a hint that the RNAi machinery could indeed be involved in tethering *hsp-16.2* to the nuclear periphery in the uninduced as well as in the induced state. Since RNAi experiments against components of the RNAi machinery might not be very efficient and cause secondary effects, this experiment needs to be repeated with strains expressing a stop mutation of the different RNAi factors. Even more important is to analyse the expression level and see whether also *hsp-16.2* in *C. elegans* is cotranscriptionally silenced to adapt the amount of transcript to the need of the situation.

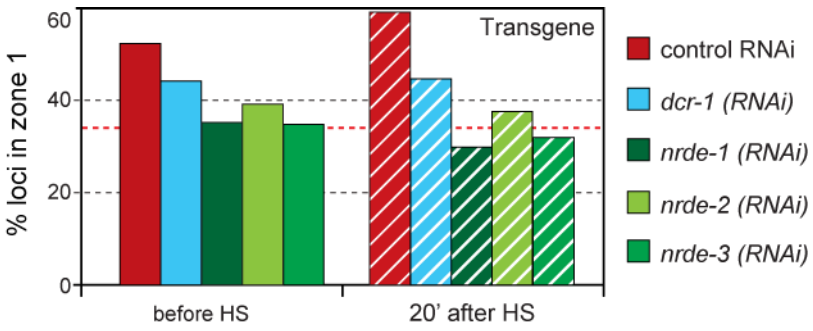

Figure 11: Localisation of *hsp-16.2* in reduced levels of different components of the RNAi machinery RNAi experiment performed for 3 generations in *dcr-1* and 2 generations for all the others. First number: percentage in zone 1; second number: spots counted. Before HS: control (48%; 326), *dcr-1* (41%; 48), *nrde-1* (35%; 41), *nrde-2* (39%; 90), *nrde-3* (35%; 88). After HS: control (56%, 393) *dcr-1* (44%; 47), *nrde-1* (30%; 30), *nrde-2* (38%; 83), *nrde-3* (32%; 81)

In a study in which *C elegans* DCR-1 was mutated, Welker and colleagues found that many misregulated genes are found on the X chromosome (Welker et al., 2007). In another study it was shown that at least in germ cells, *C. elegans* DCR-1 also interacts with the nuclear pore complex (Beshore et al., 2011). Interestingly, it has been shown in *Drosophila* that a large percentage of the X chromosome interacts with the nuclear pore complex and that association with the nuclear pore complex is involved in dosage compensation (Mendjan et al., 2006; Vaquerizas et al., 2010). In summary, Dicer is located at nuclear pores in *S. pombe* and *C. elegans*, it is involved in gene regulation on the X chromosome in *C. elegans*, and we know that dosage compensation takes place at nuclear pores in *Drosophila* (Beshore et al., 2011; Emmerth et al., 2010; Mendjan et al., 2006; Welker et al., 2007). Together with the results I show, we can speculate that the RNAi machinery is localised at nuclear pores in *C. elegans* and is involved in co-transcriptional gene silencing under uninduced conditions. To be sure, there remain many experiments to do in order to understand this phenomenon.

With these preliminary data, we show that the gene gating hypothesis may have some merit in worms. In addition we lend some support to the hypothesis that cotranscriptional gene silencing might keep the heat shock locus in check so that an appropriate level of transcript is made. These could both be valid reasons for pore association of *hsp-16.2* and more generally for heat-inducible genes.

References

Beshore, E.L., T.J. McEwen, M.C. Jud, J.K. Marshall, J.A. Schisa, and K.L. Bennett. 2011. C. elegans Dicer interacts with the P-granule component GLH-1 and both regulate germline RNPs. *Dev Biol*. 350:370-381.

Blobel, G. 1985. Gene gating: a hypothesis. *Proc Natl Acad Sci U S A*. 82:8527-8529.

Burkhart, K.B., S. Guang, B.A. Buckley, L. Wong, A.F. Bochner, and S. Kennedy. 2011. A pre-mRNA-associating factor links endogenous siRNAs to chromatin regulation. *PLoS Genet*. 7:e1002249.

Cernilogar, F.M., M.C. Onorati, G.O. Kothe, A.M. Burroughs, K.M. Parsi, A. Breiling, F. Lo Sardo, A. Saxena, K. Miyoshi, H. Siomi, M.C. Siomi, P. Carninci, D.S. Gilmour, D.F. Corona, and V. Orlando. 2011. Chromatin-associated RNA interference components contribute to transcriptional regulation in Drosophila. *Nature*. 480:391-395.

Emmerth, S., H. Schober, D. Gaidatzis, T. Roloff, K. Jacobeit, and M. Buhler. 2010. Nuclear retention of fission yeast Dicer is a prerequisite for RNAi-mediated heterochromatin assembly. *Dev Cell*. 18:102-113.

Guang, S., A.F. Bochner, K.B. Burkhart, N. Burton, D.M. Pavelec, and S. Kennedy. 2010. Small regulatory RNAs inhibit RNA polymerase II during the elongation phase of transcription. *Nature*. 465:1097-1101.

Guang, S., A.F. Bochner, D.M. Pavelec, K.B. Burkhart, S. Harding, J. Lachowiec, and S. Kennedy. 2008. An Argonaute transports siRNAs from the cytoplasm to the nucleus. *Science*. 321:537-541.

Mendjan, S., M. Taipale, J. Kind, H. Holz, P. Gebhardt, M. Schelder, M. Vermeulen, A. Buscaino, K. Duncan, J. Mueller, M. Wilm, H.G. Stunnenberg, H. Saumweber, and A.

Akhtar. 2006. Nuclear pore components are involved in the transcriptional regulation of dosage compensation in Drosophila. *Mol Cell*. 21:811-823.

Patel, M.R., and K. Shen. 2009. RSY-1 is a local inhibitor of presynaptic assembly in C. elegans. *Science*. 323:1500-1503.

Simonis, N., J.F. Rual, A.R. Carvunis, M. Tasan, I. Lemmens, T. Hirozane-Kishikawa, T. Hao, J.M. Sahalie, K. Venkatesan, F. Gebreab, S. Cevik, N. Klitgord, C. Fan, P. Braun, N. Li, N. Ayivi-Guedehoussou, E. Dann, N. Bertin, D. Szeto, A. Dricot, M.A. Yildirim, C. Lin, A.S. de Smet, H.L. Kao, C. Simon, A. Smolyar, J.S. Ahn, M. Tewari, M. Boxem, S. Milstein, H. Yu, M. Dreze, J. Vandenhaute, K.C. Gunsalus, M.E. Cusick, D.E. Hill, J. Tavernier, F.P. Roth, and M. Vidal. 2009. Empirically controlled mapping of the Caenorhabditis elegans protein-protein interactome network. *Nat Methods*. 6:47-54.

Spector, D.L., and A.I. Lamond. 2011. Nuclear speckles. *Cold Spring Harb Perspect Biol*. 3.

Vaquerizas, J.M., R. Suyama, J. Kind, K. Miura, N.M. Luscombe, and A. Akhtar. 2010. Nuclear pore proteins nup153 and megator define transcriptionally active regions in the Drosophila genome. *PLoS Genet*. 6:e1000846.

Welker, N.C., J.W. Habig, and B.L. Bass. 2007. Genes misregulated in C. elegans deficient in Dicer, RDE-4, or RDE-1 are enriched for innate immunity genes. *Rna*. 13:1090-1102.

Woolcock, K.J., R. Stunnenberg, D. Gaidatzis, H.R. Hotz, S. Emmerth, P. Barraud, and M. Buhler. 2012. RNAi keeps Atf1-bound stress response genes in check at nuclear pores. *Genes Dev*. 26:683-692.

Chapter 4: Concluding remarks and future prospects

In this thesis I have investigated the localisation of the *hsp-16.2* gene that encodes a small heat shock protein, in *C. elegans* embryos. Using two different types of transgenes that enable locus tracking by live fluorescence imaging, we could show that the promoter of this gene is sufficient to position the locus near the nuclear periphery, although in a less efficient manner than at the endogenous locus. We characterized *cis* as well as *trans* factors that are involved in the peripheral localisation of the *hsp-16.2* locus. From our work we can draw two major conclusions:

I) A *C. elegans* heat inducible gene interacts with the nuclear pore complex

The endogenous *hsp-16.2* locus, as well as small transgenes derived from bombardment and a single copy ectopic insertion that contains the *hsp-16.2* promoter driving the *mCherry* coding region, bearing an intron and a 3'UTR from the *unc-54* gene, are preferentially localised to the nuclear periphery, not only after heat shock induction but already in their non-induced state.

Refinement of the localisation data using a high resolution Structural Illumination Microscopy and Chromatin immunoprecipitation confirm that the *hsp-16.2* promoter position colocalizes with nuclear pores particularly in the induced state, and not with components of the nuclear lamina meshwork (i.e. LMN-1 or LEM-2). In other higher eukaryotes it was previously shown that stress-inducible genes interact with the nuclear pore complex and it was found that nucleoporins can influence gene regulation in a number of ways (Capelson et al., 2010; Kalverda et al., 2010). However, not all these gene-nucleoporin interactions take place at the nuclear periphery, since for a subpopulation of nucleoporins a fraction of the population in a soluble form, that diffuses through the nucleoplasm (for review see (Capelson et al., 2010)). Our combined microscopic/ChIP analyses provide two strong arguments against an interaction of *hsp-16.2* with soluble nucleoporins. First, high resolution microscopy shows that the locus is near the nuclear envelope, in a manner strongly correlated with the ChIP results. Secondly, our ChIP analysis was performed with a membrane spanning, poorly soluble nucleoporin (NPP-13 (in mammals Nup93), reducing the likelihood that the interaction we score takes place in the nuclear lumen.

We found that not only the interaction of the *hsp-16.2* promoter with the nuclear pore complex, but also the array of factors that mediate the interaction are conserved among yeast, flies and worms. The transcription factor HSF-1 together with its binding site in the heat shock element (HSE), are essential for the efficient activation of stress-inducible genes in all species analysed (Anckar and Sistonen, 2011), and both the factor and its binding sites are important for peripheral localization of the locus. In addition to the HSE sites we found a second *cis*-acting element in the *hsp-16.2* promoter, called HSAS, which both promotes anchoring and contributes to efficient *hsp-16.2* expression (GuhaThakurta et al., 2002), and data not shown). In our hands ENY-2, the homologue

of yeast Sus1, is also essential for peripheral localisation of *hsp-16.2*. Sus1 in yeast and E(y)2/ENY-2 in flies was shown to be part of two complexes (SAGA and TREX), which regulate both gene activation and export of the mRNA. ENY-2 appears to serve as a physical link between these complexes and the nuclear pore (Garcia-Oliver et al., 2011).

It is important to mention that at present we do not know if other heat inducible genes or even stress-inducible genes interact with the nuclear pore complex, and if they do, whether they use the same anchorage pathway.

II) Peripheral localisation is dependent on the RNA polymerase II

Using temperature sensitive mutants of the RNA polymerase II (pol II) we found that a shift from permissive to restrictive temperature is enough to abandon peripheral localisation of bombardment derived transgenes carrying the *hsp-16.2* locus. The resulting random distribution within the nucleus persists upon heat shock gene activation. It has been suggested that the two mutations we used cause a dissociation of RNA pol II either through loss of template binding or by disrupting the interaction between *C. elegans* AMA-1 and RBP-2, the catalytic and major subunits of RNA pol II.

The fact that the endogenous locus, which has a bidirectional promoter, is located more peripherally than the two types of transgenes, in which the transcription is on only one side of the promoter, encouraged us to create a single copy insertion with an *hsp-16.2* promoter flanked by *mCherry* on either side. This renders it more similar to the endogenous promoter, which drives not only *hsp-16.2* but also *hsp-16.41*. We find that a single copy integration of this functional bidirectional promoter increases the percentage of *hsp-16.2* localised at the periphery.

Taken together with the fact that RNA pol II is important for localisation at the periphery, I suggest two possible interpretations: I) It may be simply the presence of pol II that contacts nuclear pores, explaining why a bidirectional promoter with two RNA polymerases loaded, enhances the peripheral localisation. This is only valid if one imagines that there is something unique or special about the engaged pol II at this locus, for otherwise all promoters should be pore-associated. II) Alternatively, the link to nuclear pores may be mediated through the transcripts or transcript associated proteins. The increased transcript levels due to the bidirectional promoter, would thus account for the increased peripheral localisation. So far, we cannot rule out one or the other possibility.

An argument for the latter interpretation is the fact that loss of ENY-2, which is present in SAGA and in the TREX complex which contributes to mRNA transport and export, abolishes peripheral localisation as well. It is possible that both explanations are true, and that RNA pol II links the gene to the nuclear periphery, as does the accumulated transcript.

Preliminary data presented here also suggest that the processing of transcripts is involved in tethering *hsp-16.2* to the nuclear periphery. We found that disruption of RSY-

1, a protein interacting with ENY-2, results only in the release of *hsp-16.2* upon heat induction. Looking at the predicted protein structure suggests that it may have splicing activity, since the sequence has a quite high resemblance to the serine/arginine rich splicing factors in mouse and humans. For the moment, however, its splicing activity is purely speculative and needs to be tested before we can conclude that splicing is involved in the peripheral localisation of *hsp-16.2*.

So far the involvement of the RNAi machinery in the interaction of *hsp-16.2* with the nuclear pore complex is also speculative. From the literature we know that in *S. pombe* Dicer is localised at nuclear pores and that disruption of Dicer leads to an up-regulation of several heat shock genes (Emmerth et al., 2010; Woolcock et al., 2012). Similarly, in *Drosophila* it was shown that the disruption of DCR2 and AGO2 results in an up-regulation of *Hsp70* and *Hsp68* under uninduced conditions, while it has no influence on the heat-shock-mediated gene activation (Cernilogar et al., 2011). In worms it was shown that DCR-1 localises at the nuclear pores in the germ line (Beshore et al., 2011). Preliminary data presented in this thesis show that upon down-regulation of DCR-1 or other components of the nuclear RNAi deficient (Nrde) pathway, the peripheral localisation of *hsp-16.2* is reduced or lost. This indicates that also in *C. elegans* the RNAi machinery may be involved in tethering heat shock loci to the nuclear pore complex, controlling the level of mRNA expression by cotranscriptional gene silencing. This aspect, however, needs further study.

Future prospects

An important question that remains open is whether the presence of RNA pol II per se, or in addition the presence of transcripts, is crucial for a peripheral localisation. This can be tested in several ways. On one hand the analysis of expression levels of the mutant *cis* and *trans* elements can indicate whether transcription levels are comparable when the locus is found in the nuclear lumen to levels when the locus is found at the periphery. Another means to test this would be to tether *hsp-16.2* to nuclear pores and see whether or not expression levels change.

The preliminary data in Chapter 3 opens the door to an interesting future study on the involvement of these proteins in the documented association of stress-induced promoters with the nuclear pore. On one hand, it would be interesting to see if RSY-1 is a splicing factor, by comparing the level of unprocessed and processed RNA in the *rsy-1* knockout. In addition it is important to investigate the distribution of RSY-1 protein in embryonic nuclei, and to test its potential interaction with nuclear pores by high resolution microscopy.

A very competitive topic is the involvement of RNAi machinery components and cotranscriptional gene silencing as a functional reason for the interaction of *hsp-16.2* with the nuclear pore complex. Here it is important to obtain and use stop mutations in the RNAi machinery components, since any further analysis of the RNAi machinery

might not be very efficient, if one uses RNAi methodology itself to generate the mutant state. Having stop mutations crossed to the *hsp-16.2* transgene would not only allow the analysis of the gene localisation, but also its expression level. If the expression of heat shock genes is fine-tuned by the RNAi machinery in *C. elegans*, we expect to see an up-regulation of transcript in the mutant strains prior to heat shock. For DCR-1 an interaction with nuclear pores was shown in the germ-line of *C. elegans* but for the NRDE factors no precise localisation study has been performed (Beshore et al., 2011).

From the study we performed it remains open whether other heat inducible loci, or even other stress inducible genes, show a similar behaviour and relocate to nuclear pores upon induction. This could be addressed with genome wide ChIP assays that use antibodies against a pore component (preferentially the one used in our paper). We would then use next generation sequencing to reveal which genes interact with nucleoporins upon induction. Microscopy analysis would ensure that these interactions primarily take place at the nuclear periphery and not in the nuclear lumen.

In this thesis I have shown that *hsp-16.2* interacts with nuclear pores and I shed light on different *cis* and *trans* elements that are involved in this process. One important finding was that the presence of RNA pol II is important for peripheral localisation not only upon induction, but already prior to induction. If this is solely due to the presence of RNA pol II and associated proteins, or is due to the presence of transcripts, remains unresolved. In the future it will be interesting to further investigate the significance of co-transcriptional gene silencing and also of the putative splicing factor RSY-1 in stress gene positioning at nuclear pores. A more global attempt to analyse if other stress inducible loci in *C. elegans* behave in a similar way to the one we describe for *hsp-16.2*.

References

Anckar, J., and L. Sistonen. 2011. Regulation of HSF1 function in the heat stress response: implications in aging and disease. *Annu Rev Biochem*. 80:1089-1115.

Beshore, E.L., T.J. McEwen, M.C. Jud, J.K. Marshall, J.A. Schisa, and K.L. Bennett. 2011. C. elegans Dicer interacts with the P-granule component GLH-1 and both regulate germline RNPs. *Dev Biol*. 350:370-381.

Capelson, M., Y. Liang, R. Schulte, W. Mair, U. Wagner, and M.W. Hetzer. 2010. Chromatin-bound nuclear pore components regulate gene expression in higher eukaryotes. *Cell*. 140:372-383.

Cernilogar, F.M., M.C. Onorati, G.O. Kothe, A.M. Burroughs, K.M. Parsi, A. Breiling, F. Lo Sardo, A. Saxena, K. Miyoshi, H. Siomi, M.C. Siomi, P. Carninci, D.S. Gilmour, D.F. Corona, and V. Orlando. 2011. Chromatin-associated RNA interference components contribute to transcriptional regulation in Drosophila. *Nature*. 480:391-395.

Emmerth, S., H. Schober, D. Gaidatzis, T. Roloff, K. Jacobeit, and M. Buhler. 2010. Nuclear retention of fission yeast dicer is a prerequisite for RNAi-mediated heterochromatin assembly. *Dev Cell*. 18:102-113.

Garcia-Oliver, E., V. Garcia-Molinero, and S. Rodriguez-Navarro. 2011. mRNA export and gene expression: The SAGA-TREX-2 connection. *Biochim Biophys Acta*.

GuhaThakurta, D., L. Palomar, G.D. Stormo, P. Tedesco, T.E. Johnson, D.W. Walker, G. Lithgow, S. Kim, and C.D. Link. 2002. Identification of a novel cis-regulatory element involved in the heat shock response in Caenorhabditis elegans using microarray gene expression and computational methods. *Genome Res*. 12:701-712.

Kalverda, B., H. Pickersgill, V.V. Shloma, and M. Fornerod. 2010. Nucleoporins directly stimulate expression of developmental and cell-cycle genes inside the nucleoplasm. *Cell*. 140:360-371.

Woolcock, K.J., R. Stunnenberg, D. Gaidatzis, H.R. Hotz, S. Emmerth, P. Barraud, and M. Buhler. 2012. RNAi keeps Atf1-bound stress response genes in check at nuclear pores. *Genes Dev*. 26:683-692.

Abbreviations List (all described in text)

AC	Astrocytes
ChIP	Chromatin Immuno-Precipitation
chr V	Chromosome V
Da	Daltons
DAM-ID	DNA-Adenine Methyltransferase IDentification
DSIF	DRB Sensitivity Inducing Factor
ESC	Embryonic Stem Cells
FISH	Fluorescent In Situ Hybridisation
GRS	Gene Recruitment Sequence
HAT	Histone Acetyl Transferase
HDAC	Histone Deacetylase
HP1	Heterochromatin Protein 1
HS	Heat Shock (10 minutes @ 34°C)
HSAS	Heat Shock Associated Site
HSE	Heat Shock Element
HSF-1	Heat Shock transcription Factor 1
LAD	Lamina-Associated Domain
NE	Nuclear Envelope
NELF	Negative Elongation Factor
NPC	Nuclear Pore Complex
TREX	TRanscription and EXport complex
Pol II	RNA polymerase II
P-TEFb	Positive Transcription Elongation Factor b
rt	room temperature
S2 cells	Schneider 2 *Drosophila* cells
SAGA	Spt-Ada-Gcn-Acetyltransferase
SAMS	S-Adenosyl Methyltransferase
SR-SIM	Super-Resolution Structured Illumination Microscopy
ts	temperature sensitive
TSS	Transcription Start Site

Acknowledgements

I am thankful to my supervisor, Susan Gasser for her continuous support and guidance throughout my PhD, as well as to Julie Ahringer and Dirk Schübeler for fruitful discussions during the committee meetings. Special thanks go to Peter Meister, who introduced me to the world of *Caenorhabditis elegans* as well as to various microscopy techniques. With his enthusiasm and curiosity for experiments, I enjoyed working with him.

I appreciated the enjoyable atmosphere in the lab with room for many work-related but also personal discussions. Also the readiness to help with technical or practical issues is a habit in the lab that I am grateful for. Without Monika Tsai, who is running the lab in a very well organised way, and Razel Arpagaus who is always concerned about lab consumables, daily life in the lab would have been much less comfortable.

During all that time in the lab, Véronique Kalck was a great help not only for technical assistance and fruitful discussions but also as a very enjoyable person. For the maintenance of plenty of worm strains and the freezing of them I thank Monique Thomas and special thanks go also to Helder Ferreira for suggestions for experiments and changes in phrasing.

Without the introduction of Jan Pielage to the high resolution Structured Illumination Microscope I would not have been able to detect this fantastic world.

Life in FMI is also much easier thanks to the facilities. Iskra Katic is very helpful with all kinds of questions about *C. elegans* and is encouraging communication between the worm labs. The training in microscopy and the maintenance of the microscopes is nicely taken care of by Laurent Gelman and Steven Bourke, who have a lot of patience to help. Without the help of Aaron Ponti and Raphael Thierry image analysis would not be at such a high level and I am thankful to both for additional insights into this field. Finally I would like to thank Christel Genoud to introduce me to the world of electron microscopy, even though we did not apply it in the end.

Last but not least I would like to thank our collaborators in Chapel Hill, Jason Lieb, Kohta Ikegami and Xuefei Wang, who did the ChIP experiments for our paper.